

Synthetic Routes Approaching Functional Micro-Block Copolymers of γ -Substituted ϵ -Caprolactones

by

Sarah M. Craig

B.S. Chemistry, University of Rochester, 2021

Submitted to the Graduate Faculty of the
Dietrich School of Arts and Sciences in partial fulfillment
of the requirements for the degree of
Master of Science

University of Pittsburgh

2024

UNIVERSITY OF PITTSBURGH
DIETRICH SCHOOL OF ARTS AND SCIENCES

This thesis was presented

by

Sarah M. Craig

It was defended on

December 12, 2023

and approved by

Jennifer Laaser, Ph.D., University of Pittsburgh Department of Chemistry

Yiming Wang, Ph.D., University of Pittsburgh Department of Chemistry

Thesis Advisor: Tara Meyer, Ph.D., University of Pittsburgh Department of Chemistry and
McGowan Center for Regenerative Medicine

Copyright © by Sarah M. Craig

2024

Synthetic Routes Approaching Functional Micro-Block Copolymers of γ -Substituted ϵ -Caprolactones

Sarah M. Craig, M.S.

University of Pittsburgh, 2024

Described herein is a generalizable process towards the synthesis micro-block copolymers of γ -substituted ϵ -caprolactone moieties with reliable block alternation based on thermodynamic preferences in olefin metathesis. These micro-block copolymeric materials, containing oligomeric segments of multiple repeat unit types, inhabit a unique property space and can be used to probe the interface between alternating-like and block-like copolymer bulk behavior when synthesized at scale. The limitations of functional pendant groups are explored, demonstrating that the strategy is limited by both the solubility of the pendant group and its tolerance towards the anionic ring opening strategy employed for chain growth. Based on findings that pendant ester groups are most reactive towards anionic ring opening methods, the major product— chains terminated by an annulation event that occurs via intramolecular transesterification— is thus characterized and the mechanism used to inform alternate potential catalytic approaches. The product distribution of an aluminum salen catalyst with more sterically precluded coordination sites is found to slightly favor the linear product as opposed to its annulated counterpart, more so than is evidenced in the traditional aluminum alkoxide catalyzed oligomerization of the same γ -ester substituted ϵ -caprolactone monomer. While this change in preference is modest, such an improvement is indicative of potential options for attainable further improvements in the selectivity and tolerance

in anionic ring-opening polymerizations of lactides, potentially providing a plethora of options for bespoke functionalized biocompatible polymer materials.

Table of Contents

1.0 Introduction	1
1.1 Micro-Block Copolymer Utility	1
1.2 Previous Syntheses of Microblock Copolymers	2
1.3 Targeted Characteristics of Micro-Block Components Used in This Work	4
1.4 Polymers of Substituted ϵ-Caprolactones	4
1.5 Modes of γ-Carbonyl Substituted ϵ-Caprolactone Reactivity	6
1.6 Unique Behavioral Regime of Micro-Block Copolymers	7
1.7 Use of ADMET (Acyclic Diene Metathesis) for Polymerization of Macromonomers	8
1.8 Thesis Contents	8
2.0 Synthesis of Multiblock ϵ-Caprolactone Copolymers Bearing Pendant Amides	10
2.1 Results and Discussion	10
2.2 Conclusion	17
3.0 Investigation of Oligomerization Strategies for γ-Ester-Substituted ϵ- Caprolactone Moieties	18
3.1 Results and Discussion	20
3.1.1 Aluminum Tri-alkoxide Catalyzed γ-Ester Substituted ϵ-Caprolactone Oligomerization	20
3.1.2 Evaluation of γ-Ester ϵ-Caprolactone Oligomerization Catalyzed by an Aluminum Catalyst Bearing a Jacobsen Ligand Framework	26
3.2 Conclusion	28

4.0 Experimental Procedures	29
4.1 Materials and Instrumentation	29
4.1.1 Materials	29
4.1.2 NMR Spectroscopy.....	30
4.1.3 Size Exclusion Chromatography	30
4.1.4 MALDI-ToF MS	30
4.2 Synthesis of γ-Substituted ϵ-Caprolactones	31
4.2.1 4-Oxocyclohexane-1-carboxylic acid (2)	31
4.2.2 N-isopropyl-4-Oxocyclohexane-1-carboxamide (3, R=iPr).....	31
4.2.3 4-Oxo-N-propylcyclohexane-1-carboxamide (3, R=nPr).....	32
4.2.4 CL _{iPrA}	32
4.2.5 CL _{nPrA}	33
4.2.6 CL _{COOEt}	34
4.3 Diblock Macromonomer Synthesis	34
4.4 End Group Modification of γ-Substituted ϵ-Caprolactone Oligomers	35
4.5 Polymerization of Macromonomers	36
4.6 N,N'-bis(3,5-di-tert-butylsalicylidene)-1,2-cyclohexane-diamino aluminum isopropoxide (Al-salen) catalyst synthesis	36
4.7 Oligomerization of CL_O using Al(salen) catalyst	37
4.8 Kinetic Testing of CL_{COOEt} using Al(OR)₃ and Al(salen) catalysts	37
5.0 Future Directions	38
5.1 Alternative Synthetic Strategies	38
5.1.1 Catalyst	39

5.1.2 Monomer	39
5.2 Bulk Material Testing	40
5.2.1 Hydrophilicity.....	41
5.2.2 Mechanical Properties	41
5.2.3 Thermal Properties	42
Appendix A Spectral Data Associated with Monomer Syntheses	43
Appendix A.1 4-Oxocyclohexane-1-Carboxylic Acid Proton Chemical Shift Assignments & NMR Spectrum	43
Appendix A.2 N-Isopropyl 4-Oxocyclohexane-1-Carboxamide Proton Chemical Shift Assignments & NMR Spectrum	45
Appendix A.3 4-Oxo-N-Propylcyclohexane-1-Carboxamide Proton Chemical Shift Assignments & NMR Spectrum	47
Appendix A.4 N-Isopropyl-7-Oxooxepane-4-Carboxamide (CL _{iPrA}) Proton Chemical Shift Assignments & NMR Spectrum.....	49
Appendix A.5 7-Oxo-N-Propyloxepane-4-Carboxamide (CL _{nPrA}) Proton Chemical Shift Assignments & NMR Spectrum	51
Appendix A.6 Ethyl 7-Oxooxepane-4-Carboxylate (CL _{COOEt}) Proton Chemical Shift Assignments & NMR Spectrum	53
Appendix B Spectral Data Associated with Syntheses of γ -Substituted ϵ -Caprolactone Oligomers	55
Appendix B.1 1,3-Butenol and Hydroxyl Capped Oligo- ϵ -Caprolactone (CL _{o15-OH}) Proton Chemical Shift Assignments & NMR Spectrum.....	55

Appendix B.2 1,3-Butenol and Hydroxyl Capped Oligo- ϵ -Caprolactone- <i>block</i> - ϵ - Caprolactone- γ -Isopropyl Amide (CL _O 10-CL _{iPrA} 5-OH) Chemical Shift Assignments, ¹³ C and ¹ H NMR Spectra, and SEC.....	57
Appendix B.3 1,3-Butenol and Hydroxyl Capped Oligo- ϵ -Caprolactone- <i>block</i> - ϵ - Caprolactone- γ -N-propyl Amide (CL _O 10-CL _{nPrA} 5-OH) Chemical Shift Assignments, ¹³ C and ¹ H NMR Spectra, SEC, and MALDI-TOF.	60
Appendix C Spectral Data Associated with End Group Modifications of γ -Substituted ϵ -Caprolactone Oligomers.....	64
Appendix C.1 1,3-Butenol and Acrylate- Capped Oligo- ϵ -Caprolactone (CL _O 15) Proton Chemical Shift Assignments & NMR Spectrum.....	64
Appendix C.2 1,3-Butenol and Acrylate- Capped Oligo- ϵ -Caprolactone- <i>block</i> - ϵ - Caprolactone- γ -Isopropyl Amide (CL _O 10-CL _{iPrA} 5) Proton Chemical Shift Assignments, ¹ H NMR Spectrum, and MALDI-TOF Spectrum.	66
Appendix D Spectral Data Associated with Polymerization of γ -Substituted ϵ - Caprolactone Oligomers.....	68
Appendix D.1 ADMET-Synthesized Poly- ϵ -caprolactone (p[CL _O 15]) Proton Chemical Shift Assignments, ¹ H NMR Spectrum, and MALDI-TOF Spectrum.	68
Appendix D.2 ADMET-Synthesized Poly-[Oligo-(ϵ -Caprolactone)- <i>block</i> -(ϵ - Caprolactone- γ -Isopropyl Amide)] (p[CL _O 10-CL _{iPrA} 5]) Proton Chemical Shift Assignments, ¹ H NMR Spectrum, and MALDI-TOF Spectrum.	71
Appendix E Spectral Data Associated with Syntheses of γ -Ester-Substituted ϵ - Caprolactone Oligomers and Al-Salen Catalyst.....	74

Appendix E.1 1,3-Butenol and 2-Oxotetrahydrofuran Capped Oligo-(ϵ-Caprolactone)- <i>block</i>-(ϵ-Caprolactone-γ-Ethyl Ester) (CL₀₈-CL_{COOE_n)}	
NMR Spectra, SEC, and MALDI-TOF	75
Appendix E.2 Aluminum Tri-1,3-Butenoxide Catalyzed ϵ-Caprolactone-γ-Ethyl Ester Oligomer	
Chemical Shift Assignments and NMR Spectrum	78
Appendix E.3 N,N'-bis(3,5-di-tert-butylsalicylidene)-1,2-cyclohexane-diamino aluminum isopropoxide (Al-Salen) Catalyzed ϵ-Caprolactone Oligomer	
Chemical Shift Assignments and NMR Spectrum	80
Appendix E.4 N,N'-bis(3,5-di-tert-butylsalicylidene)-1,2-cyclohexane-diamino aluminum isopropoxide (Al-Salen) Catalyzed ϵ-Caprolactone-γ-Ethyl Ester Oligomer	
Chemical Shift Assignments and NMR Spectrum	82
Bibliography	84

List of Tables

Table 1. Comparison of micro-block copolymerization strategies	3
Table 2. Oligomer block ratios and molecular weights as compared to reactant ratios	16
Table 3. Polymer molecular weight data as compared to targeted molecular weights.	16
Table 4. Ratios of monomers used for CL_O , CL_{nPrA} , and CL_{iPrA} micro-block copolymerizations	35
Table 5. 1H NMR Shift Assignment for 4-Oxocyclohexane-1-Carboxylic Acid.....	43
Table 6. 1H NMR Shift Assignment for N-Isopropyl 4-Oxocyclohexane-1-Carboxamide...	45
Table 7. 1H NMR Shift Assignment for 4-Oxo-N-Propylcyclohexane-1-Carboxamide.	47
Table 8. 1H NMR Shift Assignment for N-Isopropyl-7-Oxooxepane-4-Carboxamide (CL_{iPrA}).	49
Table 9. 1H NMR Shift Assignment for 7-Oxo-N-Propyloxepane-4-Carboxamide (CL_{nPrA}).	51
Table 10. 1H NMR Shift Assignment for Ethyl 7-Oxooxepane-4-Carboxylate (CL_{COOEt})...	53
Table 11. 1H NMR Shift Assignment for 1,3-Butenol- and Hydroxyl- Capped Oligo- ϵ -Caprolactone (CL_{O15-OH}).....	55
Table 12. 1H and ^{13}C NMR Shift Assignments for 1,3-Butenol- and Hydroxyl- Capped Oligo- ϵ -Caprolactone- <i>block</i> - ϵ -Caprolactone- γ -Isopropyl Amide ($CL_{O10-CL_{iPrA}5-OH}$)....	57
Table 13. 1H and ^{13}C NMR Shift Assignments for 1,3-Butenol- and Hydroxyl- Capped Oligo- ϵ -Caprolactone- <i>block</i> - ϵ -Caprolactone- γ -N-propyl Amide ($CL_{O10-CL_{nPrA}5-OH}$). ...	60
Table 14. 1H NMR Shift Assignments for 1,3-Butenol- and Acrylate- Capped Oligo- ϵ -Caprolactone (CL_{O15}).	64

Table 15. ¹H NMR Shift Assignments for 1,3-Butenol- and Acrylate- Capped Oligo-ϵ-Caprolactone-<i>block</i>-ϵ-Caprolactone-γ-Isopropyl Amide (CL_O10-CL_{iPrA}5).....	66
Table 16. ¹H NMR Shift Assignments for ADMET-Synthesized Poly-ϵ-caprolactone (p[CL_O15]).	68
Table 17. ¹H NMR Shift Assignments for ADMET-Synthesized Poly-[Oligo-(ϵ-Caprolactone)-<i>block</i>-(ϵ-Caprolactone-γ-Isopropyl Amide)] (p[CL_O10-CL_{iPrA}5]). ...	71
Table 18. ¹H and ¹³C NMR Shift Assignments for 1,3-Butenol and 2-Oxotetrahydrofuran Capped Oligo-(ϵ-Caprolactone)-<i>block</i>-(ϵ-Caprolactone-γ-Ethyl Ester) (CL_O8-CL_{COOEt}).....	75
Table 19. ¹H NMR Shift Assignment for Aluminum Tri-1,3-Butenoxide Catalyzed ϵ-Caprolactone-γ-Ethyl Ester Oligomer.	78
Table 20. ¹H NMR Shift Assignment for N,N'-bis(3,5-di-tert-butylsalicylidene)-1,2-cyclohexane-diamino aluminum isopropoxide (Al-Salen) Catalyzed ϵ-Caprolactone Oligomer.	80
Table 21. ¹H NMR Shift Assignment for N,N'-bis(3,5-di-tert-butylsalicylidene)-1,2-cyclohexane-diamino aluminum isopropoxide (Al-Salen) Catalyzed ϵ-Caprolactone-γ-Ethyl Ester Oligomer.....	82

List of Figures

Figure 1. Previously reported strategies towards micro-block copolymerization.	2
Figure 2. Possible product outcomes of substituted cyclohexanone oxidation.....	5
Figure 3. Prominent transesterification mechanisms evident in polymerization of γ -ester substituted ϵ -caprolactone monomers.....	7
Figure 4. Synthesis of γ -substituted ϵ -caprolactone monomer units.....	11
Figure 5. The synthetic route followed to prepare the micro-block copolymer.....	12
Figure 6. ^1H NMR spectra of the olefin region of heterotelechelic $\text{CL}_{\text{O}15}$ bearing a terminal olefin and a terminal acrylate under ADMET conditions.	13
Figure 7. A segment of the MALDI-TOF spectrum of the di-micro-block co-oligomer of CLO and CLiPrA ,	15
Figure 8. SEC of $\text{CL}_{\text{O}15}$ before and after undergoing ADMET polymerization.....	16
Figure 9. Previously reported active structures of Al-salen catalysts in the polymerization of cyclic esters.	19
Figure 10. Size Exclusion Chromatogram (SEC) of di-block oligomer containing CLO and CL_{COOEt}	20
Figure 11. Experimental MALDI-TOF spectrum of $\text{CLO}8\text{-CL}_{\text{COOEt}}4$ (lines) overlaid with model mass distribution of $\text{CLO}8\text{-CL}_{\text{COOEt}}4$ (points).....	21
Figure 12. The mechanism of chain-end annulation in γ -ester-substituted ϵ -caprolactone moieties, labeled with component molecular weights observable by MALDI-TOF.	22
Figure 13. The mechanism of rearrangement as enabled by the radical cationic character induced in MALDI-TOF, labeled with observable component molecular weights. .	23

Figure 14. ^1H NMR spectra of CL_{COOEt} oligomerization over the course of 72 hours, with diagnostic peaks labeled.	24
Figure 15. Concentration of monomer, cyclic, and linear components measured over time relative to initial CL_{COOEt} concentration.	25
Figure 16. ^1H NMR spectra of CL_{COOEt} oligomerization at 15 minute and 72 hour timepoints.	27
Figure 17. Synthetic Route for Diblock Macromonomer Synthesis.....	34
Figure 18. Synthetic Route for end group modification of γ -substituted ϵ -caprolactone oligomers.....	35
Figure 19. Synthetic route for polymerization of macromonomers as applied to $\text{p}[\text{CL}_{\text{O15}}]$	36
Figure 20. ^1H NMR Spectrum of 4-oxocyclohexane-1-carboxylic acid. 400 MHz, CDCl_3 ..	44
Figure 21. ^1H NMR Spectrum of N-Isopropyl 4-Oxocyclohexane-1-Carboxamide. 400 MHz, CDCl_3	46
Figure 22. ^1H NMR Spectrum of N-Isopropyl 4-Oxocyclohexane-1-Carboxamide. 400 MHz, CDCl_3	48
Figure 23. ^1H NMR Spectrum of N-Isopropyl-7-Oxooxepane-4-Carboxamide (CL_{iPrA}). 400 MHz, CDCl_3	50
Figure 24. ^1H NMR Spectrum of 7-Oxo-N-Propyloxepane-4-Carboxamide (CL_{nPrA}). 400 MHz, CDCl_3	52
Figure 25. ^1H NMR Spectrum of Ethyl 7-Oxooxepane-4-Carboxylate (CL_{COOEt}). 400 MHz, CDCl_3	54

Figure 26. ¹ H NMR Spectrum of 1,3-Butenol- and Hydroxyl- Capped Oligo-ε-Caprolactone (CL _O 15-OH). 400 MHz, CDCl ₃	56
Figure 27. ¹ H NMR Spectrum of 1,3-Butenol- and Hydroxyl- Capped Oligo-ε-Caprolactone- <i>block</i> -ε-Caprolactone-γ-Isopropyl Amide (CL _O 10-CL _{iPrA} 5-OH). 400 MHz, CDCl ₃ . 58	58
Figure 28. ¹³ C NMR Spectrum of 1,3-Butenol- and Hydroxyl- Capped Oligo-ε-Caprolactone- <i>block</i> -ε-Caprolactone-γ-Isopropyl Amide (CL _O 10-CL _{iPrA} 5-OH). 500 MHz, CDCl ₃ . 59	59
Figure 29. SEC Chromatogram of 1,3-Butenol- and Hydroxyl- Capped Oligo-ε-Caprolactone- <i>block</i> -ε-Caprolactone-γ-Isopropyl Amide (CL _O 10-CL _{iPrA} 5-OH).	59
Figure 30. ¹ H NMR Spectrum of 1,3-Butenol- and Hydroxyl- Capped Oligo-ε-Caprolactone- <i>block</i> -ε-Caprolactone-γ-N-propyl Amide (CL _O 10-CL _{nPrA} 5-OH). 400 MHz, CDCl ₃ . 61	61
Figure 31. ¹³ C NMR Spectrum of 1,3-Butenol- and Hydroxyl- Capped Oligo-ε-Caprolactone- <i>block</i> -ε-Caprolactone-γ-N-propyl Amide (CL _O 10-CL _{nPrA} 5-OH). 500 MHz, CDCl ₃ . 62	62
Figure 32. SEC Chromatogram of CL _O 10-CL _{nPrA} 5-OH taken in THF, calibrated to polystyrene standards.....	62
Figure 33. MALDI-TOF spectra of CL _O 10-CL _{nPrA} 5-OH, masses shown with Na ⁺ adducts.63	63
Figure 34. ¹ H NMR Spectrum of 1,3-Butenol- and Acrylate- Capped Oligo-ε-Caprolactone (CL _O 15) 400 MHz, CDCl ₃	65
Figure 35. ¹ H NMR Spectrum of 1,3-Butenol- and Acrylate- Capped Oligo-ε-Caprolactone- <i>block</i> -ε-Caprolactone-γ-Isopropyl Amide (CL _O 10-CL _{iPrA} 5). 400 MHz, CDCl ₃	67
Figure 36. MALDI- TOF Spectrum of 1,3-Butenol- and Acrylate- Capped Oligo-ε-Caprolactone- <i>block</i> -ε-Caprolactone-γ-Isopropyl Amide (CL _O 10-CL _{iPrA} 5).....	67
Figure 37. ¹ H NMR Spectrum of ADMET-Synthesized Poly-ε-caprolactone (p[CL _O 15]). 400 MHz, CDCl ₃	69

Figure 38. SEC chromatogram of ADMET-Synthesized Poly- ϵ -caprolactone (p[CL_o15]). 69

**Figure 39. MALDI-TOF Spectra of ADMET-Synthesized Poly- ϵ -caprolactone (p[CL_o15]).
..... 70**

**Figure 40. ¹H NMR Spectrum of ADMET-Synthesized Poly-[Oligo-(ϵ -Caprolactone)-*block*-
(ϵ -Caprolactone- γ -Isopropyl Amide)] (p[CL_o10-CL_{iPrA}5]). 400 MHz, CDCl₃..... 72**

**Figure 41. SEC Chromatogram of ADMET-Synthesized Poly-[Oligo-(ϵ -Caprolactone)-
block-(ϵ -Caprolactone- γ -Isopropyl Amide)] (p[CL_o10-CL_{iPrA}5]). 73**

**Figure 42. MALDI-TOF Spectra of ADMET-Synthesized Poly-[Oligo-(ϵ -Caprolactone)-
block-(ϵ -Caprolactone- γ -Isopropyl Amide)] (p[CL_o10-CL_{iPrA}5]). 73**

**Figure 43. ¹H NMR Spectrum of 1,3-Butenol and 2-Oxotetrahydrofuran Capped Oligo-(ϵ -
Caprolactone)-*block*-(ϵ -Caprolactone- γ -Ethyl Ester) (CL_o8-CL_{COEt}n). 400 MHz,
CDCl₃. 76**

**Figure 44. ¹³C NMR Spectrum of 1,3-Butenol and 2-Oxotetrahydrofuran Capped Oligo-(ϵ -
Caprolactone)-*block*-(ϵ -Caprolactone- γ -Ethyl Ester) (CL_o8-CL_{COEt}n). 500 MHz,
CDCl₃. 76**

**Figure 45. SEC of 1,3-Butenol and 2-Oxotetrahydrofuran Capped Oligo-(ϵ -Caprolactone)-
block-(ϵ -Caprolactone- γ -Ethyl Ester) (CL_o8-CL_{COEt}n). 77**

**Figure 46. MALDI-TOF Spectra of 1,3-Butenol and 2-Oxotetrahydrofuran Capped Oligo-
(ϵ -Caprolactone)-*block*-(ϵ -Caprolactone- γ -Ethyl Ester) (CL_o8-CL_{COEt}n). 77**

**Figure 47. ¹H NMR Spectrum of Aluminum Tri-1,3-Butenoxide Catalyzed ϵ -Caprolactone-
 γ -Ethyl Ester Oligomer. 400 MHz, CDCl₃. 79**

Figure 48. ^1H NMR Spectrum of $\text{N,N}'$-bis(3,5-di-tert-butylsalicylidene)-1,2-cyclohexane-diamino aluminum isopropoxide (Al-Salen) Catalyzed ϵ-Caprolactone Oligomer after 72 h. 400 MHz, CDCl_3.....	81
Figure 49. ^1H NMR Spectrum of $\text{N,N}'$-bis(3,5-di-tert-butylsalicylidene)-1,2-cyclohexane-diamino aluminum isopropoxide (Al-Salen) Catalyzed ϵ-Caprolactone-γ-Ethyl Ester Oligomer after 72 h. 400 MHz, CDCl_3.....	83

1.0 Introduction

1.1 Micro-Block Copolymer Utility

The natural world boasts an abundance of polymeric materials—spider silk, mussel adhesives, insect wings—with wide-ranging combinations of desirable properties—strength and flexibility, adhesion and water resistance, tunable moduli and low densities.^{1,2,3,4} Many members of this unique class of materials consist of tandem repeat proteins, composed of mid-sized segments of amino acid chains long enough to impart combinations of the characteristic bulk properties of each repeat unit. Minimal microphase segregation, in contrast with more pronounced effects seen with typical block copolymers, is observed only when repeat unit block lengths are sufficiently short.⁵ Synthetically, materials occupying this approximate area, containing short blocks of repeat units between 3-15 repeat units, are known as microblock copolymers. This sequencing capability, easily achieved *in vivo* by ribosomes, is difficult to access at the benchtop or in an industrial setting, as shown by the singular mass-produced example of this motif being polyurethanes.

Though a singular category of commodity polymer, polyurethane materials account for 6% of total polymer production as of 2019 and are seen as foams, thermoplastics, coatings, adhesives, and fabric fibers amongst other applications.⁶ Such a range of functionality is imparted by relatively simple functional groups; polyurethanes are synthesized as microblock-like copolymers via step growth condensation reactions between phenyl diisocyanate ‘hard blocks’ and alkyl diol chain extenders or ‘soft blocks’ to create urethane linkages. While this approach is industrially

facile, it limits both the scope of accessible functional groups and the lower bound of dispersity due to the step-growth methodology.

1.2 Previous Syntheses of Microblock Copolymers

On smaller scales, microblock copolymerizations involving more complex functional groups have been exhibited, though these typically require iterative growth sequences, extensive sequential additions to living systems, or template design (Figure 1).⁷⁻¹²

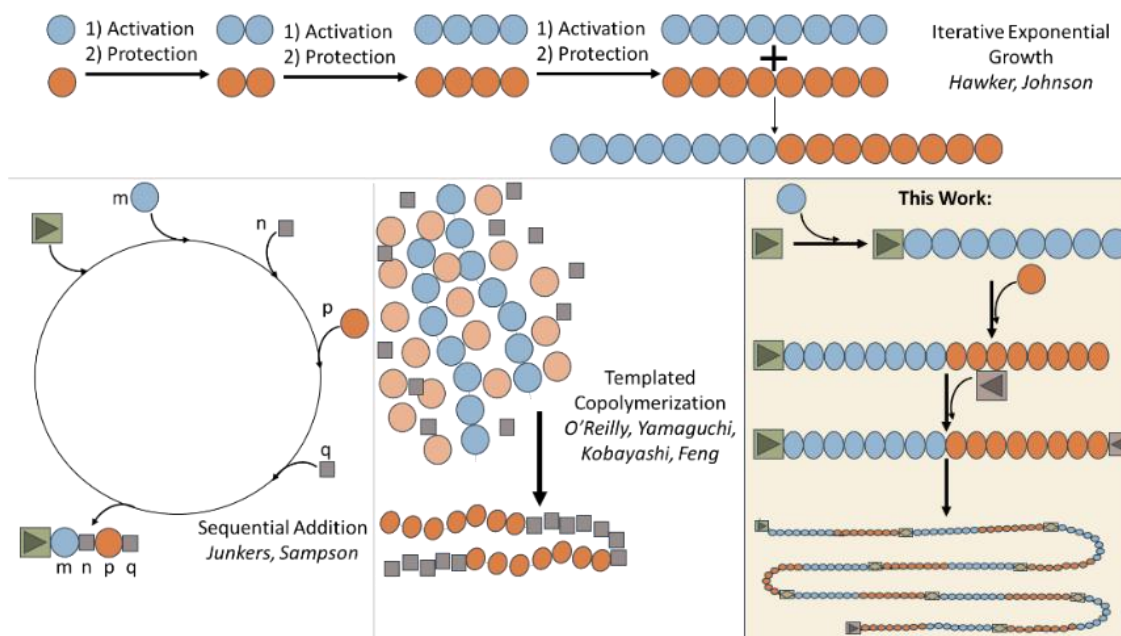


Figure 1. Previously reported strategies towards micro-block copolymerization.

Each previously reported method for microblock copolymer synthesis—iterative growth, sequential addition, and templated copolymerization—balances a combination of synthetic material qualities (Table 1). While iterative growth is capable of producing exponentially high molecular weight polymers with monodisperse lengths, the preparation requires multiple steps to

achieve each increase in chain length and is often not generalizable beyond specific monomer types. Sequential addition approaches are typically one-pot procedures, making them much less synthetically demanding than iterative growth methods, but this results in a wider molecular weight distribution and necessitates numerous additions to access high molecular weights. In many cases, these one-pot strategies are also highly tailored to certain monomer varieties that require separate preparation. Templated systems, though attractive in terms of producing materials like those found in nature, are currently limited to biologically based systems which can express only sequences of nucleotides, or charged ionomers which assemble into extended systems based on electrostatic interactions.^{13, 14}

Table 1. Comparison of micro-block copolymerization strategies

	Block Length Uniformity	Preparation	Polymer MW	Monomer Functionality
Iterative Growth	High	Intensive	Low-High	Moderate
Sequential Addition	Moderate	Moderate	Moderate	Moderate
Templated Copolymerization	Low	Moderate-Intensive	Moderate	Moderate
<i>This Work</i>	<i>Moderate</i>	<i>Moderate</i>	<i>Moderate-High</i>	<i>High</i>

We attempt here to solve this issue of synthetic difficulty by coupling a short chain oligomerization with a single sequential addition of a second repeat unit to create a di-microblock oligomer. In this system, both end groups can be defined as different olefin types, resulting in metathesis between end groups occurring in a defined head-to-tail ratio.¹⁵ This method allows for full spectroscopic characterization of the oligomeric-scale macromonomers prior to polymerization, enabling production of medium to high molecular weight polymers characterized with similar rigor as oligomers.

1.3 Targeted Characteristics of Micro-Block Components Used in This Work

To best examine minute differences between block lengths, repeat units with stark property contrasts are necessary. In this work, blocks with differing hydrogen bonding capabilities are used— ϵ -caprolactone, a hydrogen bond acceptor; γ -substituted ϵ -caprolactone bearing an ester functional group, a pendant hydrogen bond acceptor; and γ -substituted ϵ -caprolactone with a pendant amide, a hydrogen bond donor. Poly- ϵ -caprolactone is well-characterized in the literature and is known to be a flexible material with a low glass transition temperature.^{16, 17} The γ -substituted ϵ -caprolactone moieties are less common but have been previously synthesized and oligomerized, and polymers such as poly-NIPAM which have pendant amide motifs tend to display sensitive thermal and solution-phase properties along with higher glass transition temperatures due to their hydrogen bonding capabilities.^{16, 18, 19} Functionalization at the γ -position further enables modularity in terms of substitution, as the carboxylic acid produced along the synthetic route can hold any variety of amine-functionalized pendant via condensation.

1.4 Polymers of Substituted ϵ -Caprolactones

Of readily available ϵ -caprolactone monomers, those with substitutions in the α - and γ -positions are most common. The Baeyer-Villiger reaction is frequently used to produce both unsubstituted and substituted ϵ -caprolactone monomers from cyclohexanone derivatives.²⁰ Due to this strategy, the cyclohexanone derivatives substituted in the 2- and 4- positions produce α - (or ϵ - , depending on substituent identity) and γ - substituted products, respectively, with high regioselectivity; as shown in Figure 2, cyclohexanone derivatives substituted in the 3- position

have the potential to produce β - or δ - substituted ϵ -caprolactone moieties with similar likelihoods. Thus, the use of mixtures or combinations of the α - and ϵ -, and of the β - and δ - varieties for polymerization have been investigated for trends in chain growth kinetics and thermal properties of the bulk polymeric material.²¹⁻²⁴ Through these kinetic studies, it has been found that substitutions in the α - and ϵ - positions slow the rate of polymerization, leaving substitution in the γ -position the ideal choice for a monomer that can be prepared in high yield and is swiftly polymerizable while bearing complex or sterically demanding substituents. To access a functionalized α -position, it is possible to polymerize the α -Cl derivative of ϵ -caprolactone and subject the product to post-polymerization modifications; however, this comes with the drawbacks typical of post-polymerization modifications such as the necessity for a polymeric backbone that is tolerant to reaction conditions and difficulties in achieving and confirming that complete conversion has occurred.²⁵

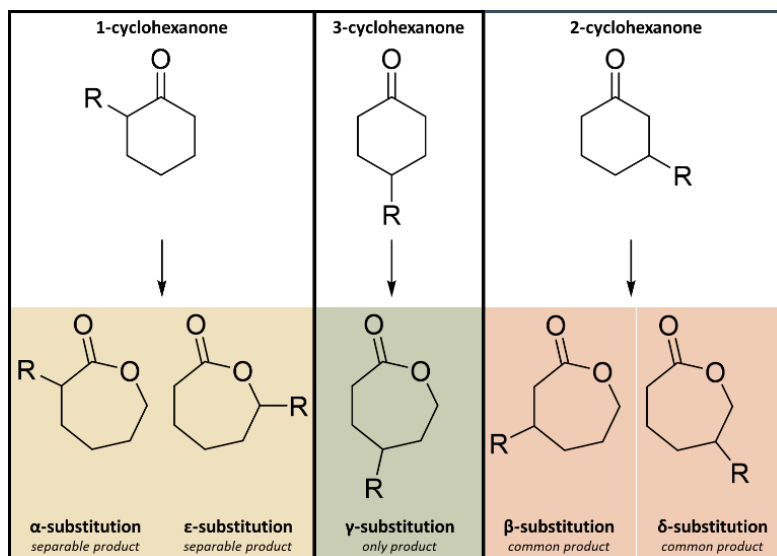


Figure 2. Possible product outcomes of substituted cyclohexanone oxidation.

As a material modifier, γ -substitutions on ϵ -caprolactone monomers have been used to impart a variety of functionality upon a polymeric backbone widely regarded for its tunable mechanical properties, biocompatibility, and degradable nature.²⁶⁻²⁸ Even a small incorporation of

functionalized ϵ -caprolactone moieties can impart effects on a range of properties, including modulus,²⁴ thermal behavior,²⁹ self-assembly,³⁰ and degradation rate,^{31, 32} amongst others. After years of usage in medical devices and implants,^{33, 34} polycaprolactone and its derivatives have also begun to be used for drug delivery applications.³⁵ Some delivery applications involve physical encapsulation of payload into copolymer hydrogels or micelles,³⁶⁻³⁸ whilst others use covalently-bound polycaprolactone-drug, -inhibitor, or -tag conjugates that can be triggered to release these payloads by environmental pH conditions.^{39, 40} Both of these methods can take advantage of selective ϵ -caprolactone functionalization, whether in using modifications to alter morphologies or by incorporating a pH trigger for molecular release.

1.5 Modes of γ -Carbonyl Substituted ϵ -Caprolactone Reactivity

At its core, the concept of ring-opening polymerization (ROP) applied to γ -carbonyl-substituted ϵ -caprolactones appears straightforward; previous research has led to methods of ϵ -caprolactone polymerization with near-nonexistent transesterification, implying a significant energetic preference for the ring-opening reaction that propagates the chain as opposed to a condensation that would instead cap the chain, for which both routes can be seen in Figure 3.⁴¹ Syntheses of γ -ester and γ -amide substituted ϵ -caprolactone derivatives have been reported, though product yields and molecular weights are often far different than the corresponding calculated values unless copolymerized with unsubstituted ϵ -caprolactone.^{18, 42, 43} Further in-depth examination of these results revealed that the rate of annulation is comparable to the rate of chain propagation to a great enough degree as to reliably terminate active chains prior to the majority of monomer being consumed.⁴⁴ The annulation described here involves the active chain end acting

as a nucleophile towards the γ -position carbonyl and replacing the corresponding pendant amine or alcohol, a condensation that can be observed by ^{13}C NMR and tracked by SEC.⁴⁵

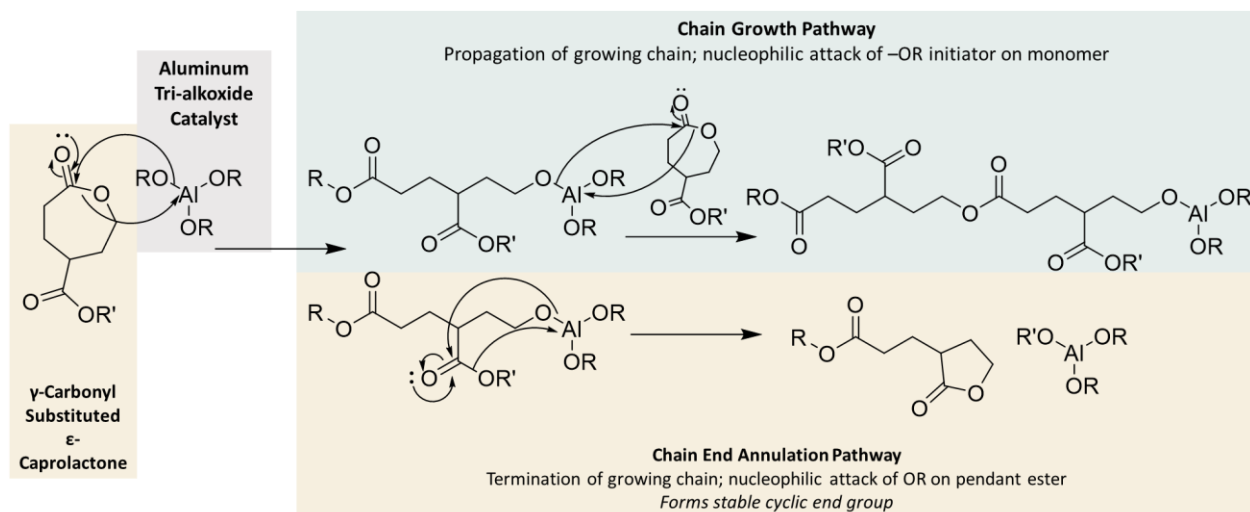


Figure 3. Prominent transesterification mechanisms evident in polymerization of γ -ester substituted ϵ -caprolactone monomers.

1.6 Unique Behavioral Regime of Micro-Block Copolymers

In the context of a bulk material behavior of a multiblock copolymer scaffold, it is well known that changing block size can have considerable effects on the morphology and behaviors of the resulting macromolecules.⁴⁶ At the micro-block scale, however, exploration of these effects are currently in a nascent stage in part due to previously discussed synthetic complexity of the regime. Recently, it was shown that even small changes on block size cause considerable effects upon interfacial rheology.⁴⁷ In an investigation of the confluence between multiblock and micro-block copolymer character, researchers found that properties such as chain flexibility and affinity for rare earth metals were controlled by the ‘patchiness,’ or functional group density within a domain—a factor that is correlated with block size down to the micro-block scale.⁴⁸

1.7 Use of ADMET (Acyclic Diene Metathesis) for Polymerization of Macromonomers

Within this work, instrumental to the head-to-tail incorporation of macromonomeric micro-block segments is the use of ADMET as a robust strategy for thermodynamically preferring addition to the olefin unit present at the head of the oligomer to that present at the oligomer's tail, a technique that is further analyzed and its rationale discussed in chapter 2. ADMET is well known as a polymerization technique with high functional group tolerance imparted by the use of Grubb's metathesis catalyst and has been previously employed for the polymerization of macromonomeric, intricately functionalized ester-backboned units.^{49, 50} Most commonly, symmetric telechelic monomers are used for ADMET polymerization to give well-defined polymer sequence, as metathesis will occur with statistical probability when only type-1 olefins are used, though the use of asymmetric monomers has been explored for ADMET in limited cases, often involving a type-1 olefin such as a terminal olefin and a type-2 olefin such as an acrylate.⁵¹⁻⁵³

1.8 Thesis Contents

In the following chapter, a generalizable strategy towards regular micro-block copolymers is described and employed to synthesize a micro-block copolymer of unsubstituted ϵ -caprolactone and ϵ -caprolactone substituted in the γ -position with an amide group. In order to explore the effects of hydrogen bonding donating micro-block size on bulk materials properties such as surface hydrophilicity and tensile strength, a similar monomeric unit lacking hydrogen bond donating capabilities was needed to provide a set of analogous baseline testing values. To this end, ϵ -caprolactone monomeric units substituted in the γ -position with an ester group were synthesized

and subjected to polymerization conditions. In chapter three of this work, the characterization of the resulting cyclic product is discussed, followed by a series of experiments using chiral salen ligands coordinated to an aluminum metal center to modulate the propagation and annulation kinetics of these ester-substituted ϵ -caprolactone monomers. The penultimate chapter details the experimental procedures and syntheses executed to obtain the data discussed in the preceding chapters, after which the final chapter puts forth a selection of alternative routes and strategies that are suitable for further investigation in pursuit of reliable installation of γ -substituted ϵ -caprolactone blocks in micro- and multi- block copolymers.

2.0 Synthesis of Multiblock ϵ -Caprolactone Copolymers Bearing Pendant Amides

In this study, a novel approach towards micro-block copolymerization for polyester synthesis is explored. Using γ -substituted ϵ -caprolactone moieties bearing ester and amide pendant groups, short oligomeric chains (5-15 repeat units) are initiated by an olefin alkoxide, extended by addition of a second γ -substituted ϵ -caprolactone species, capped with a complementary olefin end group, and polymerized by ADMET. The oligomers and resulting polymer are investigated using NMR, MALDI-TOF, and SEC techniques, demonstrating that the utility of this approach is highly monomer-dependent. It was found that the lengths of **CL_nPrA** (ϵ -caprolactone bearing an n-propyl amide at the γ -position) segments are solubility-limited; and longer **CL_iPrA** (ϵ -caprolactone bearing an isopropyl amide at the γ -position) chains can be formed in greater quantity, though with low efficiency due to a loss of end-group fidelity.

2.1 Results and Discussion

To produce these microblock copolymers, the γ -substituted monomer units were first synthesized starting from 4-keto cyclohexyl moieties oxidized via a Baeyer-Villiger reaction (Figure 4). This procedure has been adapted from the scheme used by L. Wen et al and is further described in Chapter 4.¹⁸

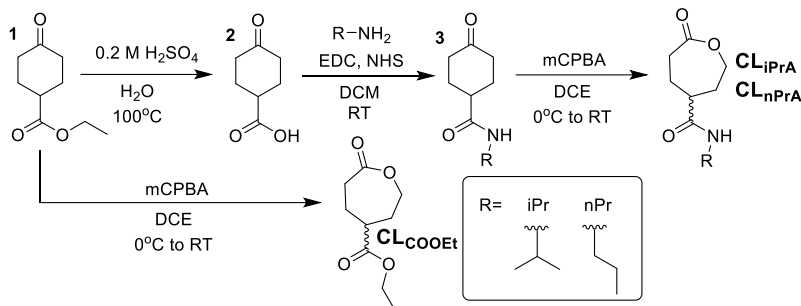


Figure 4. Synthesis of γ -substituted ϵ -caprolactone monomer units.

Ethyl-4-oxocyclohexane-1-carboxylate (**1**) was obtained at minimal expense (\$5/g) and was either immediately oxidized to form CL_{COOEt} (discussed further in Chapter 3) or acidified to form the corresponding carboxylic acid (**2**). This acid was then coupled with an amine-functionalized substituent to form the amide-bearing cyclohexanone (**3**), which was subsequently oxidized to the γ -substituted ϵ -caprolactone monomer unit ($\text{CL}_{i\text{PrA}}$, $\text{CL}_{n\text{PrA}}$). In this study, isopropyl and n-propyl amides were interrogated ($\text{CL}_{i\text{PrA}}$ and $\text{CL}_{n\text{PrA}}$, respectively); however, the versatility of the synthetic route allows for facile attachment of any oxidatively stable amine functionalized unit.

Substituted ϵ -caprolactone derivatives and well-analyzed ADMET methodology in hand, heterotelechelic diblock oligomers were formed by anionic ring opening polymerization (AROP) as precursors to the microblock copolymer produced via ADMET (Figure 5). The aluminum-catalyzed oligomerization in toluene, further discussed in chapter 4, is executed in a manner similar to that described by Dubois et al as to favor living chain growth character.⁴¹

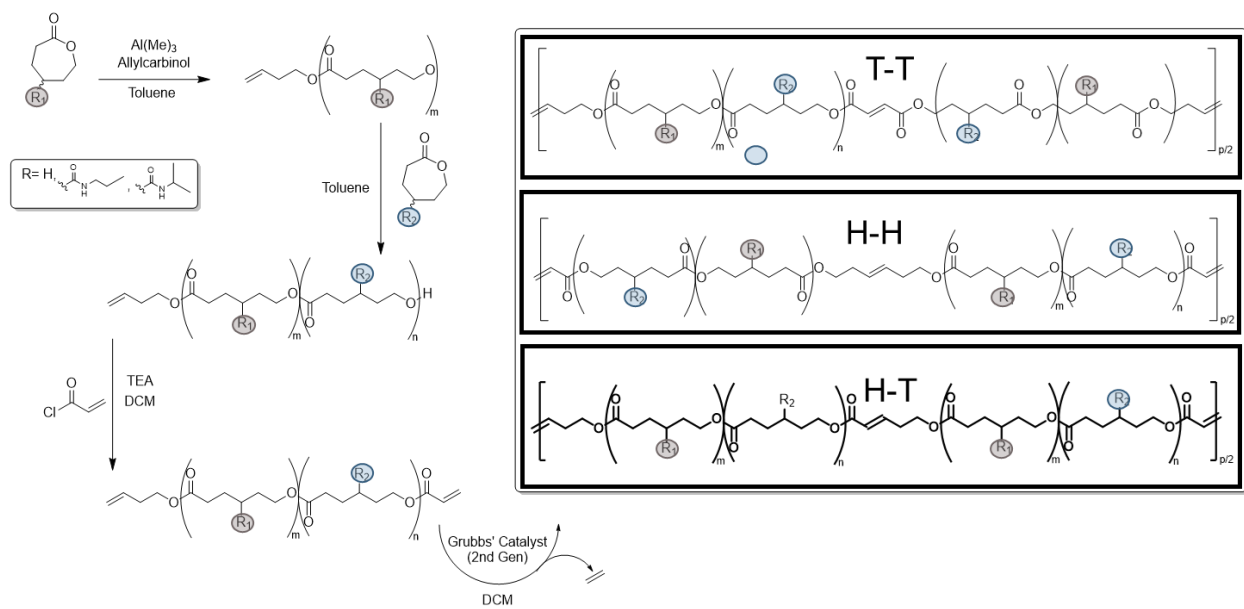


Figure 5. The synthetic route followed to prepare the micro-block copolymer.

(T-T) The Tail-to-Tail product, not formed. (H-H) The Head-to-Head product, reversibly formed. (H-T) The Head-to-Tail product, majorly formed.

Prior to oligomerization, it was vital to confirm that the asymmetric ADMET polymerization did indeed produce a robust and reliable head-to-tail product distribution. For this reason, unsubstituted ϵ -caprolactone was oligomerized and functionalized using the strategies outlined for the substituted analogs, the resulting heterotelechelic oligomer subsequently subjected to ADMET conditions to observe the progression of metathesis preferences. Full conversion of the capped species was confirmed by ^1H NMR observation of a 1:1 ratio of acrylate protons to terminal olefin protons, ensuring stoichiometric equivalence between the electron-deficient acrylate type-2 olefin and the electron-rich, sterically unhindered type-1 olefin end groups. Using a second-generation Grubbs' catalyst to subject the oligomers to metathesis conditions, it was observed that the head-to-head product (**H-H**) and head-to-tail (**H-T**) products first formed in approximately equivalent amounts at room temperature (Figure 6). Once the temperature of the system was raised to 40°C , the reaction rate increased and the ratio between **H-T** and **H-H** product shifted from 1:1

to 3:1 with no **T-T** product. This outcome is characteristic of type 1 and type 2 olefin cross metathesis; homodimerization between type 1 olefins is fast but the homodimers are consumable, while homodimerization between type 2 olefins is exceedingly slow.¹⁵ By contrast, cross metathesis between a type 1 and a type 2 olefin results in internal olefin products that have a high energetic barrier to undergoing further metathesis, generating selectivity in product distribution.

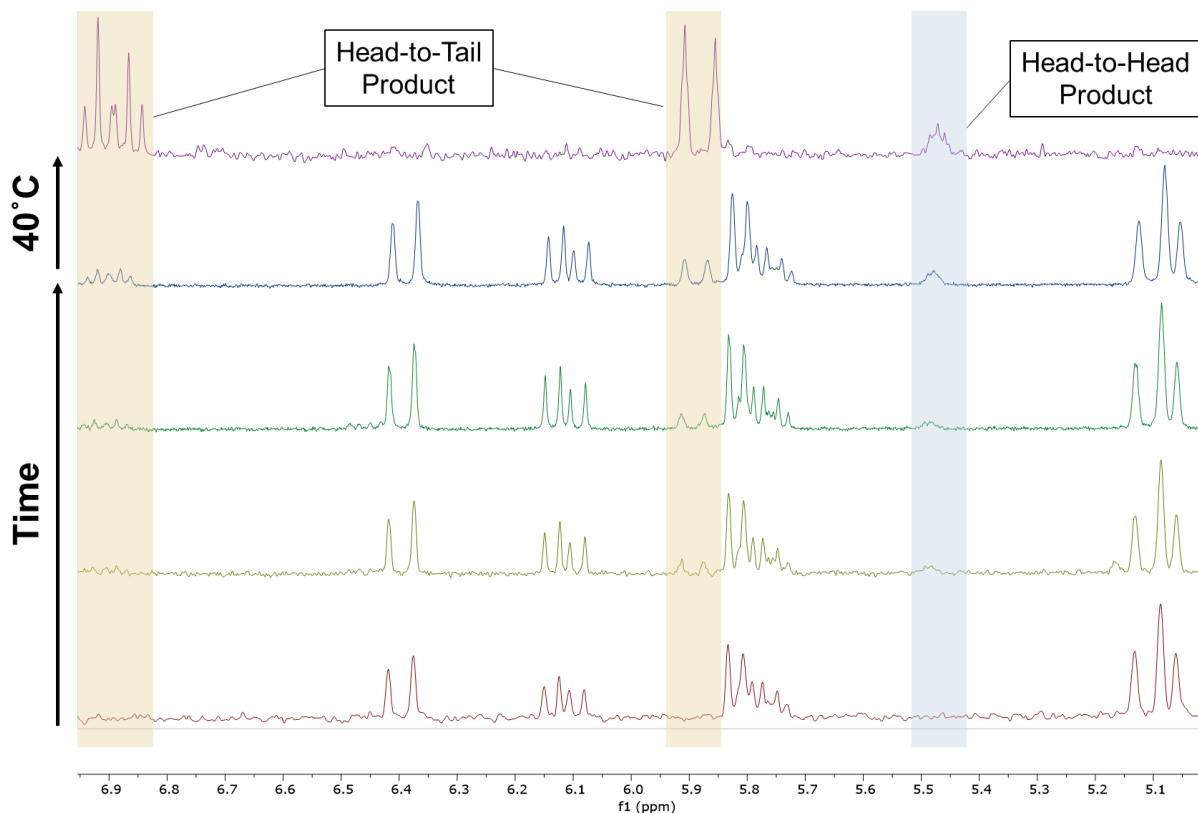


Figure 6. ^1H NMR spectra of the olefin region of heterotelechelic **CLo15** bearing a terminal olefin and a terminal acrylate under ADMET conditions.

The oligomerization of the γ -substituted monomers was initiated in a $\text{N}_{2(g)}$ atmosphere with allylcarbinol and catalyzed by trimethyl aluminum, ring-opening the first ϵ -caprolactone species and defining the initial end group to be a terminal olefin. When the first monomer had fully reacted, a subsequent substituted monomer was added and similarly allowed to react until fully consumed. For unsubstituted caprolactone (**CLo**), this conversion was evidenced by the disappearance of the ^1H NMR peak for the proton in the ϵ position at 4.12 ppm in CDCl_3 , and for

the amide-substituted lactones such conversion was shown by the disappearance of the multiplet at 2.9 ppm. As **CL_O** has a very exothermic enthalpy of ring opening, this addition was executed at -78°C. Substitution at the gamma position, by changing the preferred conformation of the ring structure, decreases the magnitude of the ring opening enthalpy and thus required reactions of the γ -substituted ϵ -caprolactone species to be performed at higher temperatures (100°C). In these experiments, block lengths ranging from 5-10 repeat units were targeted in order to achieve varied chain lengths within the microblock regime. Unfortunately, oligomerization of **CL_{nPrA}** did not progress beyond two repeat units due to insolubility of the component as a result of high H-bonding propensity permitted by the alkyl chain's minimal steric hindrance. For this reason, investigation of the diblock oligomeric system and corresponding polymers was conducted mainly using **CL_O** and **CL_{iPrA}** repeat units. Degrees of polymerization were determined via ¹HNMR, available in the supporting information, and calculated for caprolactone based on the methylene peak at 4.06 ppm, for **CL_{iPrA}** based on the pendant methyl doublet at 1.12 ppm, and for **CL_{nPrA}** based on its pendant's methyl triplet at 0.9 ppm.

The oligomers were further analyzed by MALDI-TOF spectrometry. For the **CL_O** homooligomer, a difference of 114 amu was visible between peaks, coinciding with the molar mass of a single **CL_O** repeat unit. In the **CL_O-CL_{iPrA}** system, the MALDI-TOF spectra depict the ensemble of peaks that would be present for the Na⁺-ionized desired diblock oligomer (Figure 7). Each peak seen here is the summation of a 23 amu Na⁺ ion, a 71.05 amu alkoxy olefin end group, a 56.03 amu acrylate end group, 'n' **CL_O** units each having a mass of 114.07 amu, and 'm' **CL_{iPrA}** units each having a mass of 199.12 amu. Series are present for various numbers of **CL_O** units in the block present adjacent to the **CL_{iPrA}** segment containing repeat unit values centered around an average of five, though this is somewhat visually distorted by the decreased ionization potential

for higher molecular weight species. Following complete monomer consumption, the alkoxy chain was capped with acryloyl chloride, defining the second end group to be an acrylate.

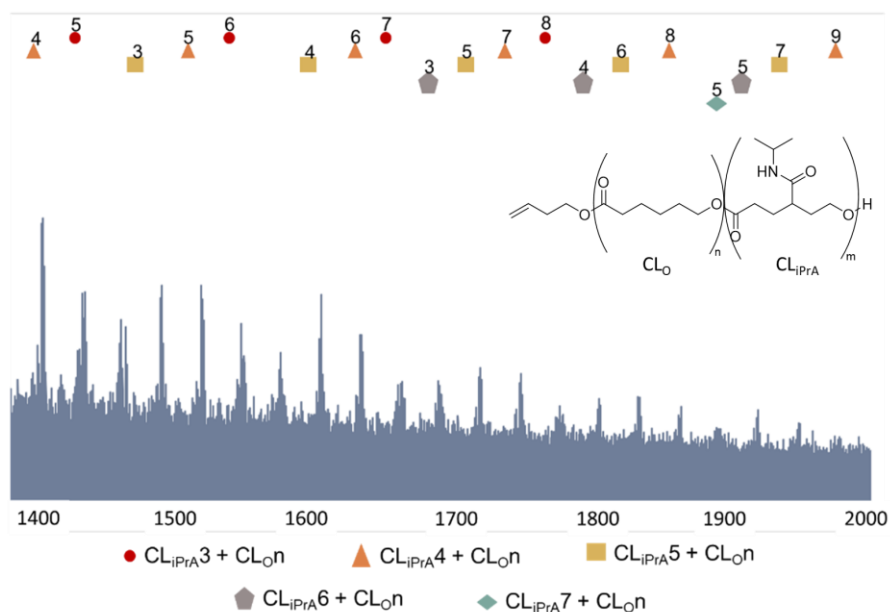


Figure 7. A segment of the MALDI-TOF spectrum of the di-micro-block co-oligomer of CLO and CLiPrA, series labeled by number of amide-bearing units, number of lactone units labeled above each symbol.

Throughout the synthesis of these materials, products were further monitored by size exclusion chromatography (SEC). From the chromatograms of **CLO15** homo-oligomer and its resulting homopolymer, the oligomer was fully consumed under ADMET conditions to produce a combination of cyclic oligomer and 11 kDa polymer, equivalent to an average of five chained oligomers (Figure 8). The cyclic oligomers—likely produced as dimers of short chains, which have a propensity to taken on a coiled conformation—appear at higher elution times than the linear oligomer due to the cyclization-induced coiled conformation of the chain, causing it to occupy a smaller volume.

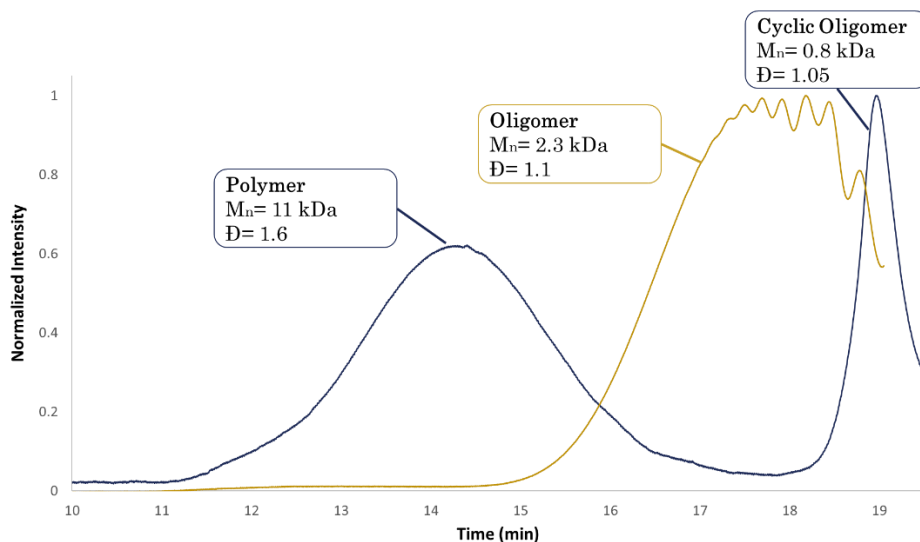


Figure 8. SEC of CLo15 before and after undergoing ADMET polymerization.

SEC of oligomer (gold), ADMET-produced polymer (blue, left) and cyclic products (blue, right).

Oligomers and polymers investigated here were analyzed by NMR, SEC, and MALDI-TOF spectrometry (Table 2, Table 3). These species were found to have relatively narrow dispersities and similar degrees of polymerization to those targeted.

Table 2. Oligomer block ratios and molecular weights.

Oligomer	CL _O : CL _A Feed Ratio	CL _O : CL _A NMR Ratio	Target Mn (Da)	Mn (NMR) (Da)	Mn (SEC) (Da)	Mw (SEC) (Da)	Đ (SEC)
CL _O 15	15:0	11.5:0	1838	1438	2300	2500	1.1
CL _O 10-CL _{nPrA} 5	10:5	5.5:0.9	2263	933.7	1300	1600	1.2
CL _O 10-CL _{iPrA} 5	10:5	11.4:4.8	2263	2383	615	701	1.1

Table 3. Polymer molecular weight data.

Polymer	Target Mn (kDa)	Mn (NMR) (kDa)	Mn (SEC) (kDa)	Mw (SEC) (kDa)	Đ (SEC)
CL _O 15	15	17	11.8	20.1	1.7
CL _O 10-CL _{iPrA} 5	24	12	20.9	40.2	1.9

2.2 Conclusion

Through these data, it can be concluded that the characteristics of the pendant groups attached at the γ -position to ϵ -caprolactone monomers can introduce steric effects that dictate the effectiveness of the micro-block copolymerization methods described here. While the methodology itself is robust, functional-group tolerant and capable of producing high-yielding regio-regular copolymers, as seen in the model polycaprolactone case, the process is limited by the extent to which incorporated monomers can form heterotelechelic oligomers with high chain-end fidelity. Thus, monomers such as $\text{CL}_{n\text{PrA}}$, which produce oligomers that become insoluble in commodity solvents at short chain lengths and are characterized by high melting temperatures, are not ideal for use in this methodology as they render the necessary subsequent solution-phase post-oligomerization modifications highly difficult and thereby prevent the formation of micro-block copolymers. Similarly, monomers such as $\text{CL}_{i\text{PrA}}$, which are capable of undergoing transesterification reactions that annulate chain ends when monomer concentrations are sufficiently low via a competing reaction, are not ideal for use with this copolymerization strategy due to the low yield of linear species relative to their annulated counterparts and with consideration of monomer input, though it is possible to form small quantities of the targeted polymer using these monomers through the strategy described here. This concept is further explored in chapter 3.

This strategy may be best employed using γ -substituted ϵ -caprolactone monomers for which the pendant group is unreactive with respect to the anionic alkoxide species that propagates the chain growth mechanism. Examples would include alkyl and phenyl substitutions, which could produce polymeric substrates suitable for systematic investigation of the effects of other, weaker non-covalent interactions, such as π -stacking, on the bulk properties of the material.

3.0 Investigation of Oligomerization Strategies for γ -Ester-Substituted ϵ -Caprolactone Moieties

In the pursuit of synthesizing ϵ -caprolactone moieties bearing pendant ester groups in the γ -position, it has been found that chain length is limited by the propensity of the active chain end to undergo an annulation with the pendant group which thereby terminates the chain.^{44, 45} Here, these products are characterized by MALDI-TOF mass spectroscopy, ^1H and ^{13}C NMR, and SEC, and these characterizations are used further to evaluate the effect of an alternate catalytic system on the product distribution of a CL_0 and CL_{COOEt} diblock oligomerization.

When the mechanism of polymerization for CL_0 using an aluminum tri-alkoxide catalyst is considered, it is apparent that the Al metal center is capable of initiating three chains, and further equilibrates in its active state between species bearing coordination numbers of 4, 5, and 6 with the carbonyl components of the ϵ -caprolactone monomer units associating to the catalyst.⁵⁴ With an unsubstituted ϵ -caprolactone monomer, this is often a beneficial quality of a catalytic system that has been investigated to such a point that transesterification can be reliably discouraged; however, at the higher temperatures required to ring-open substituted ϵ -caprolactone species due to their increased reactivity, substituted ϵ -caprolactone species are more susceptible to transesterification typically observed in the form of backbiting.⁵⁵ As unsubstituted ϵ -caprolactone⁵⁶ as well as γ - and α -alkylated ϵ -caprolactone species⁵⁷ have been polymerized successfully by employing salen ligand scaffolds on aluminum alkoxy catalysts, we have hypothesized that these catalytic systems may offer some utility in the polymerization of γ -ester and γ -amide substituted ϵ -caprolactone monomers. Per mechanistic investigations of the Al-salen catalyzed systems, Al-salen catalysts offer two open coordination sites for use by the propagating

ϵ -caprolactone species.^{58, 59} Based largely on these findings, we hypothesize here that the use of a sterically crowded Al-salen catalytic species for polymerization of γ -ester substituted ϵ -caprolactone monomers will decrease the likelihood of intra-chain annulation and thus result in products having higher degrees of polymerization than those synthesized via high-coordinate $\text{Al}(\text{OR})_3$ catalytic systems.

In this work, the catalyst interrogated for use in γ -ester ϵ -caprolactone polymerization consists of a salen mesityl ligand scaffold bearing an enantiopure cyclohexyl substituent as shown in Figure 9, similar to a species previously used for polymerization of lactide monomers.⁶⁰ This was synthesized by the procedure described in a recent collaboration between the Meyer and Coates groups, a process which is further described in chapter four.⁶¹

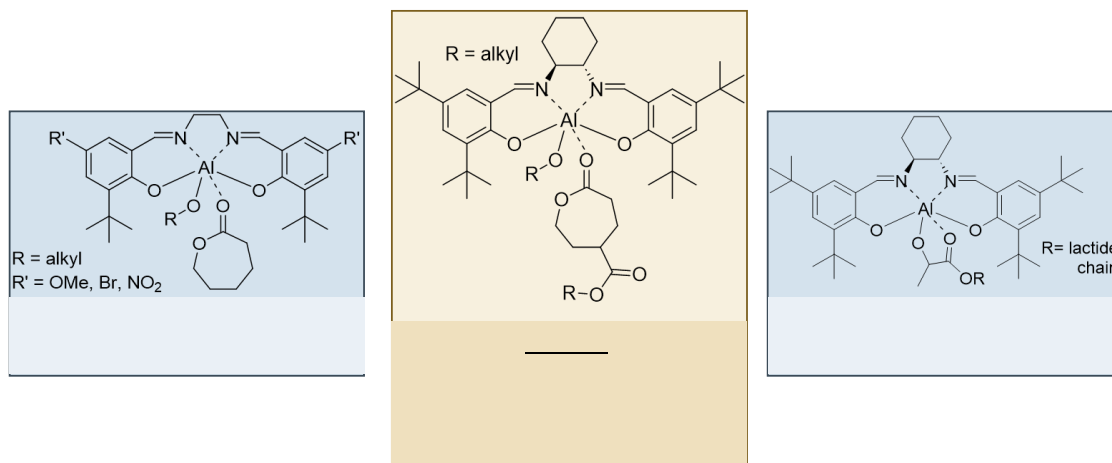


Figure 9. Previously reported active structures of Al-salen catalysts in the polymerization of cyclic esters.

3.1 Results and Discussion

3.1.1 Aluminum Tri-alkoxide Catalyzed γ -Ester Substituted ϵ -Caprolactone Oligomerization

While aluminum tri-alkoxide catalysts functioned sufficiently in the synthesis of the compounds reported in chapter 3, their application to forming the diblock oligomer of CL_O and CL_{COOEt} did not result in the formation of the desired product. By SEC, it was seen that poor initiation of the CL_{COOEt} block by the CL_O block occurred, and that the diblock that was formed was not of the anticipated molar mass, as is shown in Figure 10. While the former of these observations is common in block copolymer synthesis by chain growth sequential addition strategies, the typical result of this situation is that the second initiated block is longer than calculated due to a greater ratio of monomer to initiator being present; thus, the resulting shorter second block was likely indicative of a termination event.

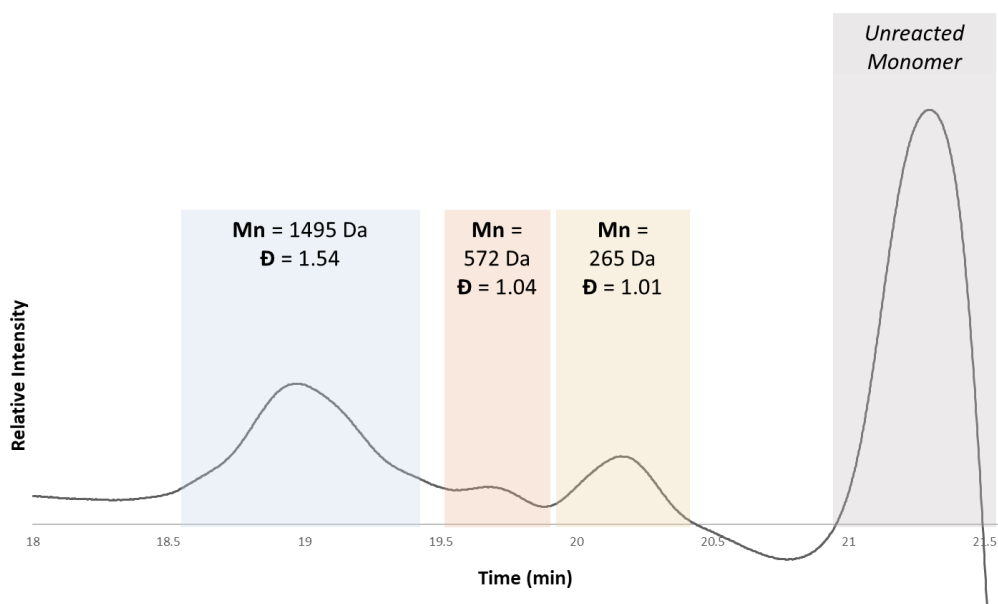


Figure 10. Size Exclusion Chromatogram (SEC) of di-block oligomer containing CL_O and CL_{COOEt} .

These findings were corroborated by the MALDI-TOF spectrum collected of the di-block oligomer synthesized with a ratio of 8:4:1 with respect to ϵ -caprolactone, γ -COOEt substituted ϵ -caprolactone, and alkoxy olefin initiator. In Figure 11, the spectrum of this di-block oligomer is shown overlaid with a spectrum modeled using the same olefin end group (1,3-butenol), average degrees of polymerization of 8 in ϵ -caprolactone and 4 in γ -COOEt-substituted ϵ -caprolactone, with intensity in a normal distribution and a standard deviation of 2 repeat units for each block—consistent with previous experiments as discussed in chapter 2. This simulated spectrum takes into account only the major isotopic species for simplicity, but nonetheless displays that the experimental spectrum contains populations of much lower molecular weight than those anticipated, considering as well that the 500-3000 Da range is within a regime previously established as having good ionization efficiency for polyester species. A predominant trend in the lower molecular weight region along with a longer periodic series separated by a mass of 114 Da, can be interpreted here as a combination of inefficient initiation of the second block and limited addition of the substituted monomer to the series of unsubstituted repeat units.

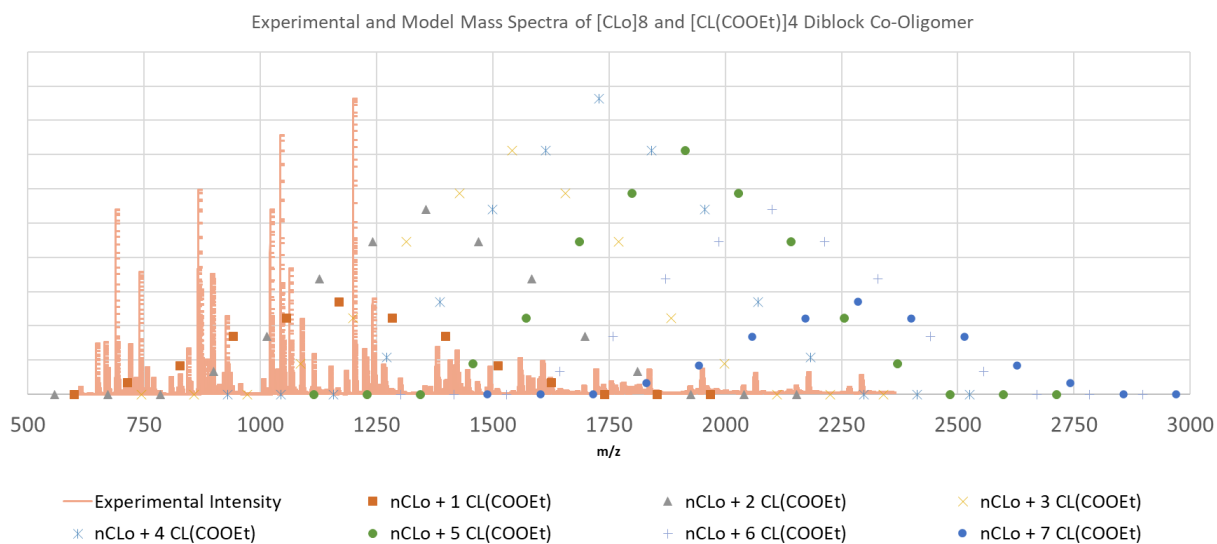


Figure 11. Experimental MALDI-TOF spectrum of CLo8-CLCOOEt4 (lines) overlaid with model mass distribution of CLo8-CLCOOEt4 (points).

Besides these trends evidenced by the SEC trace and echoed by the data seen in the MALDI-TOF spectrum, the data in this spectrum further elucidate both the mechanism by which the chain growth is terminated and the root of the underlying inconsistencies between the modeled spectrum and the spectrum obtained experimentally. Coinciding with the phenomenon discussed by Stefan et al and Fukushima et al, the MALDI-TOF spectrum depicts a common loss of 45 Da from the expected molecular weight of the di-block oligomer due to the annulation of chain ends, as shown in Figure 12.^{44, 45} The mechanism shown involves the nucleophilic attack of the active alkoxide chain end on the carbonyl as a unimolecular process; however, as this premise is the mechanistic basis for the anionic chain growth undergone by the lactone, it can easily be facilitated by acidic, basic, and organometallic catalysis.

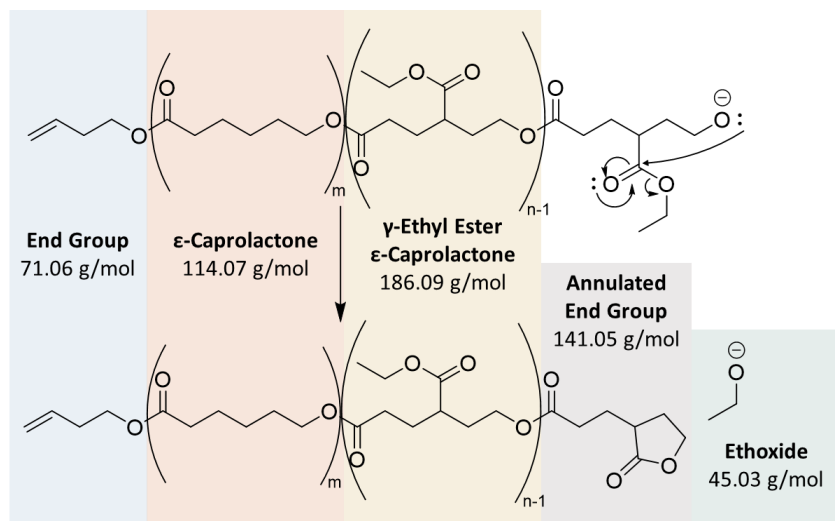


Figure 12. The mechanism of chain-end annulation in γ -ester-substituted ϵ -caprolactone moieties, labeled with component molecular weights observable by MALDI-TOF.

Combinations of these molecular weights comprise the populations seen in the spectrum reported in Figure 11, shown in greater detail in Appendix E.1, Figure 46. The populations which appear in addition to this involve the oligomers initiated via the severed ethoxide, noted by the 26 Da decrease in molecular weight from the butenol-initiated oligomers and by their identity as CL_{COOEt} homooligomers, due to CL_O having been completely consumed prior to the reaction.

Though MALDI-TOF is a soft ionization technique which discourages fragmentation, the energetic input is often enough to cause further reactivity and related fragmentation within molecular species, which in the case of the oligomeric segments of CL_{COOEt} be seen by the additional release of 28 Da fragments via the rearrangement depicted in Figure 13.

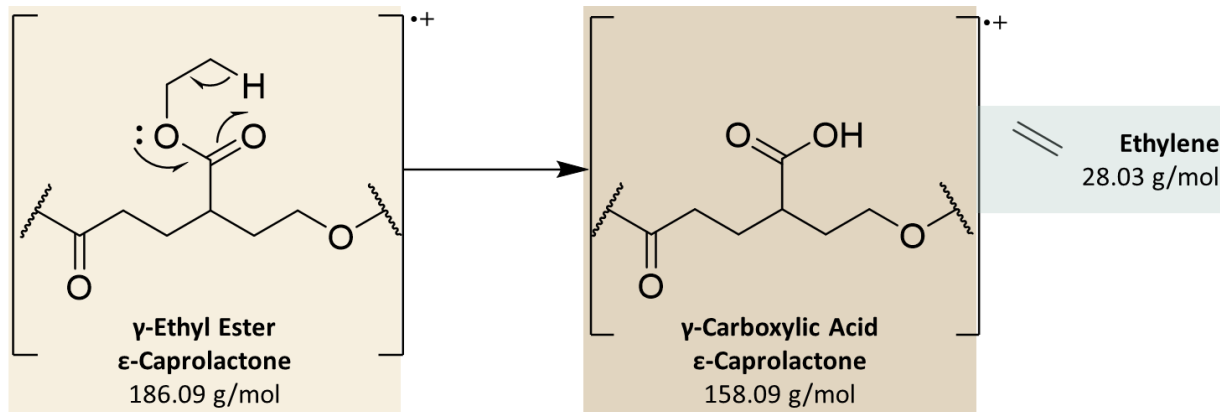


Figure 13. The mechanism of rearrangement as enabled by the radical cationic character induced in MALDI-TOF, labeled with observable component molecular weights.

By ^{13}C NMR spectroscopy, the carbon atoms involved in the linear and cyclic components can be seen distinctly, and are labeled in the spectrum available in Appendix E.1, Table 18 and Figure 44. In the ^1H NMR spectrum, peaks for linear, cyclic, end group, and monomeric components overlap at times, but a set of diagnostic peaks shown in Figure 14 have been obtained through thorough assignment of the spectrum, also available in Appendix E. Proton assignment to chemical shift regions enabled calculation of relative species presence; as shown in Figure 14, these regions were integrated and correlated to the corresponding number of protons for each species that is represented within them as individual peaks were not cleanly integrable.

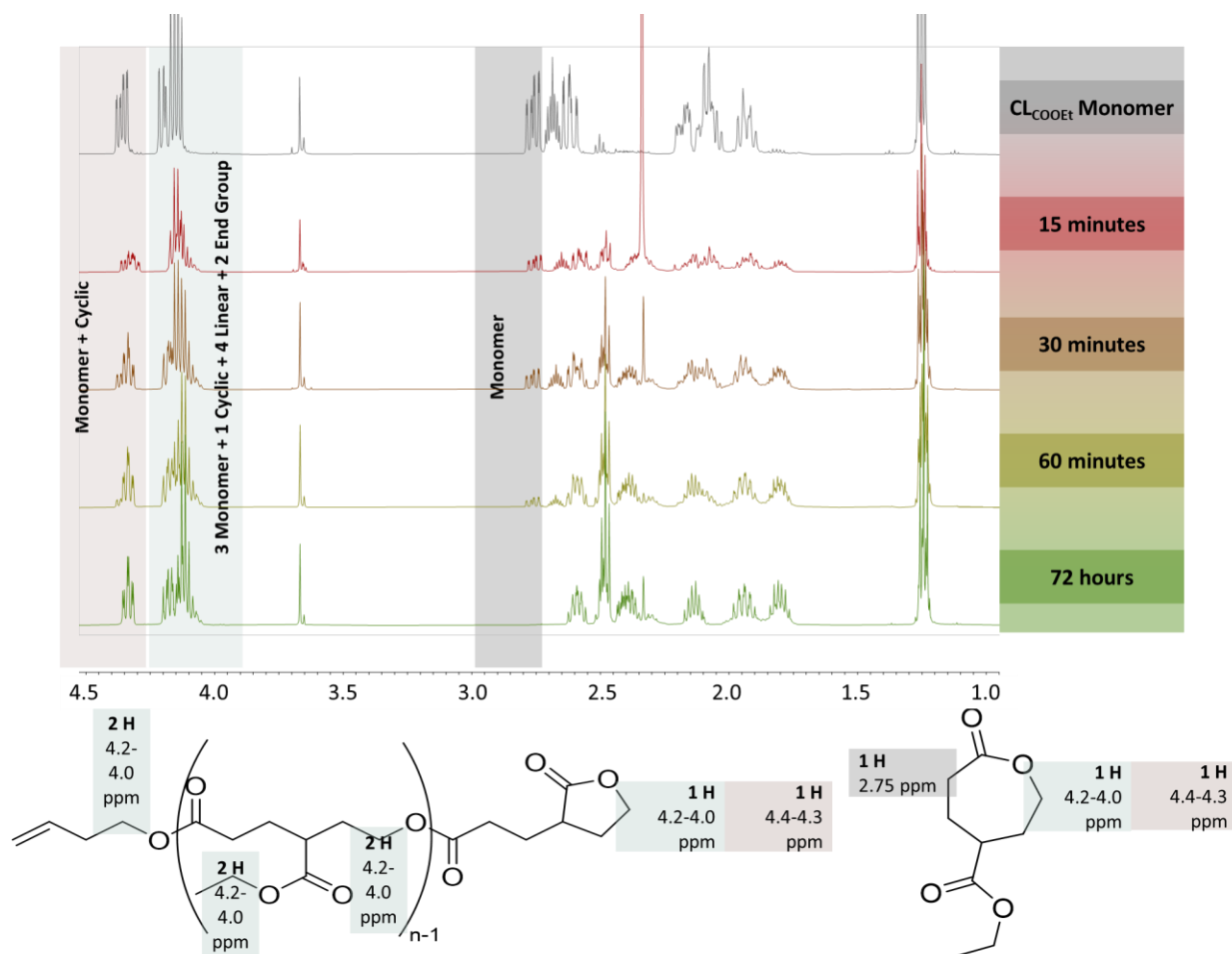


Figure 14. ^1H NMR spectra of CL_{COOEt} oligomerization over the course of 72 hours, with diagnostic peaks labeled.

By employing these assignments, a kinetic study (Figure 15) was conducted of the aluminum tri-butenol anionic catalyst system as it pertains to the oligomerization of CL_{COOEt} . From this study, it appears that the chain growth and annulation begin at comparable initial rates; however, active linear species are readily converted to their cyclic counterparts while the annulated species are energetically more stable and unable to return to the more reactive state. Additionally, while chains are rendered inactive by chain-end annulation, the ejected ethoxide components are able to further initiate oligomerization of otherwise unreacted monomers. This is seen as a steady consumption of monomer alongside an initially fast annulation rate, which then slows as the supply of active chain ends dwindles, finally increasing cyclic product formation linearly as freed

ethoxide species initiate further lactone ring opening. At the end point, the species remaining in solution include butenol oxyanion- and ethoxy- initiated oligomers, some of which contain internal linear components preceding an annulated end group.

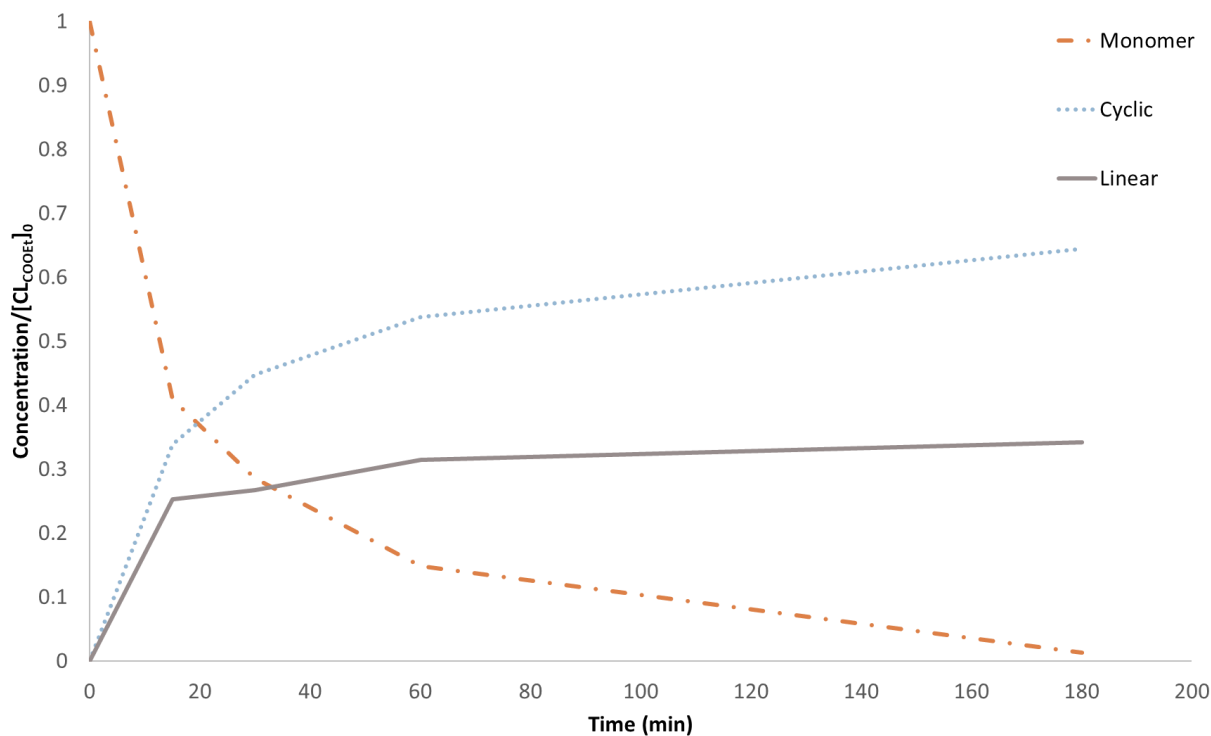


Figure 15. Concentration of monomer, cyclic, and linear components measured over time relative to initial CL_{COOEt} concentration.

With the relevant components of the CL_{COOEt} oligomer reliably assigned using the known catalytic system discussed in chapter 2, these data were then able to be used to obtain the product distributions from the application of the Al-salen catalyst to the oligomerization of the γ -ethyl ester ϵ -caprolactone monomer.

3.1.2 Evaluation of γ -Ester ϵ -Caprolactone Oligomerization Catalyzed by an Aluminum Catalyst Bearing a Jacobsen Ligand Framework

Using the methodology previously employed for aluminum tri-alkoxide catalyzed oligomerization of CL_O , CL_{COOEt} , CL_{iPrA} , and CL_{nPrA} , the Al(salen) system (synthesized as described in chapter 4) was first tested on CL_O and subsequently applied to CL_{COOEt} monomer in order to analyze the product distribution and reaction rate. The Al(salen) catalyst proved robust in the oligomerization of CL_O , resulting in a degree of polymerization similar to the calculated value per chapter 4 and as seen in Appendix E.3. However, when employed for the oligomerization of the ester-substituted ϵ -caprolactone variant, room temperature oligomerization proceeded at a rate unable to be tracked at time scales comparable to those used for the analogous tri-alkoxy aluminum catalyzed experiment. The product distribution, unchanged between 15 minutes and 72 hours of reaction time, contained a greater concentration of the annulated component in comparison to linear component than that given by the aluminum tri-alkoxide catalyst, as can be seen spectroscopically in Figure 16. At both of these timepoints, calculated in the manner depicted in Figure 14, the reaction mixture contained a ratio of 0.09:0.45:0.46 monomer:cyclic:linear components, all normalized to the initial monomer concentration.

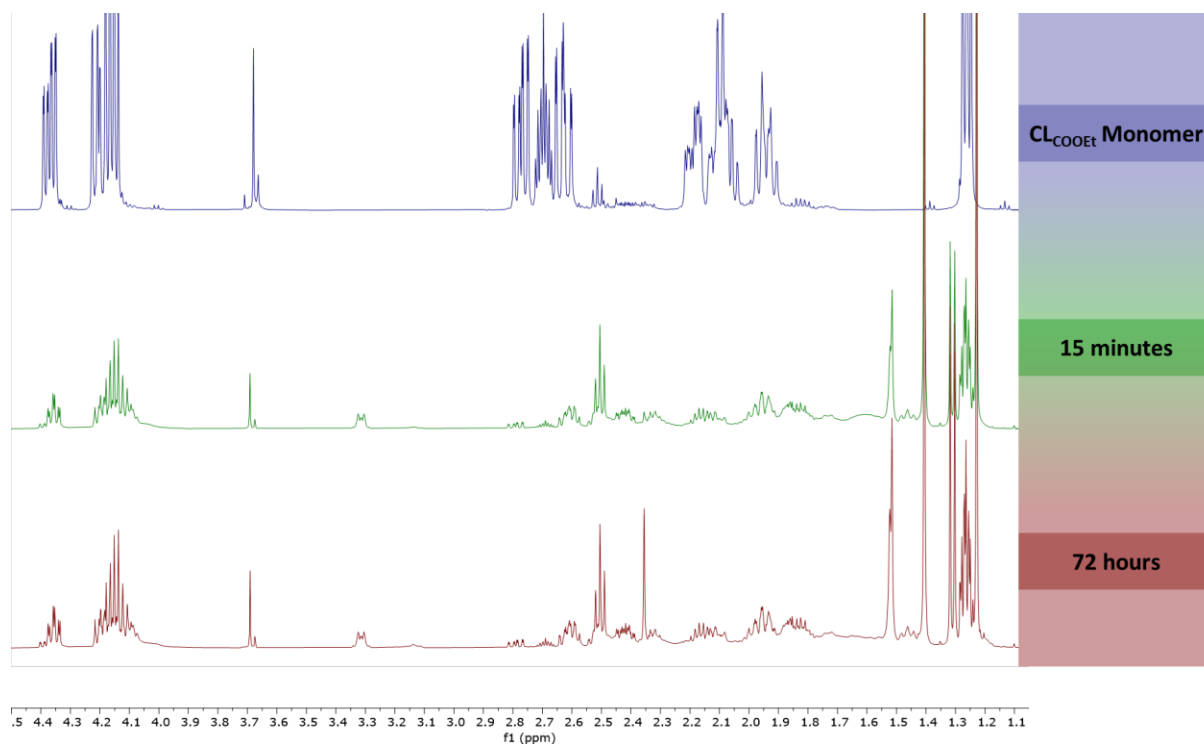


Figure 16. ^1H NMR spectra of CL_{COOEt} oligomerization at 15 minute and 72 hour timepoints.

While the $\text{Al}(\text{salen})$ catalytic system generated a product distribution with a higher ratio of linear components than that given by the aluminum tri-alkoxy system, this modest increase is accompanied by a decrease in monomer consumption, indicating that each chain end was nonetheless annulated by 15 min of reaction time. From these experiments, it is evident that the $\text{Al}(\text{salen})$ catalyst is incapable of inhibiting the intramolecular transesterification that occurs at room temperature within γ -ester substituted ϵ -caprolactone ring-opening polymerizations. Based on the mechanism of reactivity, it is likely that the weakness of the alkoxide coordination to the Al center results in sufficient distance between the reactive components to allow for more sterically demanding reactants, such as the pendant ester group, to react with the active chain end. Further, due to the high rate of the reaction, it is evident that room temperature conditions provide overly satisfactory input of thermal energy to the reaction; considering that ring-opening reactions are

typically more exothermic than linear transesterification reactions, it is possible that decreased reaction temperatures would further favor the linear product over its annulated counterpart.

3.2 Conclusion

In this chapter, the rationale for characterizing oligomeric species of CL_{COOEt} as bearing annulated chain ends was explored through the lens of SEC, MALDI-TOF, and NMR spectroscopy, resulting in a thorough analysis of these compounds sufficient for application to the characterization of similar γ -ester substituted ϵ -caprolactone moieties. Pursuant to recent research, it was found that annulation of chain ends is a common transesterification reaction that occurs with carbonyl-containing ϵ -caprolactone compounds, affected only minimally by the polymerization strategy employed. The employment of an $\text{Al}(\text{salen})$ catalyst for this oligomerization displayed modest increases in linear chain growth rate relative to chain end annulation rate; however, this increase is not yet suitably large to reliably produce oligomeric species with defined functional chain ends. While lowering the temperature of the reaction may further improve these relative rates, it is likely that these findings would be best used to inform future research into improved catalytic methods or preferred monomer systems to produce reliably heterotelechelic poly(pendant ester) compounds.

4.0 Experimental Procedures

4.1 Materials and Instrumentation

4.1.1 Materials

All experiments were carried out in oven-dried or flame-dried glassware under an atmosphere of N₂ using standard Schlenk line techniques unless otherwise noted. Monomers and their precursors¹⁸ were prepared according to previously published protocols. Dichloromethane (DCM, Fisher) was purified by a Solvent Dispensing System by J. C. Meyer by passing over two columns of neutral alumina. ϵ -Caprolactone (CL_O) was purchased from Fisher Scientific, dried over CaH₂ and distilled before use. 1,3-Butenol was purchased from Fisher Scientific, stored over K₂CO₃ for dryness, and filtered before use. Aluminum isopropoxide (99.99%) was purchased from Thermo Scientific and stored under N₂. All other chemicals were used without further purification. Ethyl 4-keto cyclohexane carboxylate, N-hydroxysuccinimide (NHS), and trimethyl aluminum were purchased from Fisher Scientific. Triethylamine (TEA) and 1-Ethyl-3-(3-dimethylaminopropyl)carbodiimide (EDC) were purchased from Sigma-Aldrich. Diphenyl ether was purchased from Acros Organics. Grubbs 2nd generation catalyst (G2) was purchased from AK Scientific. Deuterated NMR solvent (CDCl₃) was purchased from Cambridge Isotope Laboratories. Methanol (MeOH) and diethyl ether were purchased from Fisher Scientific. Anhydrous, inhibitor-free Tetrahydrofuran (THF, >99.9%) was purchased from Alfa Aesar.

4.1.2 NMR Spectroscopy

^1H (400 and 500 MHz) and ^{13}C (100 and 125 MHz) NMR spectra were obtained using Bruker spectrometers and are reported as δ values in ppm relative to the reported solvent. Splitting patterns are abbreviated as follows: singlet (s), doublet (d), triplet (t), quartet (q), multiplet (m), broad (br), and combinations thereof.

4.1.3 Size Exclusion Chromatography

Molecular weights and dispersities were obtained on a TOSOH HLC-8320GPC EcoSEC equipped with two columns (TSKgel-G3000H, TSKgel-G3000H). A mobile phase of THF inhibited with 0.025% butylated hydroxytoluene at 50 °C with a flow rate of 1 mL/min was used, reported molecular weights were obtained with a refractive index detector (TOSOH) and are relative to polystyrene standards (90, 50, 30, 9, 5, 2.5 kDa). Select SEC data were analyzed using a refractive index increment (dn/dc) of 0.060 mL/g, which was determined by the direct injection of stock solutions through the refractive index detector.

4.1.4 MALDI-ToF MS

Mass spectra were obtained on a Bruker ultrafleXtreme MALDI-ToF instrument. An accelerating voltage of 20 kV was applied, and spectra were obtained in reflection positive mode (500 shots). The polymers were dissolved in THF to yield a concentration of 1 mg/mL. Sodium iodide (NaI) was used as the cationization agent and was dissolved in THF to form a 10 mg/mL solution. The matrix was DHB (2,5-dihydroxybenzoic acid) in THF as a 40 mg/mL solution. The

three solutions were combined in a volume ratio of 2:4:1 (polymer: DHB: NaI). The solution was then drop cast onto a 100-well MALDI plate and allowed to dry before analysis. Spectra were analyzed using Bruker flexAnalysis software package.

4.2 Synthesis of γ -Substituted ϵ -Caprolactones

4.2.1 4-Oxocyclohexane-1-carboxylic acid (2)

Using the methodology of L. Wen et al¹⁸: In a 500 mL round-bottom flask, 0.2 M H₂SO₄ (60 mmol, 300 mL) and ethyl 4-keto cyclohexane carboxylate (58.8 mmol, 10.21 g, 9.56 mL) were stirred and subsequently refluxed. After 48 h, the reaction mixture was cooled to room temperature and extracted 6x with 50 mL diethyl ether, the organic layers dried over Na₂SO₄, and solvent removed *in vacuo* to give the corresponding acid (7.5 g, 52.8 mmol, 88% yield). ¹H NMR (400 MHz, CDCl₃) δ : 2.82 (m, 1H), 2.50 (m, 2H), 2.37 (m, 2H), 2.24 (m, 2H), 2.06 (m, 2H).

4.2.2 N-isopropyl-4-Oxocyclohexane-1-carboxamide (3, R=iPr)

Using the methodology of L. Wen et al¹⁸: In a dry 250 mL round-bottom flask, 4-oxocyclohexane-1-carboxylic acid (52.8 mmol, 7.5 g) was stirred with EDC (66 mmol, 10.25 g) and NHS (66 mmol, 7.6 g) in dry DCM (100 mL) under static N_{2(g)} for 0.5 h. At this point, isopropylamine (79.2 mmol, 6.8 mL) in dry DCM (25 mL) was added dropwise over the course of 0.5 h. The reaction mixture was stirred for 3 h and subsequently filtered, and the solvent level decreased *in vacuo* to 50 mL. This solution was then rinsed thrice with NaHCO₃ (1 M, 25 mL),

dried over Na₂SO₄, and the solvent removed *in vacuo* to leave the product as a white powder (5 g, 27.3 mmol, 52% yield). ¹H NMR (400 MHz, CDCl₃) δ: 5.42 (br s, 1H), 4.08 (m, 1H), 2.49 (m, 3H), 2.33 (m, 2H), 2.14 (m, 2H); 1.98 (m, 2H); 2.06 (m, 6H).

4.2.3 4-Oxo-N-propylcyclohexane-1-carboxamide (3, R=nPr)

Using the methodology of L. Wen et al¹⁸: In a dry 200 mL round-bottom flask, 4-oxocyclohexane-1-carboxylic acid (7.04 mmol, 1.0 g) was stirred with EDC (8.79 mmol, 1.37 g) and NHS (8.79 mmol, 1.01 g) in dry DCM (100 mL) under static N_{2(g)} for 0.5 h. At this point, n-propylamine (7.74 mmol, 0.46 mL) in dry DCM (10 mL) was added dropwise over the course of 0.5 h. The reaction mixture was stirred for 3 h and subsequently filtered, and the solvent level decreased *in vacuo* to 25 mL. This solution was then rinsed thrice with NaHCO₃ (1 M, 10 mL), dried over Na₂SO₄, and the solvent removed *in vacuo* to leave the product as a white powder (0.7 g, 3.8 mmol, 54% yield). ¹H NMR (400 MHz, CDCl₃) δ: 5.53 (br s, 1H), 3.24 (td, J = 7.2, 5.8 Hz, 2H), 2.51 (m, 3H), 2.34 (m, 2H), 2.16 (m, 2H), 2.00 (m, 2H), 1.54 (h, J = 7.4 Hz, 2H), 0.93 (t, J = 7.4 Hz, 3H).

4.2.4 CL_{iPrA}

Using the methodology of L. Wen et al¹⁸: To a stirred solution of mCPBA (49 mmol, 8.4 g) in dry DCM (130 mL) at 0°C under static N_{2(g)} in a flame-dried 250 mL round-bottom flask, a solution of N-isopropyl-4-oxocyclohexane-1-carboxamide (23 mmol, 4.2 g) in dry DCM (20 mL) was slowly added over the course of 1 h. After stirring for 12 h as the reaction mixture warmed to room temperature, the mixture was exposed to atmospheric conditions, filtered, and solvent

removed *in vacuo*. The solute was then taken up in a minimal amount of DCM and precipitated in diethyl ether (50 mL). This precipitation was repeated two additional times. The product was then dried *in vacuo* to yield a white powder (2.0 g, 10.1 mmol, 44% yield). ¹H NMR (400 MHz, CDCl₃) δ: 5.25 (s, 1H), 4.50 (ddd, J = 13.8, 6.3, 2.5 Hz, 1H), 4.17 (ddd, J = 12.9, 7.7, 2.4 Hz, 1H), 4.13 – 4.00 (m, 1H), 2.91 (dd, J = 14.4, 8.5 Hz, 1H), 2.60 (ddd, J = 13.3, 10.8, 2.1 Hz, 1H), 2.37 (hept, J = 4.4 Hz, 1H), 2.15 – 1.98 (m, 3H), 1.91 (dd, J = 12.5, 11.6 Hz, 1H), 1.15 (d, J = 6.5 Hz, 6H).

4.2.5 CL_nPrA

Using the methodology of L. Wen et al¹⁸: To a stirred solution of mCPBA (10.9 mmol, 2.35 g) in dry DCM (50 mL) at 0°C under static N_{2(g)} in a flame-dried 100 mL round-bottom flask, a solution of 4-oxo-N-propylcyclohexane-1-carboxamide (5.5 mmol, 1.0 g) in dry DCM (15 mL) was slowly added over the course of 1 h. After stirring for 12 h as the reaction mixture warmed to room temperature, the mixture was exposed to atmospheric conditions, filtered, and solvent removed *in vacuo*. The solute was then taken up in a minimal amount of DCM and precipitated in diethyl ether (10 mL). This precipitation was repeated two additional times. The product was then dried *in vacuo* to yield a white powder (0.4 g, 2.01 mmol, 37% yield). ¹H NMR (400 MHz, CDCl₃) δ: 5.53 (s, 1H), 4.49 (ddd, J = 13.1, 6.2, 2.5 Hz, 1H), 4.18 (ddd, J = 13.1, 8.1, 2.4 Hz, 1H), 3.29 – 3.17 (m, 2H), 2.91 (ddd, J = 14.4, 8.5, 1.9 Hz, 1H), 2.60 (ddd, J = 14.0, 11.3, 2.2 Hz, 1H), 2.43 (tt, J = 9.3, 4.3 Hz, 1H), 2.17 – 1.99 (m, 2H), 1.92 (ddd, J = 14.3, 11.7, 9.9, 2.0 Hz, 1H), 1.52 (h, J = 7.3 Hz, 2H), 0.92 (t, J = 7.4 Hz, 3H).

4.2.6 CL_{COOEt}

Using the methodology of L. Wen et al¹⁸: To a stirred solution of mCPBA (2.9 mmol, 0.5 g) in dry DCM (10 mL) at 0°C under static N_{2(g)} in a flame-dried 100 mL round-bottom flask, a solution of ethyl 4-keto cyclohexane carboxylate (1.5 mmol, 0.25 mL) in dry DCM (5 mL) was slowly added over the course of 1 h. After stirring for 12 h as the reaction mixture warmed to room temperature, the mixture was exposed to atmospheric conditions, filtered, and solvent removed *in vacuo*. The product was then dried *in vacuo* to yield a white powder (0.4 g, 2.01 mmol, 37% yield). ¹H NMR (400 MHz, CDCl₃) δ: 4.38 (ddd, J = 13.2, 7.1, 1.8 Hz, 1H), 4.24 – 4.12 (m, 3H), 2.79 (ddd, J = 14.4, 9.1, 1.8 Hz, 1H), 2.74 – 2.55 (m, 2H), 2.28 – 2.03 (m, 3H), 1.96 (dddd, J = 14.6, 11.1, 9.3, 1.8 Hz, 1H), 1.27 (t, J = 7.1 Hz, 3H).

4.3 Diblock Macromonomer Synthesis

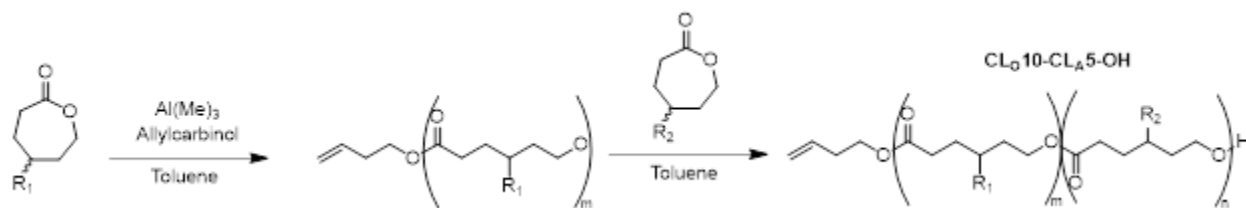


Figure 17. Synthetic Route for Diblock Macromonomer Synthesis

To a flame-dried 25 mL round-bottom flask in a N_{2(g)} atmosphere was added dry toluene (5 mL), 1 M Al(Me)₃ in hexanes (1/3 eq.), and 1,3-butenol (1 eq.). This mixture was stirred and subsequently chilled to -78°C for 15 minutes, at which point ϵ -caprolactone was added and the reaction mixture stirred for 5 h and warmed to room temperature. γ -substituted ϵ -caprolactone was then added and the reaction mixture refluxed under N_{2(g)} flow for 18 h. Following confirmation

by ^1H NMR that all monomer had been consumed, dry DCM (5 mL) and TEA (2.5 eq.) were added and the mixture chilled to 0°C . Acryloyl chloride (2 eq) was then added over the course of 0.5 h and the reaction mixture stirred, warming to room temperature. After 3 h, the reaction mixture was exposed to air and precipitated in hexanes (200 mL). The product was redissolved in DCM (50 mL) and rinsed twice with 1M HCl (20 mL), after which the solvent was partially removed *in vacuo* and the product, dissolved in a minimal amount of DCM, was precipitated in 100 mL methanol at 0°C . Oligomeric product was then dried *in vacuo*.

Table 4. Ratios of monomers used for CL_0 , $\text{CL}_{n\text{PrA}}$, and $\text{CL}_{i\text{PrA}}$ micro-block copolymerizations

Oligomer	Monomer	Ratio to Initiator	Moles (mmol)	Mass (g)	Volume (mL)
CL_015	CL_0	10	17.4	1.99	2.93
$\text{CL}_010\text{-CL}_{n\text{PrA}5}$	CL_0	10	1.00	0.11	0.108
	$\text{CL}_{n\text{PrA}}$	5	0.5	0.1	-
$\text{CL}_010\text{-CL}_{i\text{PrA}5}$	CL_0	10	2.21	0.25	0.245
	$\text{CL}_{i\text{PrA}}$	5	1.10	0.22	-
$\text{CL}_08\text{-CL}_{\text{COOEt}4}$	CL_0	8	2.25	0.26	0.25
	CL_{COOEt}	4	1.13	0.21	-

4.4 End Group Modification of γ -Substituted ϵ -Caprolactone Oligomers

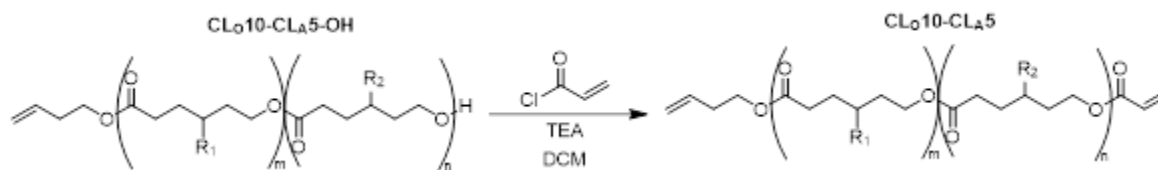


Figure 18. Synthetic Route for end group modification of γ -substituted ϵ -caprolactone oligomers

Under static $\text{N}_2(\text{g})$, the di-block oligomers bearing an $-\text{OH}$ end group (1 eq) were stirred with TEA (1.2 eq) in dry DCM (10 mL) for 0.5 h at 0°C . Acryloyl chloride (1.2 eq) in dry DCM (3 mL) was then added dropwise over 1 h and the mixture stirred overnight, during which it was warmed to room temperature. The reaction mixture was then exposed to ambient conditions and

rinsed twice with HCl (1 M, 10 mL). Solvent was evaporated until a minimal amount remained and the oligomer was precipitated twice in 10 mL methanol, the precipitate then dried *in vacuo* to produce a white powder.

4.5 Polymerization of Macromonomers

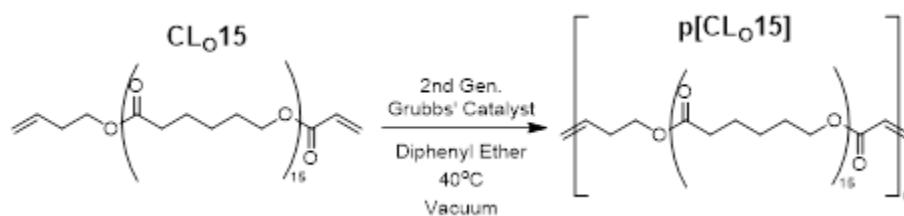


Figure 19. Synthetic route for polymerization of macromonomers as applied to p[CL₀₁₅].

In an oven-dried 1-dram vial charged with a stir bar and 2nd generation Grubbs' catalyst (5 mg), the di-olefin oligomeric product was dissolved in diphenyl ether to a 2M concentration and was stirred at 40°C under vacuum. When the product had achieved a degree of polymerization of 10 after 48 hours, the reaction mixture was cooled to room temperature, quenched with ethyl vinyl ether (0.1 mL), and precipitated in diethyl ether (50 mL).

4.6 N,N'-bis(3,5-di-tert-butylsalicylidene)-1,2-cyclohexane-diamino aluminum isopropoxide (Al-salen) catalyst synthesis

In a N₂ glovebox, solid aluminum isopropoxide (0.405 mmol, 0.042 g) was weighed into an oven-dried vial, capped and sealed with electrical tape, and removed from the glovebox. The solid was melted over four cycles using a heat gun to convert the compound from its solid

tetrameric form to its liquid trimeric form. This was then cooled and returned to the glovebox, where the N,N'-bis(3,5-di-tert-butylsalicylidene)-1,2-cyclohexane-diamine (0.405 mmol, 0.112 g) was added in 2 mL dry toluene, and the mixture subsequently capped, sealed tightly using electrical tape, and removed from the glovebox to be heated at 70°C for 72 h. After heating, the mixture was cooled and brought back into the glovebox, solvent and residual isopropanol removed *in vacuo* to leave a yellow crystalline solid (0.17 g, quantitative yield).

4.7 Oligomerization of CL_O using Al(salen) catalyst

To the dried Al salen catalyst (0.1 mmol, 0.0694 g) in a 2-dram vial in the N₂ glovebox, a solution of CL_O (1.1 mmol, 0.122 g) in dry toluene (3 mL) was added and stirred at room temperature for 4 h. This was then removed from the glovebox and solvent removed *in vacuo*, leaving the oligomer (degree of polymerization = 10) and catalyst as an off-white powder (0.12 g, quantitative yield).

4.8 Kinetic Testing of CL_{COOEt} using Al(OR)₃ and Al(salen) catalysts

In a N₂ glovebox, to a solution of catalyst (0.135 mmol, 1/3 eq initiator in Al(OR)₃ and 1 eq. initiator in Al(salen)) in dry toluene (1 mL) was added a solution of CL_{COOEt} (5 eq with respect to initiator) in toluene (1 mL) and stirred. Aliquots (0.2 mL) were taken at 15 min, 30 min, 60 min, and 72 h, dried *in vacuo*, and analyzed via ¹H NMR in CDCl₃.

5.0 Future Directions

Though the synthesis of a library of well-defined amphiphilic micro-block copolymers was not within the scope of this study, the findings herein were able to provide considerable insight and direction towards future investigations. Micro-block copolymers remain an underexplored and highly functional regime of meso-scale polymer sequencing, for which model studies indicate a rich and responsive property space. In this section, alternative synthetic strategies will be discussed, followed by an exploration of the anticipated properties suggested by micro-block copolymer theory and studies of surrounding block length scales.

5.1 Alternative Synthetic Strategies

Within this series of experiments, multiple ligand variations centered around aluminum catalysts were employed for copolymerization of ϵ -caprolactone and its γ -ester and γ -amide derivatives. In pursuit of a selection of amphiphilic micro-block copolymers, each of these components (catalytic system and monomer choice) has potential for modification to better facilitate the aforementioned research goals, and there have been promising recent developments in both areas.

5.1.1 Catalyst

Considering that the difficulties with the polymerization of γ -ester and γ -amide substituted ϵ -caprolactone moieties stem from the accessibility and compatibility of the pendant group with the ring opening catalyst, a catalyst with more selectivity either in terms of steric characteristics or energetic requirements could decrease transesterification rates. A Nd catalyst was first reported by Shen et al in 1994 for the polymerization of unsubstituted ϵ -caprolactone, which has since then been further developed into a family of Nd catalysts suitable for a variety of conditions.⁶² The mechanism of reactivity for this initial catalytic system involves coordination of Nd to the oxygen atom within the ϵ -caprolactone ring and an Al co-catalyst to both the carbonyl oxygen atom of the ϵ -caprolactone monomer as well as the alkoxy anion of the ring-opening species, though later variants take advantage of Nd's large coordination sphere and involves coordination of Nd to all three aforementioned oxygen atoms.⁶³ Using this catalyst, several γ -substituted ϵ -caprolactone varieties have been polymerized with moderate yield, though a sizeable percentage (~10%) of ester-substituted monomers still form the corresponding transesterification product.⁶⁴ The lower transesterification rate indicates the possibility of modifications to the catalyst that would further decrease this rate, or in absence of this, an option to closely monitor the polymerization and quench the reaction while a high monomer to chain end ratio remains, sacrificing reaction yield in service of chain end fidelity.

5.1.2 Monomer

If esters and amides are to represent, respectively, the H-bonding donor capable and incapable pendant block components of the amphiphilic micro-block copolymer design, it is also

possible to change the polymer backbone identity from a ring-opened ester to an alkyl unit so that a more ester- and amide- tolerant polymerization method may be employed. Gody et al have reported the use of RAFT to synthesize multiblock copolymers consisting of up to twelve blocks containing approximately ten repeat units apiece in relatively short time scales (~2 hours per block).⁶⁵ This method could feasibly be applied to a N-isopropylacrylamide and ethyl acrylate system to result in a similar system to the target material of this study; however, fewer blocks than intended would be incorporated into the resulting polymer chain and a lack of ability to dictate chain end identity would prevent further chain extension.

5.2 Bulk Material Testing

Within the class of microblock-copolymer materials, measurements that are anticipated to be affected by the degree of sequencing imposed include contact angle, differential scanning calorimetry (DSC), and mechanical testing. Polycaprolactone is known to have a relatively low T_g and T_m , though lacks mechanical toughness—however, these properties are capable of modulation via incorporation of additional repeat units.⁶⁶ In order to accurately attribute the properties observed in these experiments to the microblock length scale, controls of the corresponding copolymer composition but below and above microblock length scale are required to be measured as well for comparison. Most notably, it has been theorized that microphase segregation becomes less dependent on length as length increases;⁶⁷ however, that the contribution of surface free energies becomes more prominent as the number of blocks increases, making microphase segregation increasingly difficult with higher numbers of blocks when composition remains unchanged.⁶⁸

5.2.1 Hydrophilicity

It has been previously shown that even small incorporations of polar comonomers into hydrophobic polymer systems can decrease the material's contact angle with water.⁶⁹ Thus, at lengths of hydrogen-bonding capable units in the lower the micro-block copolymer property regime, it is anticipated that these segments of exposed components would be sufficient to increase the material's hydrophilicity. Multi-block copolymer chains have been shown to exhibit 'collapsing' behavior at sufficient length scales in such a way that precludes surface exposure of certain blocks of amphiphilic molecules.⁷⁰ For this reason, it could be expected that longer length segments of hydrogen-bonding capable blocks would be further 'collapsed,' thereby exposing fewer hydrogen-bonding capable regions and ultimately decreasing the hydrophobicity of the surface.

5.2.2 Mechanical Properties

At lengths above the micro-block regime, block-like behavior emerges within a material's mechanical properties as microphase segregation predominates—this is exemplified in the mechanisms by which mechanical failure occurs. In diblock copolymers, block lengths that result in ordered morphologies display a cavitation failure mechanism, while block lengths that produce disordered morphologies display crazing behavior at failure, approaching the modulus and behavior of the more abundant repeat unit.⁷¹ Similarly, when comparing multiblock copolymers with statistical copolymers, the multiblock copolymers display more elastomeric behavior upon addition of mechanical stress, deforming first one component before the second to result in greater elongation at break but lower tensile strength than the analogous statistical copolymer.⁷² Therefore,

one can anticipate that in a micro-block copolymer system containing components of insufficient lengths for microphase segregation a combination of these phenomena would be observed. As the morphological structures necessary to induce cavitation-based failure would not be present yet monomer A- or B- rich regions would be less aligned than necessary for crazing failure mechanisms, the failure characteristics could not be expected to align perfectly with either distinct mechanism; as A- and B- rich regions would be more linearly separated from one another, the elongation of either micro-block type would be less likely to occur in such a stepwise manner as is the case for diblock copolymers.⁷³

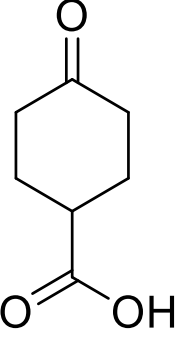
5.2.3 Thermal Properties

In amphiphilic block copolymer systems that display microphase segregation and are composed of monomers with less favorable interactions between them, it is common for multiple glass transition temperatures to be measured within a single calorimetry experiment, one being representative of each component.⁷⁴ When sequences are instead random to such an extent that microphase segregation is spatially discouraged, the glass transition temperature for the material takes on a wider range of values spanning an area between those of the two individual components.⁷⁵ Between these ranges, however, it has been modeled and theorized that alternation fractions can produce glass transition temperatures either above or below Flory-Fox predictions, dependent upon the sequencing and displaying a stronger difference when sequences are of repeated block structures rather than pseudo-random.⁷⁶

Appendix A Spectral Data Associated with Monomer Syntheses

Appendix A.1 4-Oxocyclohexane-1-Carboxylic Acid Proton Chemical Shift Assignments & NMR Spectrum

Table 5. ^1H NMR Shift Assignment for 4-Oxocyclohexane-1-Carboxylic Acid.

			
$^1\text{H-NMR}$ (400 MHz, CDCl_3)			
δ (ppm)	Mult. (J (Hz))	Int.	Assignment
2.82	m	1	CH
2.50	m	2	CH ₂
2.37	m	2	CH ₂
2.25	m	2	CH ₂
2.06	m	2	CH ₂

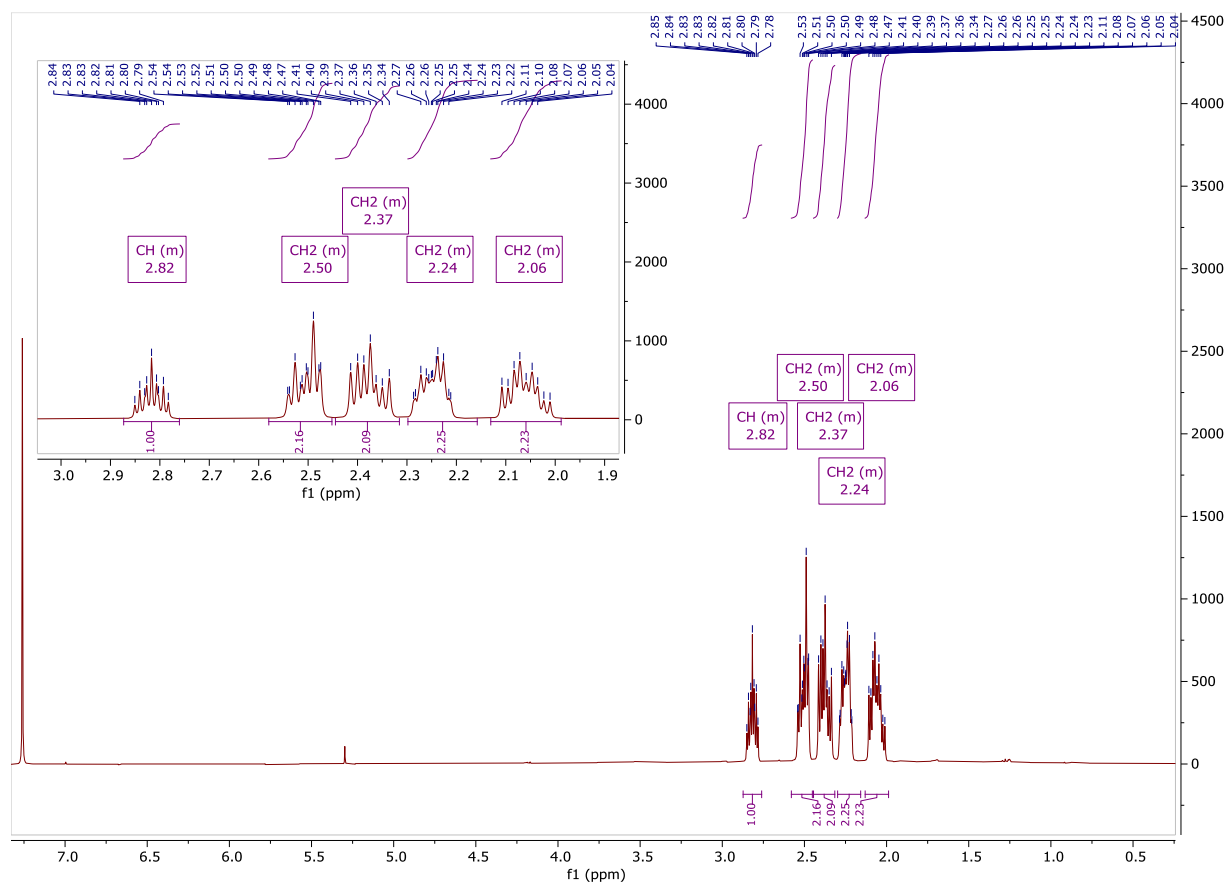
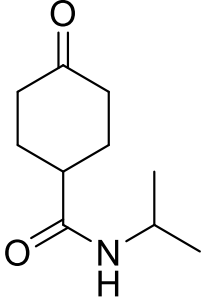


Figure 20. ^1H NMR Spectrum of 4-oxocyclohexane-1-carboxylic acid. 400 MHz, CDCl_3 .

Appendix A.2 N-Isopropyl 4-Oxocyclohexane-1-Carboxamide Proton Chemical Shift Assignments & NMR Spectrum

Table 6. ^1H NMR Shift Assignment for N-Isopropyl 4-Oxocyclohexane-1-Carboxamide.

			
$^1\text{H-NMR}$ (400 MHz, CDCl_3)			
δ (ppm)	Mult. (J (Hz))	Int.	Assignment
5.42	s	1	NH
4.08	m	1	CH
2.49	m	3	CH ₂ , CH (ring)
2.33	m	2	CH ₂ (ring)
2.14	m	2	CH ₂ (ring)
1.98	m	2	CH ₂ (ring)
1.15	d	6	CH ₃

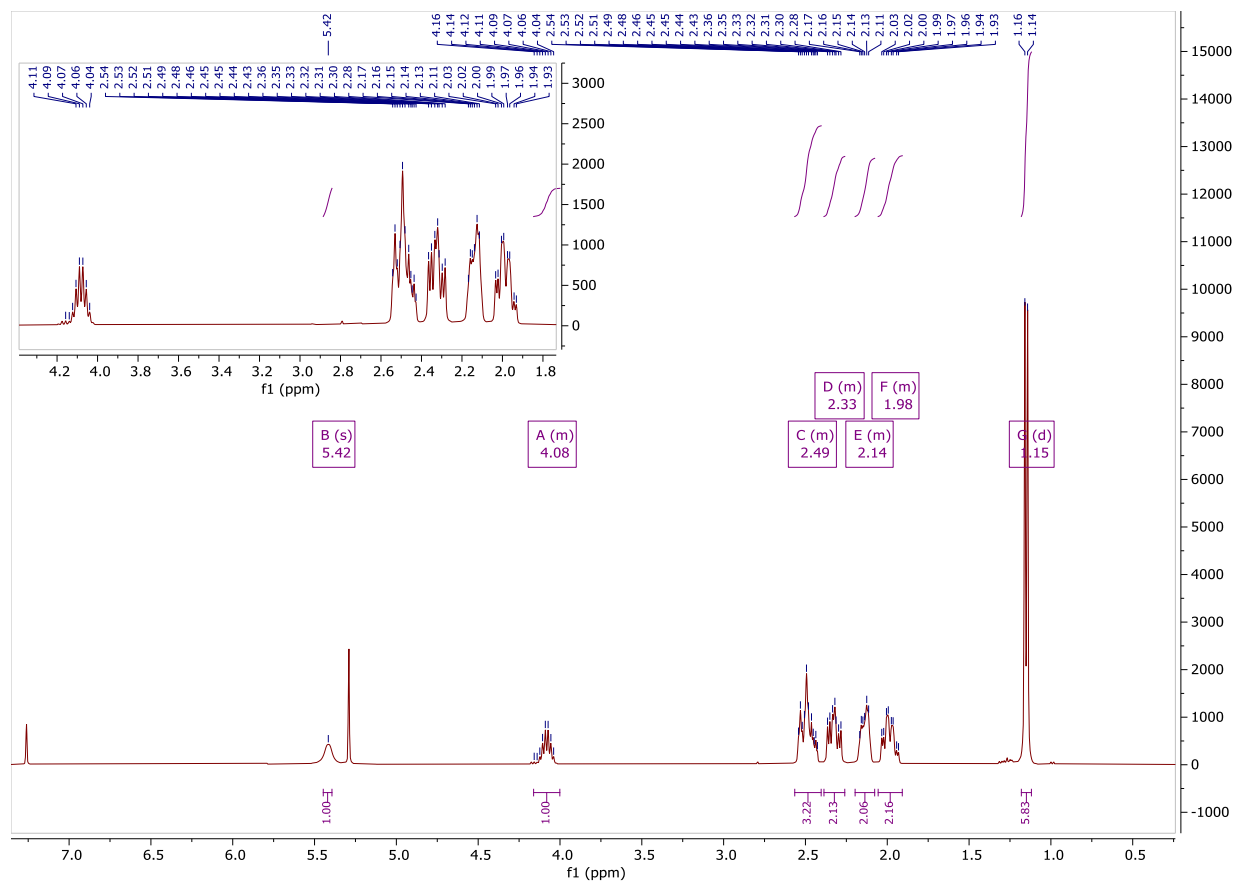
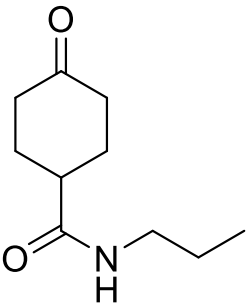


Figure 21. ^1H NMR Spectrum of N-Isopropyl 4-Oxocyclohexane-1-Carboxamide. 400 MHz, CDCl_3 .

Appendix A.3 4-Oxo-N-Propylcyclohexane-1-Carboxamide Proton Chemical Shift Assignments & NMR Spectrum

Table 7. ^1H NMR Shift Assignment for 4-Oxo-N-Propylcyclohexane-1-Carboxamide.

			
$^1\text{H-NMR}$ (400 MHz, CDCl_3)			
δ (ppm)	Mult. (J (Hz))	Int.	Assignment
5.53	s	1	NH
3.24	td (7.2, 5.8)	2	CH ₂
2.51	m	3	CH, CH ₂ (ring)
2.34	m	2	CH ₂ (ring)
2.16	m	2	CH ₂ (ring)
2.00	m	2	CH ₂ (ring)
1.54	h (7.4)	2	CH ₂
0.93	t (7.4)	3	CH ₃

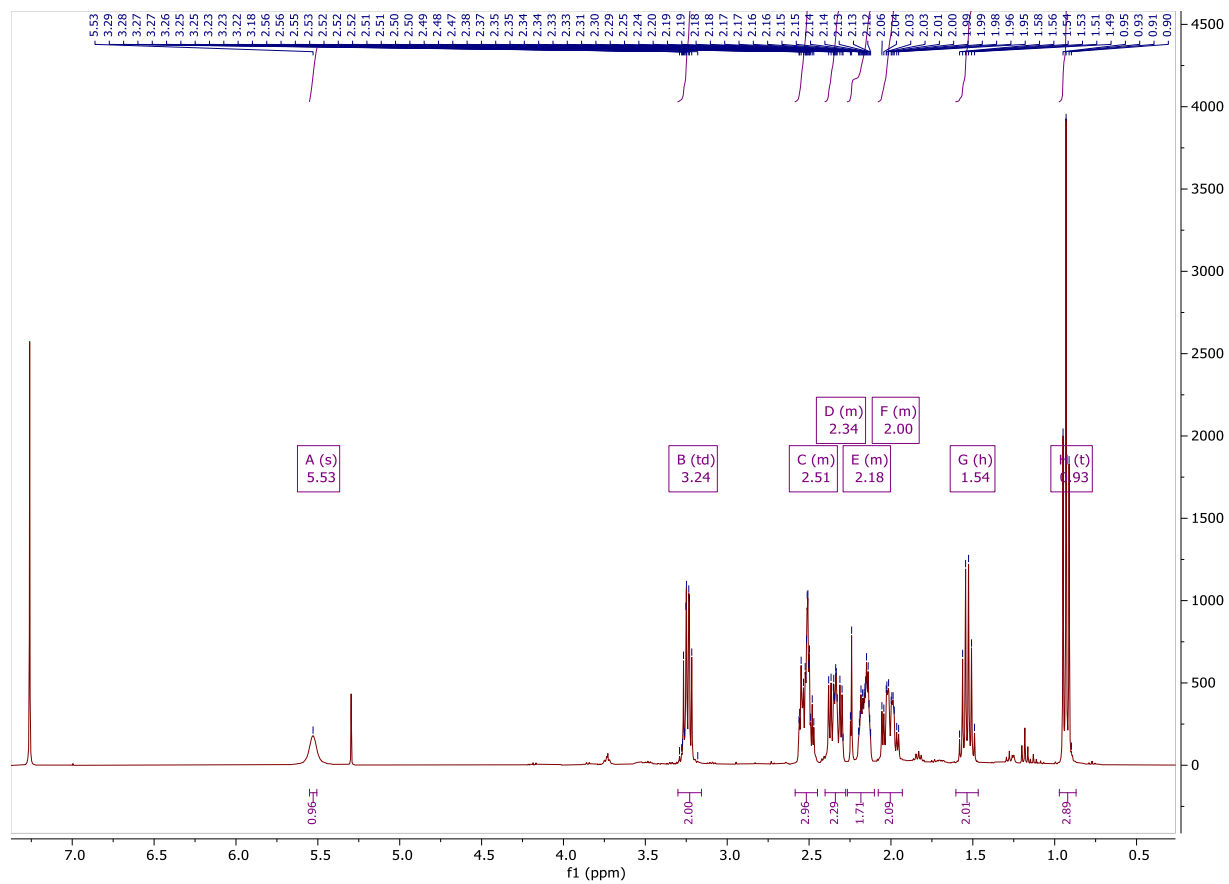
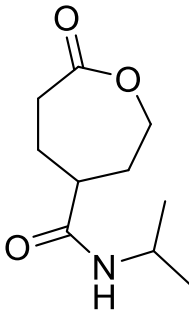


Figure 22. ¹H NMR Spectrum of N-Isopropyl 4-Oxocyclohexane-1-Carboxamide. 400 MHz, CDCl₃.

Appendix A.4 N-Isopropyl-7-Oxooxepane-4-Carboxamide (CLiPrA) Proton Chemical Shift Assignments & NMR Spectrum

Table 8. ¹H NMR Shift Assignment for N-Isopropyl-7-Oxooxepane-4-Carboxamide (CLiPrA).

			
¹H-NMR (400 MHz, CDCl₃)			
δ (ppm)	Mult. (J (Hz))	Int.	Assignment
5.25	s (br)	1	NH
4.50	ddd (13.8, 6.3, 2.5)	1	CH (ring)
4.17	ddd (12.9, 7.7, 2.4)	1	CH (ring)
4.07	m	1	CH (ring)
2.91	dd (14.4, 8.5)	1	CH (ring)
2.60	ddd (13.3, 10.8, 2.1)	1	CH (ring)
2.37	hept (4.4)	1	CH
2.07	m	3	CH, CH₂ (ring)
1.91	dd (12.5, 11.6)	1	CH (ring)
1.15	d (6.5)	6	CH₃

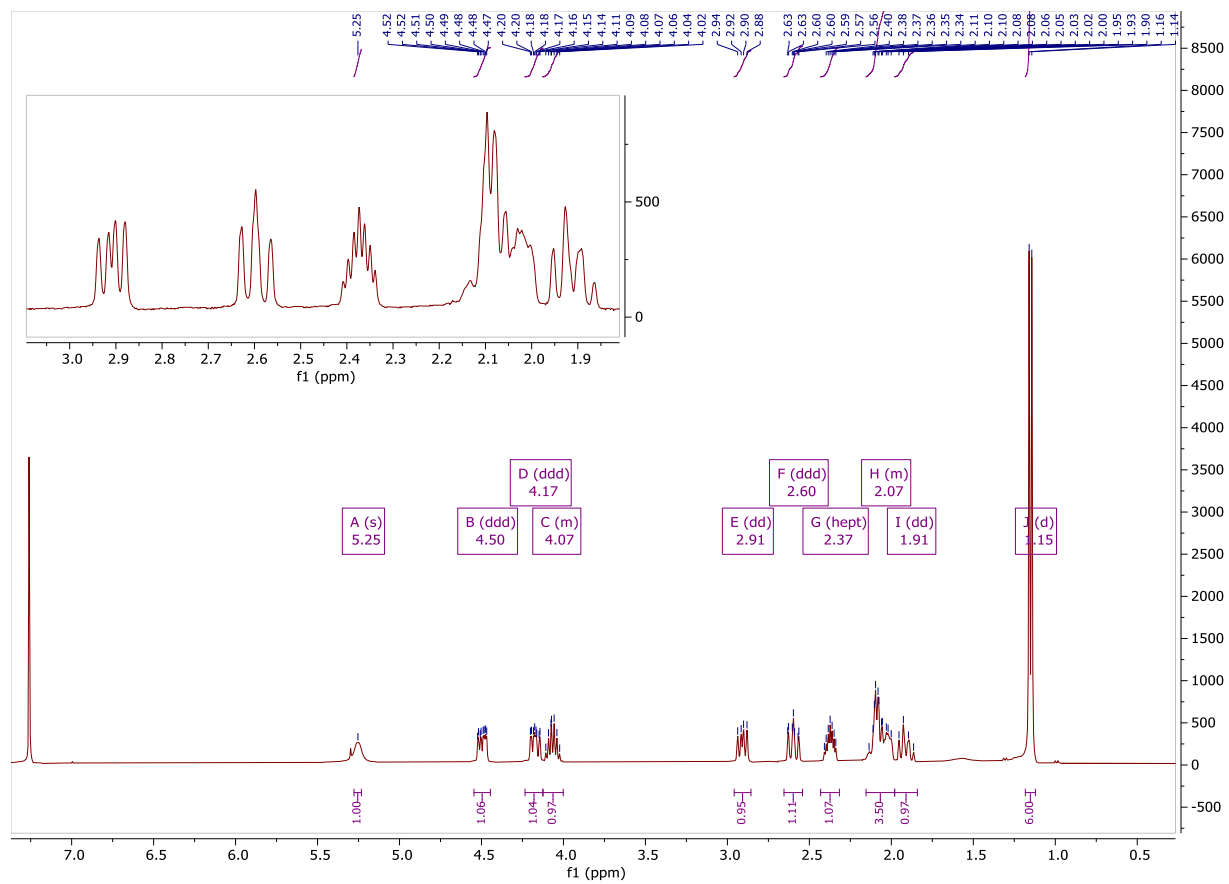
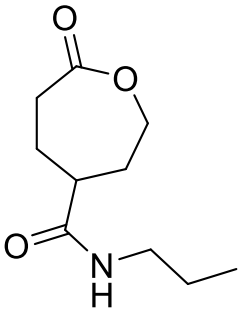


Figure 23. ¹H NMR Spectrum of N-Isopropyl-7-Oxooxepane-4-Carboxamide (CLIPrA). 400 MHz, CDCl₃.

Appendix A.5 7-Oxo-N-Propyloxepane-4-Carboxamide (CL_nPrA) Proton Chemical Shift Assignments & NMR Spectrum

Table 9. ¹H NMR Shift Assignment for 7-Oxo-N-Propyloxepane-4-Carboxamide (CL_nPrA).

			
¹H-NMR (400 MHz, CDCl₃)			
δ (ppm)	Mult. (J (Hz))	Int.	Assignment
5.53	br s	1	NH
4.49	ddd (13.1, 6.2, 2.5)	1	CH (ring)
4.18	ddd (13.1, 8.1, 2.4)	1	CH (ring)
3.22	m	2	CH₂
2.91	ddd (14.4, 8.5, 1.9)	1	CH (ring)
2.60	ddd (14.0, 11.3, 2.2)	1	CH (ring)
2.43	tt (9.3, 4.3)	1	CH (ring)
2.10	m	2	CH, CH (ring)
1.92	ddd (14.3, 11.7, 2.0)	1	CH (ring)
1.52	h (7.3)	2	CH₂
0.92	t (7.4)	3	CH₃

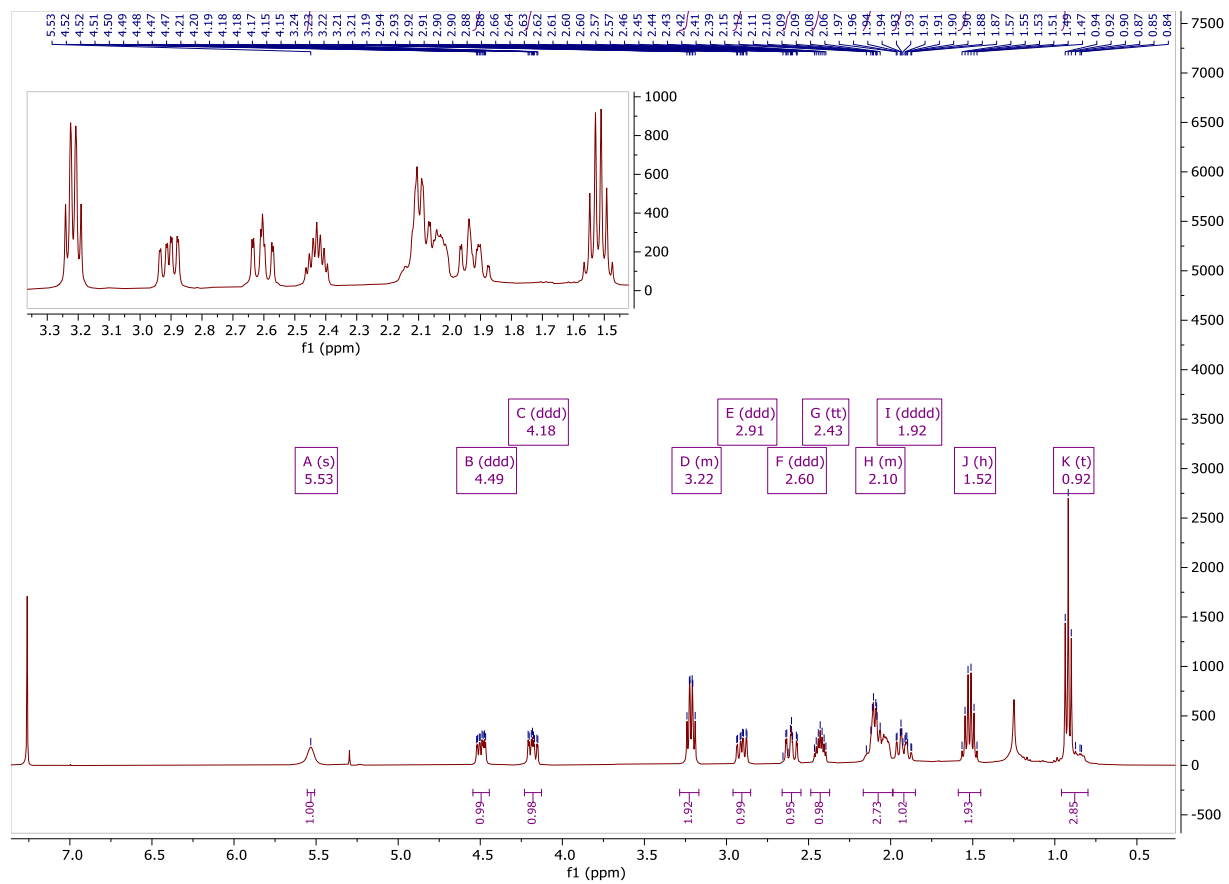
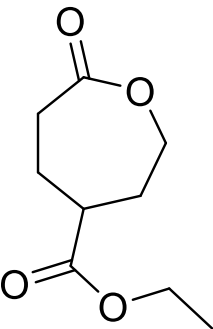


Figure 24. ¹H NMR Spectrum of 7-Oxo-N-Propyloxepane-4-Carboxamide (CL_nPrA). 400 MHz, CDCl₃.

Appendix A.6 Ethyl 7-Oxooxepane-4-Carboxylate (CL_{COOEt}) Proton Chemical Shift Assignments & NMR Spectrum

Table 10. ¹H NMR Shift Assignment for Ethyl 7-Oxooxepane-4-Carboxylate (CL_{COOEt}).

			
¹ H-NMR (400 MHz, CDCl ₃)			
δ (ppm)	Mult. (J (Hz))	Int.	Assignment
4.38	ddd (13.2, 7.1, 1.8)	1	CH (ring)
4.19	m	3	CH (ring), CH₂
2.79	ddd (14.4, 9.1, 1.8)	1	CH (ring)
2.64	m	2	CH (ring)
2.12	m	3	CH (ring)
1.96	dddd (14.6, 11.1, 9.3, 1.8)	1	CH
1.27	t (7.1 Hz)	3	CH₃

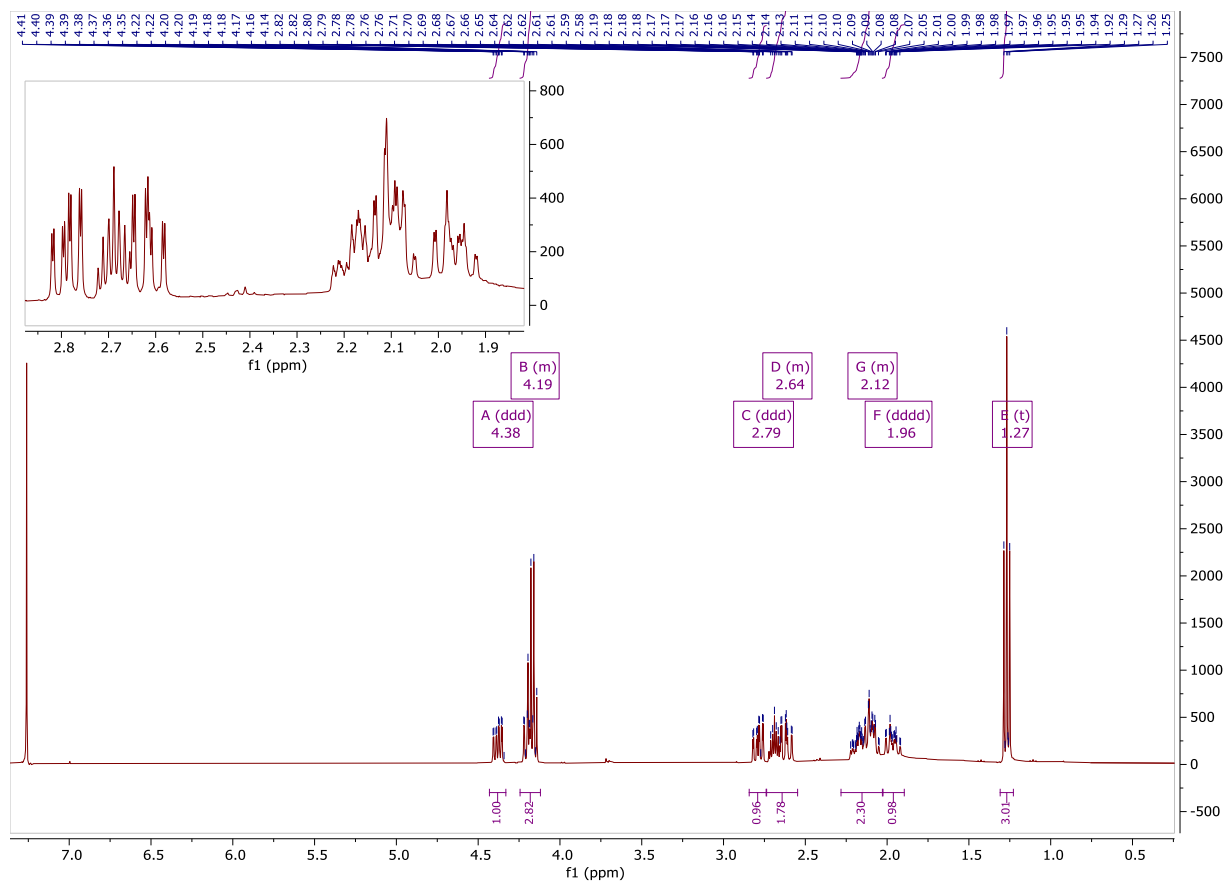


Figure 25. ¹H NMR Spectrum of Ethyl 7-Oxooxepane-4-Carboxylate (CLCOOEt). 400 MHz, CDCl₃.

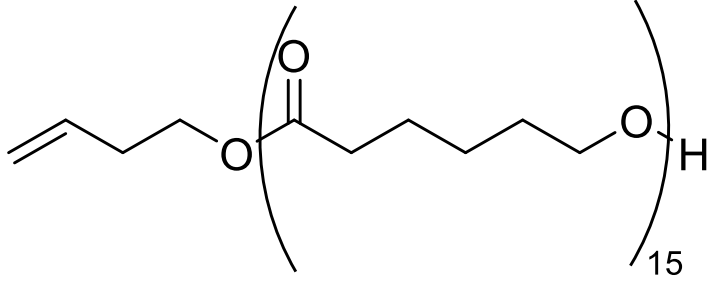
Appendix B Spectral Data Associated with Syntheses of γ -Substituted ϵ -Caprolactone

Oligomers

Appendix B.1 1,3-Butenol and Hydroxyl Capped Oligo- ϵ -Caprolactone (CLO15-OH) Proton

Chemical Shift Assignments & NMR Spectrum

Table 11. ^1H NMR Shift Assignment for 1,3-Butenol- and Hydroxyl- Capped Oligo- ϵ -Caprolactone (CLO15-OH).

			
$^1\text{H-NMR}$ (400 MHz, CDCl_3)			
δ (ppm)	Mult. (J (Hz))	Int.	Assignment
5.78	ddt (17.1, 10.2, 6.7)	1	$\text{H}_2\text{C}=\text{CH}$
5.09	m	2	$\text{H}_2\text{C}=\text{CH}$
4.13	t (6.8)	2	CH_2 (end group)
4.06	t (6.7)	20	CH_2 (internal)
3.65	q (6.2)	2	CH_2 (end group)
2.39	tt (6.7, 1.4)	2	CH_2 (end group)
2.31	m	21	CH_2 (internal)
1.64	m	47	CH_2, CH_2 (internal, end group)
1.38	m	21	CH_2 (internal)

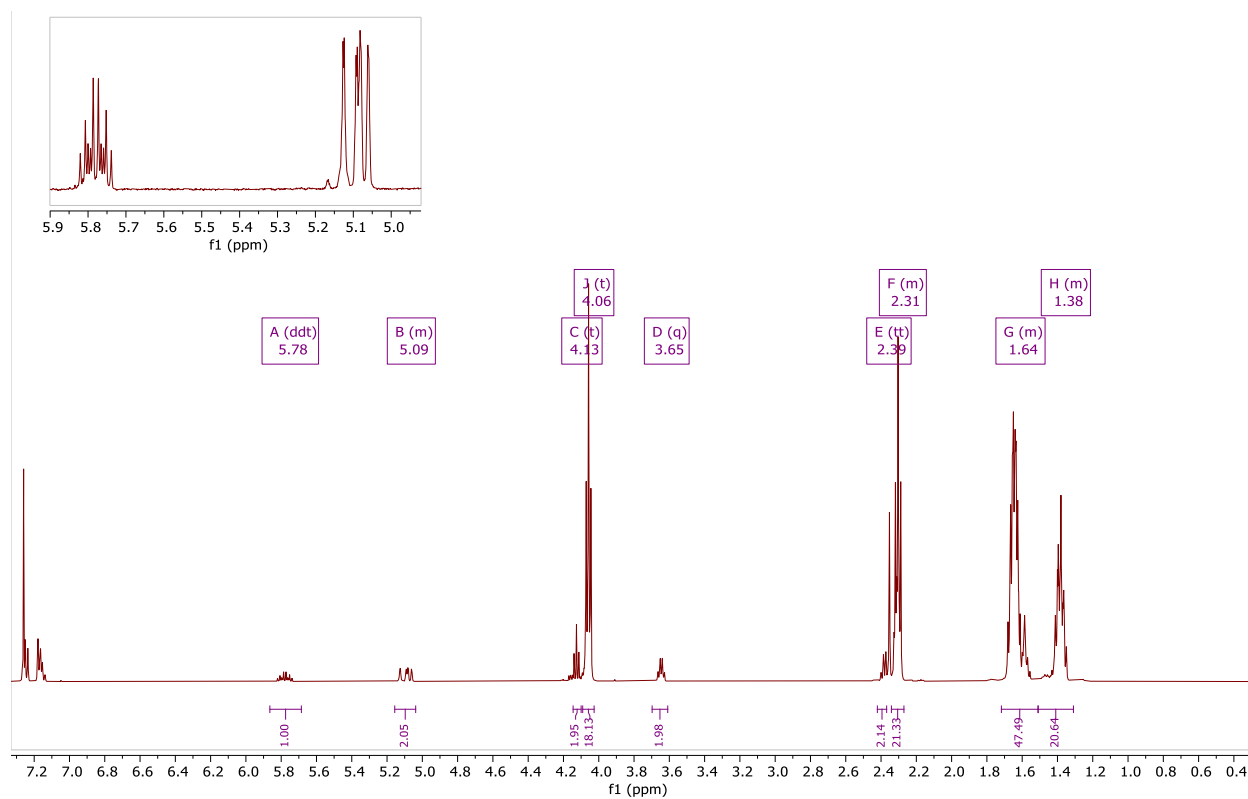
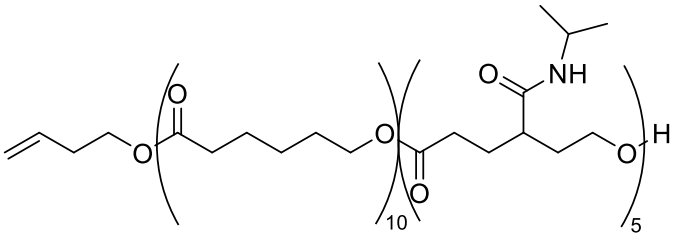


Figure 26. ¹H NMR Spectrum of 1,3-Butenol- and Hydroxyl- Capped Oligo-ε-Caprolactone (CL_o15-OH). 400 MHz, CDCl₃.

Appendix B.2 1,3-Butenol and Hydroxyl Capped Oligo- ϵ -Caprolactone-*block*- ϵ -Caprolactone- γ -Isopropyl Amide (CL_O10-CL_{iPrA}5-OH) Chemical Shift Assignments, ¹³C and ¹H NMR Spectra, and SEC.

Table 12. ¹H and ¹³C NMR Shift Assignments for 1,3-Butenol- and Hydroxyl- Capped Oligo- ϵ -Caprolactone-*block*- ϵ -Caprolactone- γ -Isopropyl Amide (CL_O10-CL_{iPrA}5-OH).

CL_O10-CL_{iPrA}5-OH				¹³ C-NMR (500 MHz, CDCl ₃)	
				δ (ppm)	Assignment
				¹H-NMR (400 MHz, CDCl₃)	
δ (ppm)	Mult. (J (Hz))	Int.	Assignment	176.5	H ₂ C=CH
5.77	m	1	H ₂ C=CH	173.88	C=O
5.10	m	2	H ₂ C=CH	173.15	C=O
4.13	m	16	CL _O CH ₂ (internal)	172.22	HN-C=O
3.67	m	12	CL _A CH ₂ (internal), CL _O CH ₂ (end group)	171.39	H ₂ C=CH
2.38	t (7.3)	8	CL _A CH ₂ (internal)	69.68	C-O
2.31	td (7.5, 3.5)	20	CL _O CH ₂ (end group, internal)	66.96	C-O
1.64	m	56	CL _O , CL _A CH ₂ (internal)	64.53	C-O
1.40	m	30	CL _O , CL _A CH ₂ (internal, end group)	63.39	C-N
1.16	d (3.4)	30	CL _A CH ₃	63.39	C-N
				23.14	CH ₃
				45.24	HN-C-(CH ₃) ₂
				34.51	CH ₂
				34.10	CH ₂
				32.04	CH ₂
				29.35	CH ₂
				28.69	CH ₂
				25.88	CH ₂
				24.94	CH ₂
				23.14	CH ₂

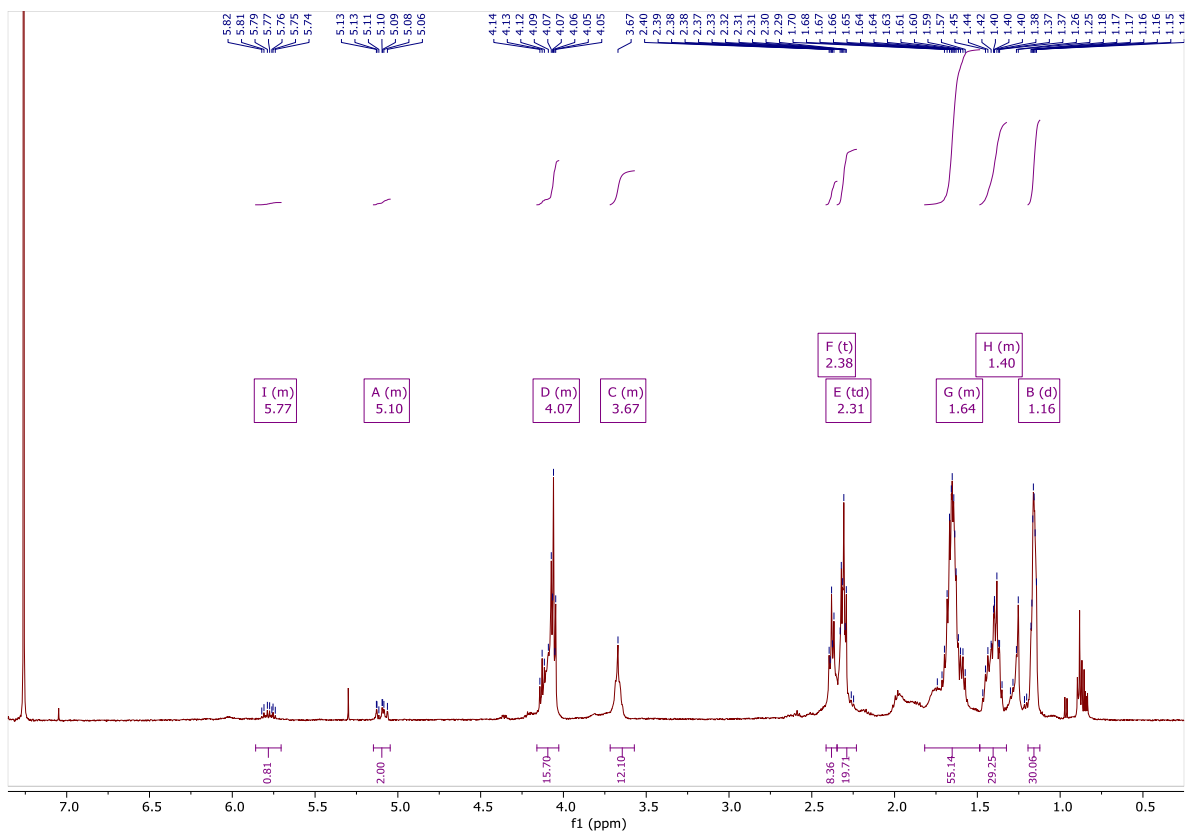


Figure 27. ^1H NMR Spectrum of 1,3-Butenol- and Hydroxyl- Capped Oligo- ϵ -Caprolactone-*block*- ϵ -Caprolactone- γ -Isopropyl Amide (CL₀10-CL_{iPrA}5-OH). 400 MHz, CDCl₃.

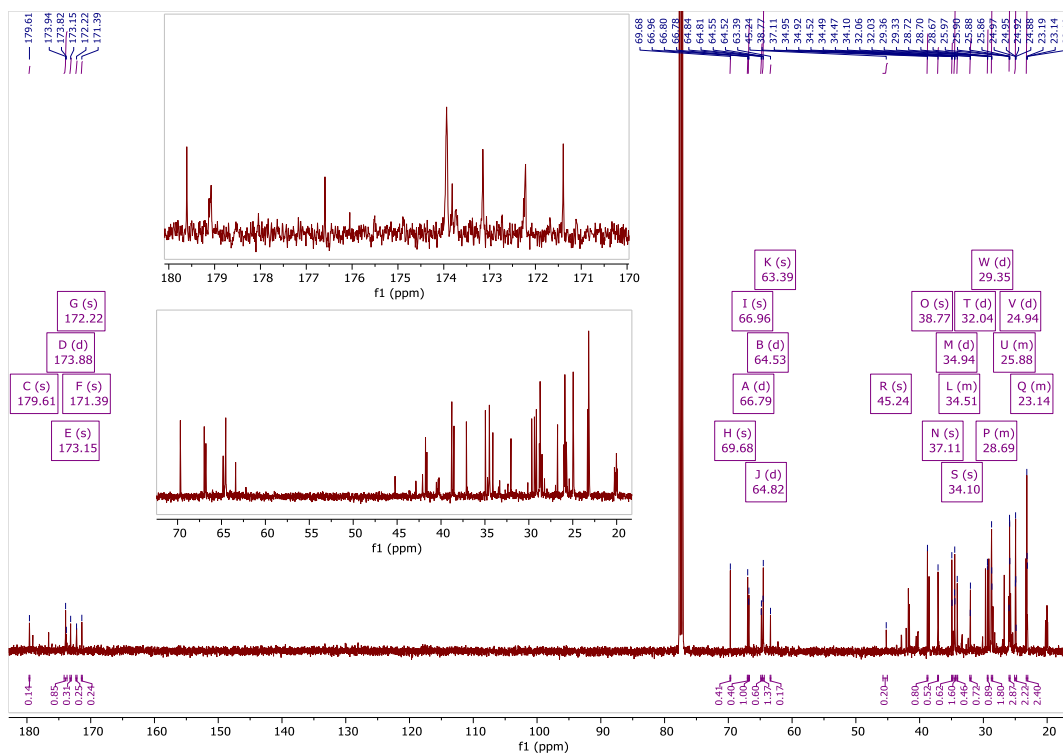


Figure 28. ^{13}C NMR Spectrum of 1,3-Butenol- and Hydroxyl- Capped Oligo- ϵ -Caprolactone-*block*- ϵ -Caprolactone- γ -Isopropyl Amide (CL_o10-CL_{iPrA}5-OH). 500 MHz, CDCl₃.

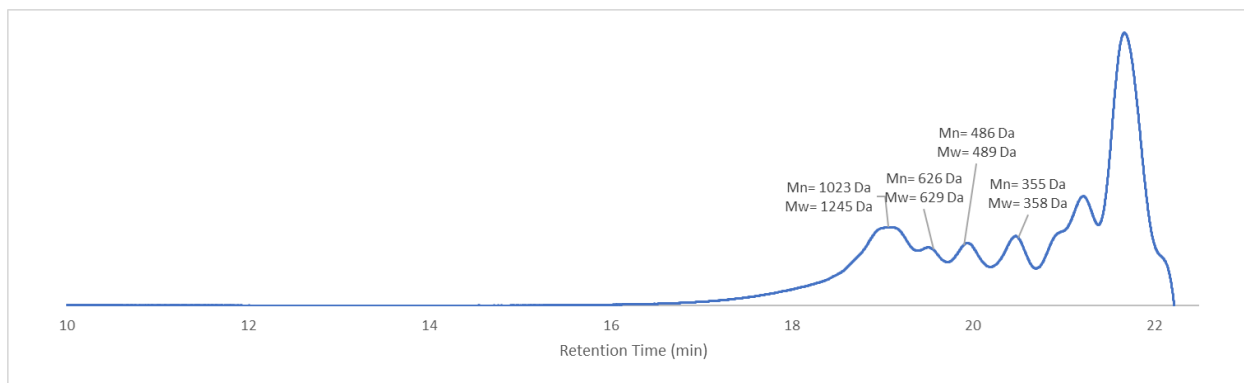
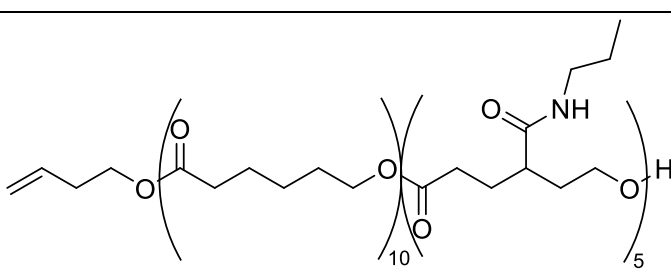


Figure 29. SEC Chromatogram of 1,3-Butenol- and Hydroxyl- Capped Oligo- ϵ -Caprolactone-*block*- ϵ -Caprolactone- γ -Isopropyl Amide (CL_o10-CL_{iPrA}5-OH).

Appendix B.3 1,3-Butenol and Hydroxyl Capped Oligo- ϵ -Caprolactone-*block*- ϵ -Caprolactone- γ -N-propyl Amide (CL₀10-CL_{nPrA}5-OH) Chemical Shift Assignments, ¹³C and ¹H NMR Spectra, SEC, and MALDI-TOF.

Table 13. ¹H and ¹³C NMR Shift Assignments for 1,3-Butenol- and Hydroxyl- Capped Oligo- ϵ -Caprolactone-*block*- ϵ -Caprolactone- γ -N-propyl Amide (CL₀10-CL_{nPrA}5-OH).

CL₀10-CL_{nPrA}5-OH				¹³ C-NMR (500 MHz, CDCl ₃)	
				δ (ppm)	Assignment
				173.69	C=O
				134.18	H ₂ C=CH
				117.31	H ₂ C=CH
¹ H-NMR (400 MHz, CDCl ₃)				64.26	C-O
δ (ppm)	Mult. (J (Hz))	Int.	Assignment	63.47	C-O
5.77	ddt (17.1, 10.2, 6.7)	1	H ₂ C=CH	62.77	C-O
5.09	m	2	H ₂ C=CH	34.30	CH ₂
4.11	t (6.7)	2	CH ₂ (end group)	33.23	CH ₂
4.05	t (6.6)	10	CL ₀ CH ₂ (internal)	32.46	CH ₂
3.64	d (11.2)	2	CH ₂ (end group)	30.45	CH ₂
3.21	t (8.3)	2	CL _A CH ₂	28.48	CH ₂
2.37	q (6.9)	2	CL _A CH ₂	25.67	CH ₂
2.30	m	10	CL ₀ CH ₂ (internal, end group)	25.41	CH ₂
1.63	m	22	CL ₀ , CL _A CH ₂ (internal)	24.76	CH ₂
1.39	m	12	CL ₀ , CL _A CH ₃ (internal, end group)		
0.91	t (7.3)	2	CL _A CH ₃		

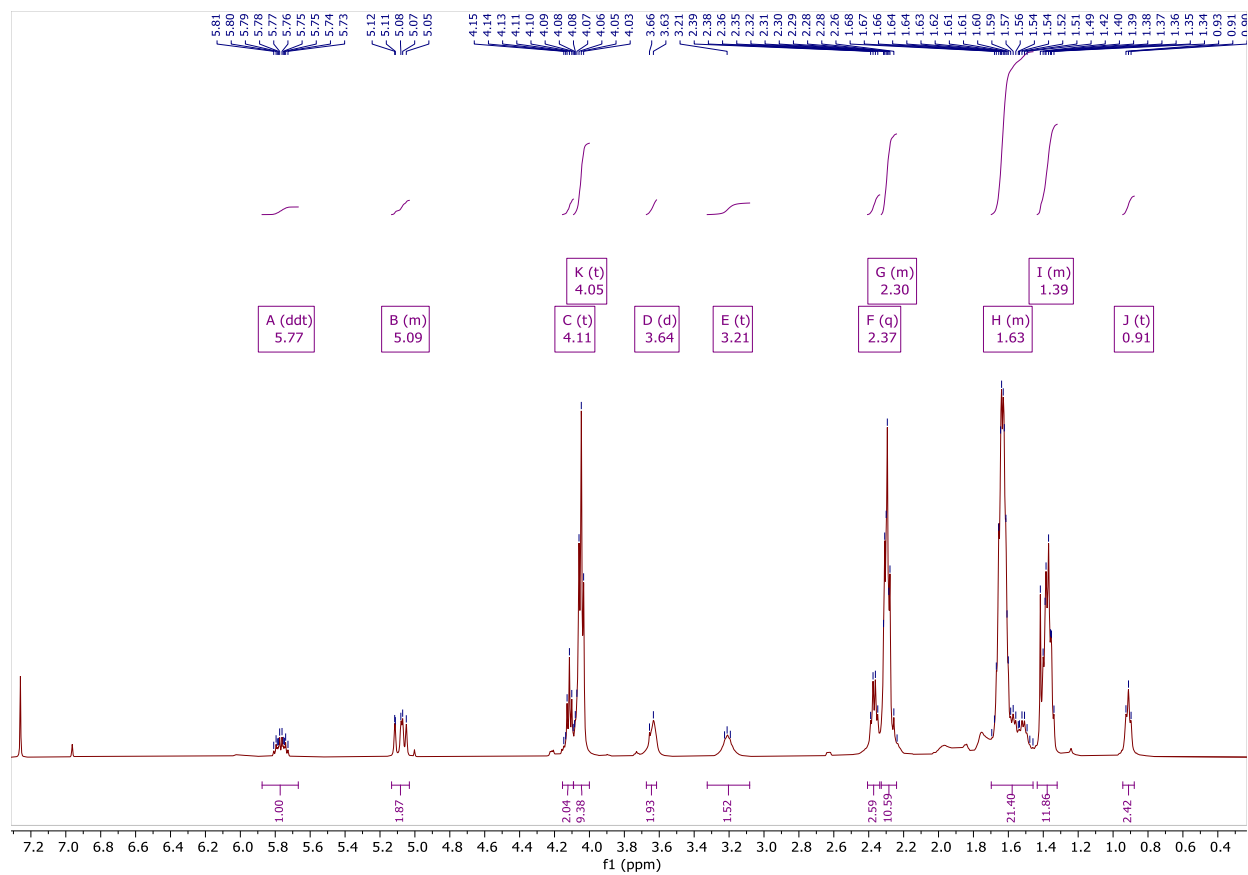


Figure 30. ¹H NMR Spectrum of 1,3-Butenol- and Hydroxyl- Capped Oligo-ε-Caprolactone-*block*-ε-Caprolactone-γ-N-propyl Amide (CL₀10-CL_nPrA5-OH). 400 MHz, CDCl₃.

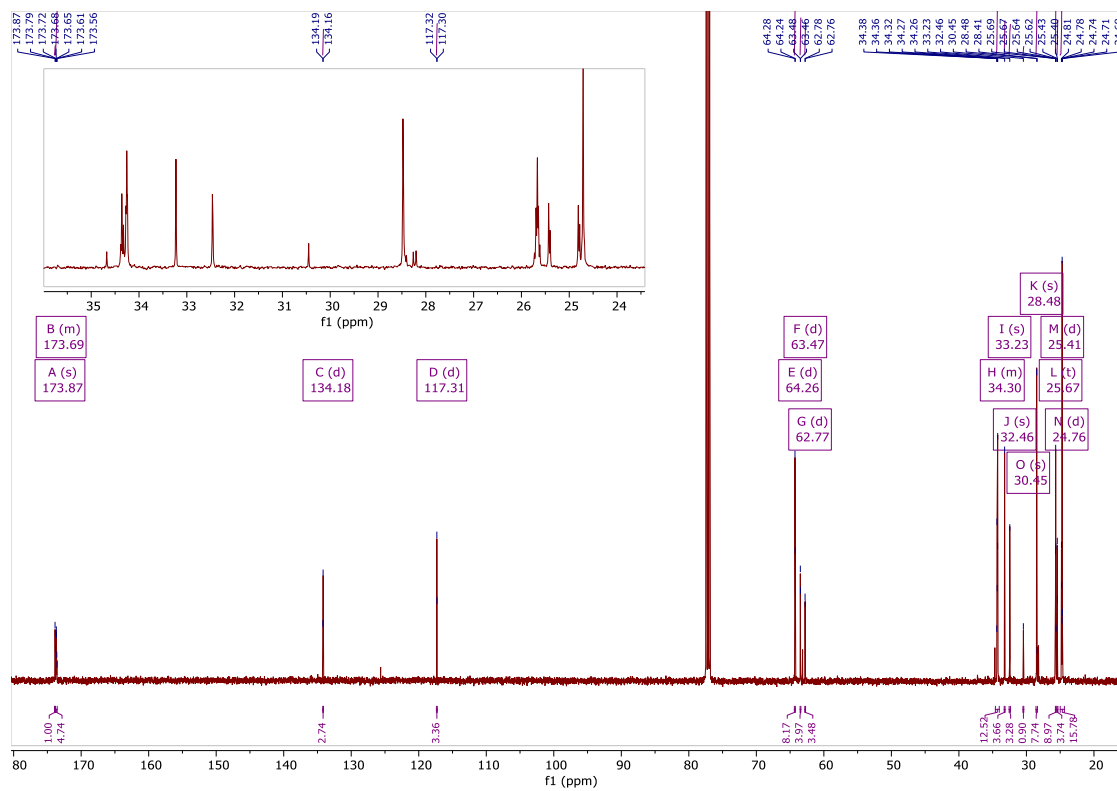


Figure 31. ¹³C NMR Spectrum of 1,3-Butenol- and Hydroxyl- Capped Oligo-ε-Caprolactone-*block*-ε-Caprolactone-γ-N-propyl Amide (CL₀10-CL_nPrA5-OH). 500 MHz, CDCl₃.

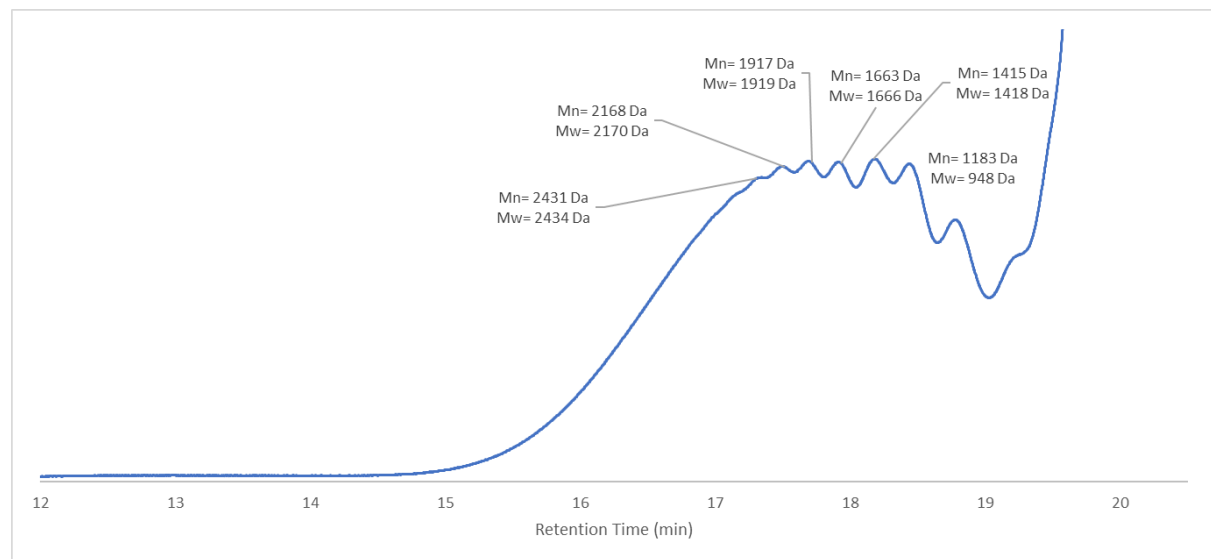


Figure 32. SEC Chromatogram of CL₀10-CL_nPrA5-OH taken in THF, calibrated to polystyrene standards.

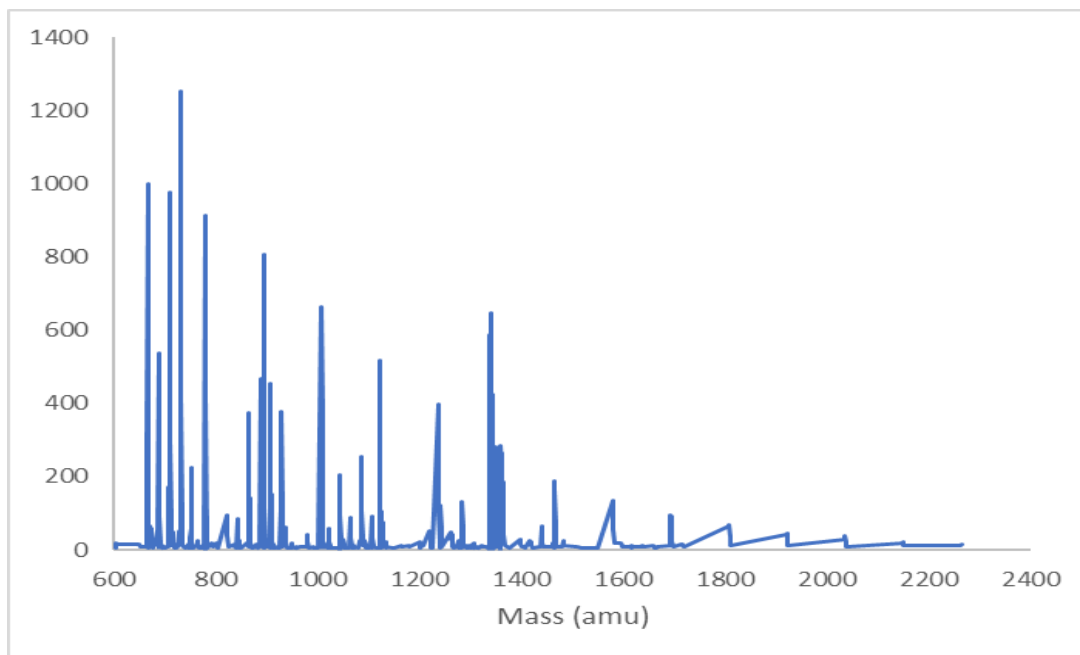
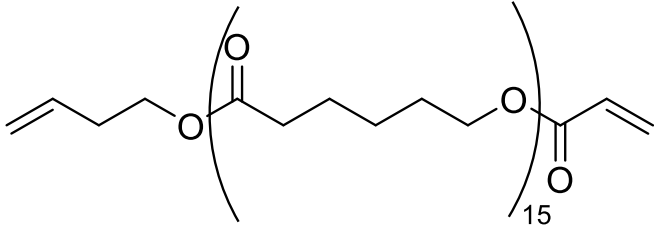


Figure 33. MALDI-TOF spectra of CL_o10-CL_{nPrA}5-OH, masses shown with Na⁺ adducts.

Appendix C Spectral Data Associated with End Group Modifications of γ -Substituted ϵ -Caprolactone Oligomers

Appendix C.1 1,3-Butenol and Acrylate- Capped Oligo- ϵ -Caprolactone (CL₀15) Proton Chemical Shift Assignments & NMR Spectrum

Table 14. ¹H NMR Shift Assignments for 1,3-Butenol- and Acrylate- Capped Oligo- ϵ -Caprolactone (CL₀15).

			
¹ H-NMR (400 MHz, CDCl ₃)			
δ (ppm)	Mult. (J (Hz))	Int.	Assignment
6.40	d (17.3)	1	H₂C=CH
6.12	m	1	H ₂ C= CH
5.82	m	2	H₂C=CH , H ₂ C= CH
5.09	m	2	H₂C=CH
4.12	m	2	CH₂ (end group)
4.06	t (6.7)	24	CH₂ (internal)
3.66	d (9.7)	2	CH₂ (end group)
2.38	t (6.9)	2	CH₂ (end group)
2.31	t (7.5)	28	CH₂ (internal, end group)
1.64	tt (10.1, 5.5)	57	CH₂ , CH₂ (internal, end group)
1.38	m	30	CH₂ (internal, end group)

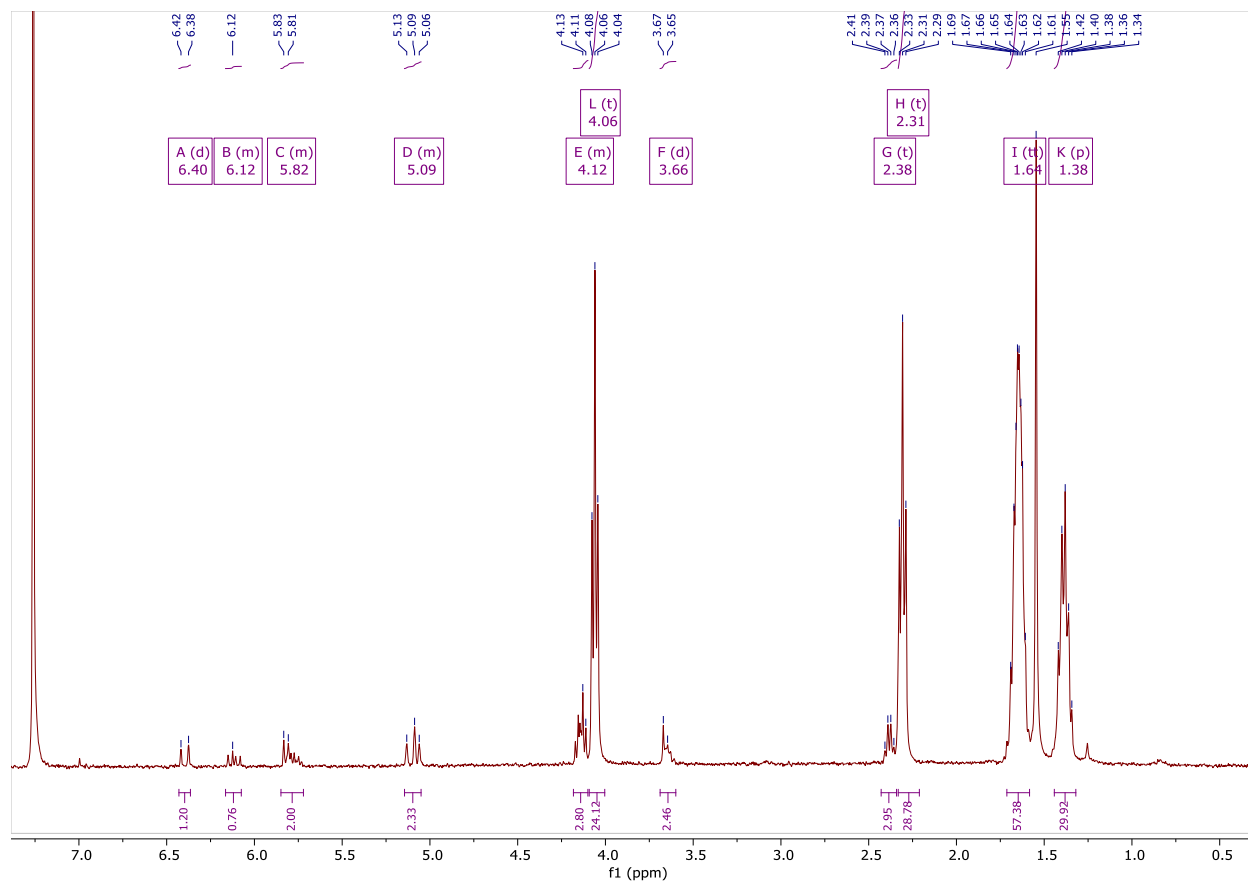


Figure 34. ¹H NMR Spectrum of 1,3-Butenol- and Acrylate- Capped Oligo-ε-Caprolactone (CLO15) 400 MHz, CDCl₃.

Appendix C.2 1,3-Butenol and Acrylate-Capped Oligo- ϵ -Caprolactone-*block*- ϵ -Caprolactone- γ -Isopropyl Amide (CL_O10-CL_{iPrA}5) Proton Chemical Shift Assignments, ¹H NMR Spectrum, and MALDI-TOF Spectrum.

Table 15. ¹H NMR Shift Assignments for 1,3-Butenol- and Acrylate-Capped Oligo- ϵ -Caprolactone-*block*- ϵ -Caprolactone- γ -Isopropyl Amide (CL_O10-CL_{iPrA}5).

¹ H-NMR (400 MHz, CDCl ₃)			
δ (ppm)	Mult. (J (Hz))	Int.	Assignment
6.40	dt (17.3, 3.1)	1	H₂C=CH
6.12	m	1	H ₂ C= CH
5.79	m	2	H ₂ C= CH ; H ₂ C= CH
5.09	m	2	H₂C=CH
4.08	m	38	CL _O , CL _A CH₂ (end group, internal)
3.72	m	6	CL _A CH₂ (internal)
2.32	m	36	CL _O CH₂ (internal)
1.64	m	56	CL _O , CL _A CH₂ (internal)
1.39	m	30	CL _O , CL _A CH₂ (internal, end group)
1.17	m	24	CL _A CH₃

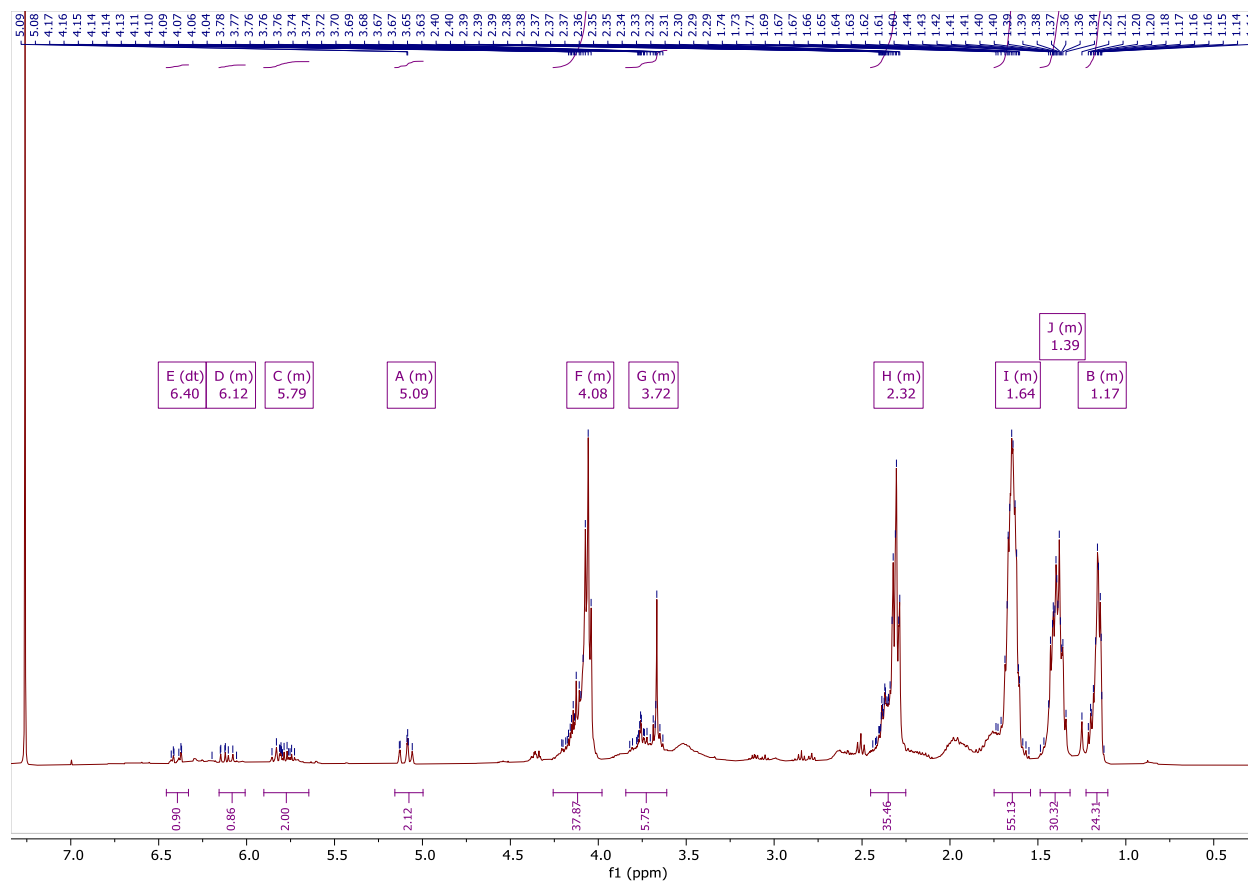


Figure 35. ¹H NMR Spectrum of 1,3-Butenol- and Acrylate- Capped Oligo-ε-Caprolactone-*block*-ε-Caprolactone-γ-Isopropyl Amide (CL_o10-CL_{iPrA}5). 400 MHz, CDCl₃.

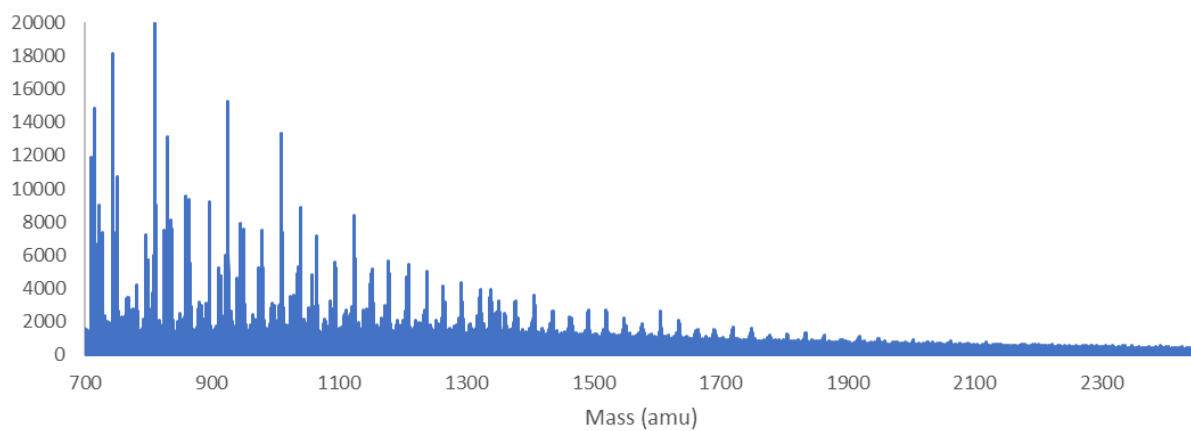
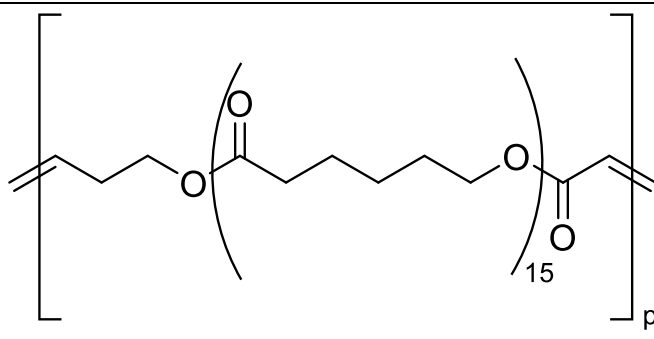


Figure 36. MALDI- TOF Spectrum of 1,3-Butenol- and Acrylate- Capped Oligo-ε-Caprolactone-*block*-ε-Caprolactone-γ-Isopropyl Amide (CL_o10-CL_{iPrA}5).

Appendix D Spectral Data Associated with Polymerization of γ -Substituted ϵ -Caprolactone Oligomers

Appendix D.1 ADMET-Synthesized Poly- ϵ -caprolactone (p[CLo15]) Proton Chemical Shift Assignments, ^1H NMR Spectrum, and MALDI-TOF Spectrum.

Table 16. ^1H NMR Shift Assignments for ADMET-Synthesized Poly- ϵ -caprolactone (p[CLo15]).

			
$^1\text{H-NMR}$ (400 MHz, CDCl_3)			
δ (ppm)	Mult. (J (Hz))	Int.	Assignment
6.91	dt (14.6, 6.9)	1	HC=CH (H-T)
5.90	d (15.8)	1	HC=CH (H-T)
5.64	m	0.35	HC=CH (H-H)
5.49	m	0.27	HC=CH (H-H)
4.06	t (6.7)	28	CH₂ (internal)
3.66	d (8.3)	2	CH₂ (end group)
2.54	q (2.54)	2	CH₂ (end group)
2.31	t (7.4)	32	CH₂ (internal, end group)
1.65	m	65	CH₂, CH₂ (internal, end group)
1.38	m	32	CH₂ (internal, end group)

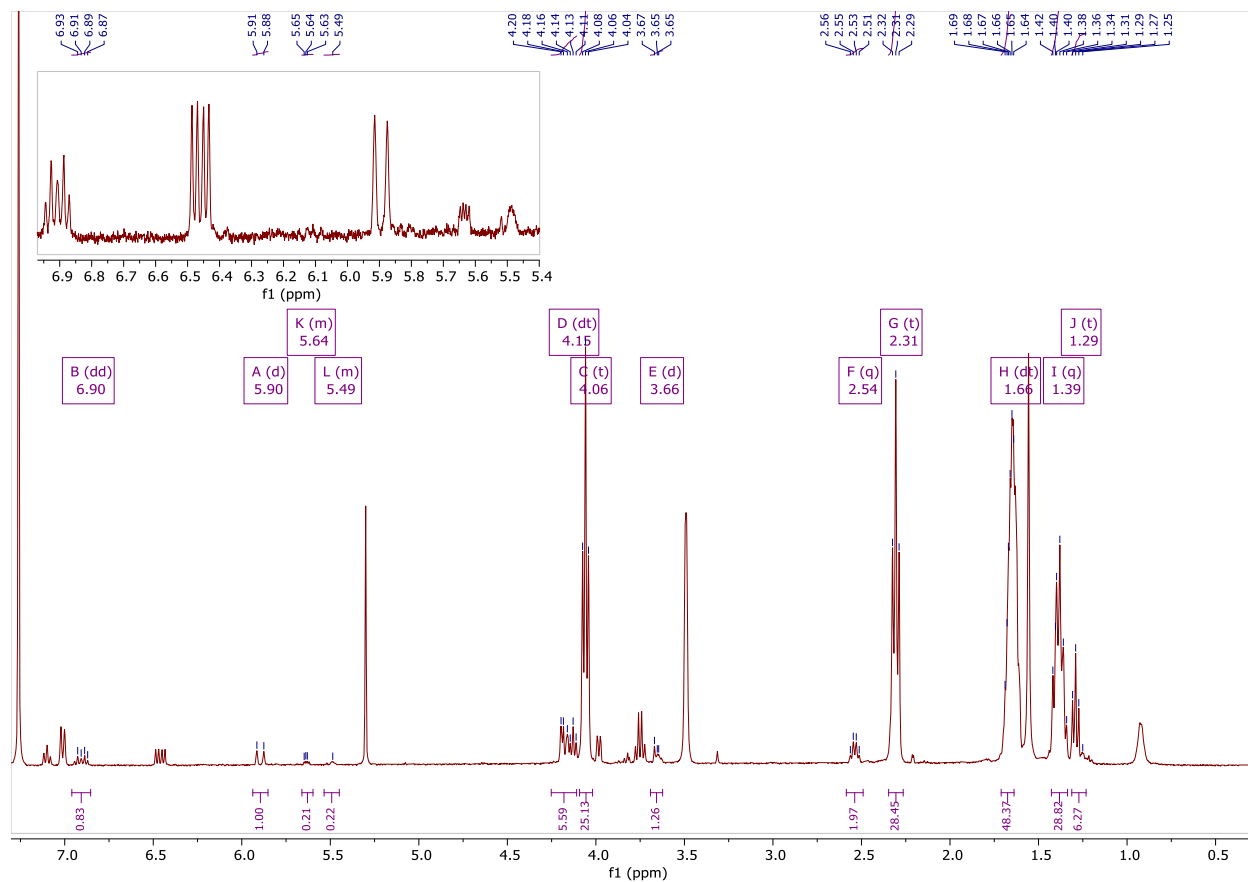


Figure 37. ^1H NMR Spectrum of ADMET-Synthesized Poly- ϵ -caprolactone (p[CL_o15]). 400 MHz, CDCl₃.

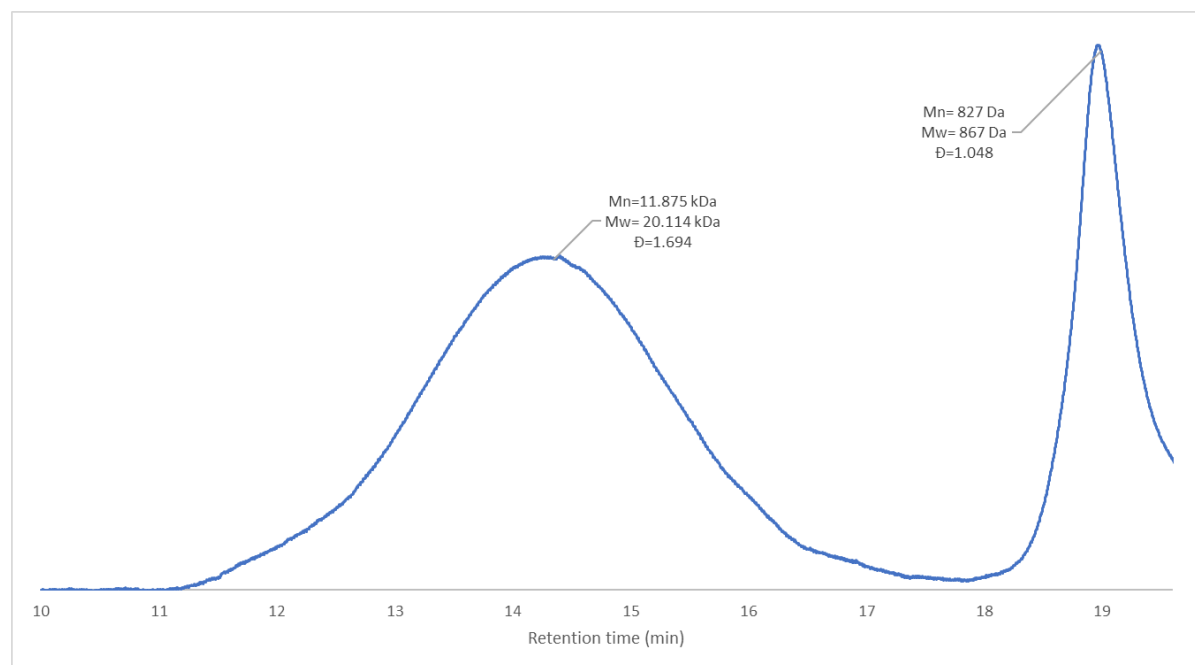


Figure 38. SEC chromatogram of ADMET-Synthesized Poly- ϵ -caprolactone (p[CL_o15]).

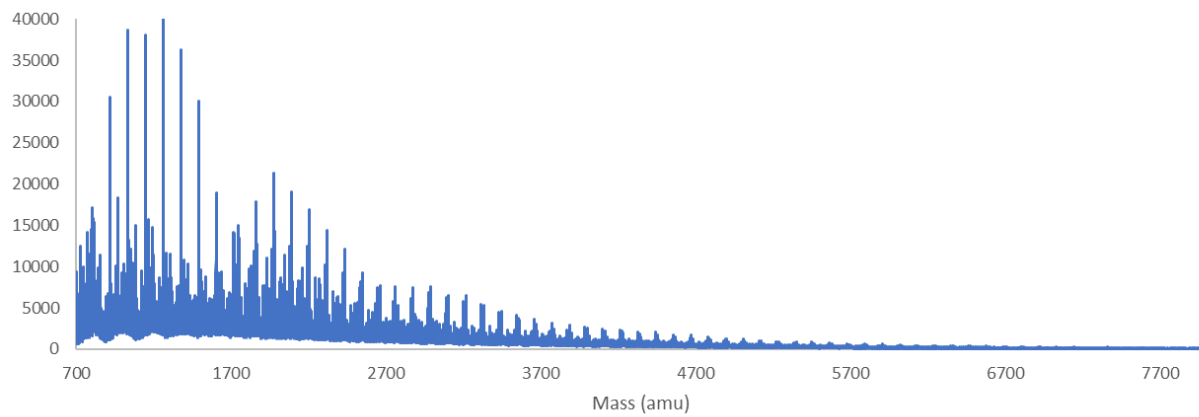


Figure 39. MALDI-TOF Spectra of ADMET-Synthesized Poly- ϵ -caprolactone (p[CLo15]).

Appendix D.2 ADMET-Synthesized Poly-[Oligo-(ϵ -Caprolactone)-*block*-(ϵ -Caprolactone- γ -Isopropyl Amide)] (p[CL_O10-CL_{iPrA}5]) Proton Chemical Shift Assignments, ¹H NMR Spectrum, and MALDI-TOF Spectrum.

Table 17. ¹H NMR Shift Assignments for ADMET-Synthesized Poly-[Oligo-(ϵ -Caprolactone)-*block*-(ϵ -Caprolactone- γ -Isopropyl Amide)] (p[CL_O10-CL_{iPrA}5]).

¹ H-NMR (400 MHz, CDCl ₃)			
δ (ppm)	Mult. (J (Hz))	Int.	Assignment
6.95	d (7.5)	1	HC=CH (H-T)
6.40	d (17.1)	1	H₂C=CH
6.12	dd (17.3, 10.5)	2	H ₂ C= CH
5.84	t (11.5)	2	HC=CH (H-T), H₂C=CH
4.35	d (7.2)	2	CH₂ (end group)
4.07	m	62	CL _O , CL _A CH₂ (end group, internal)
3.12	m	10	CL _A CH (internal)
2.51	m	2	CH₂ (end group)
2.31	m	58	CL _O , CL _A CH₂ (internal)
1.65	m	124	CL _O , CL _A CH₂ (end group, internal)
1.40	m	52	CL _O CH₂ (internal)
1.27	m	12	CL _A CH (internal)
1.16	d (6.5)	42	CL _A CH₃

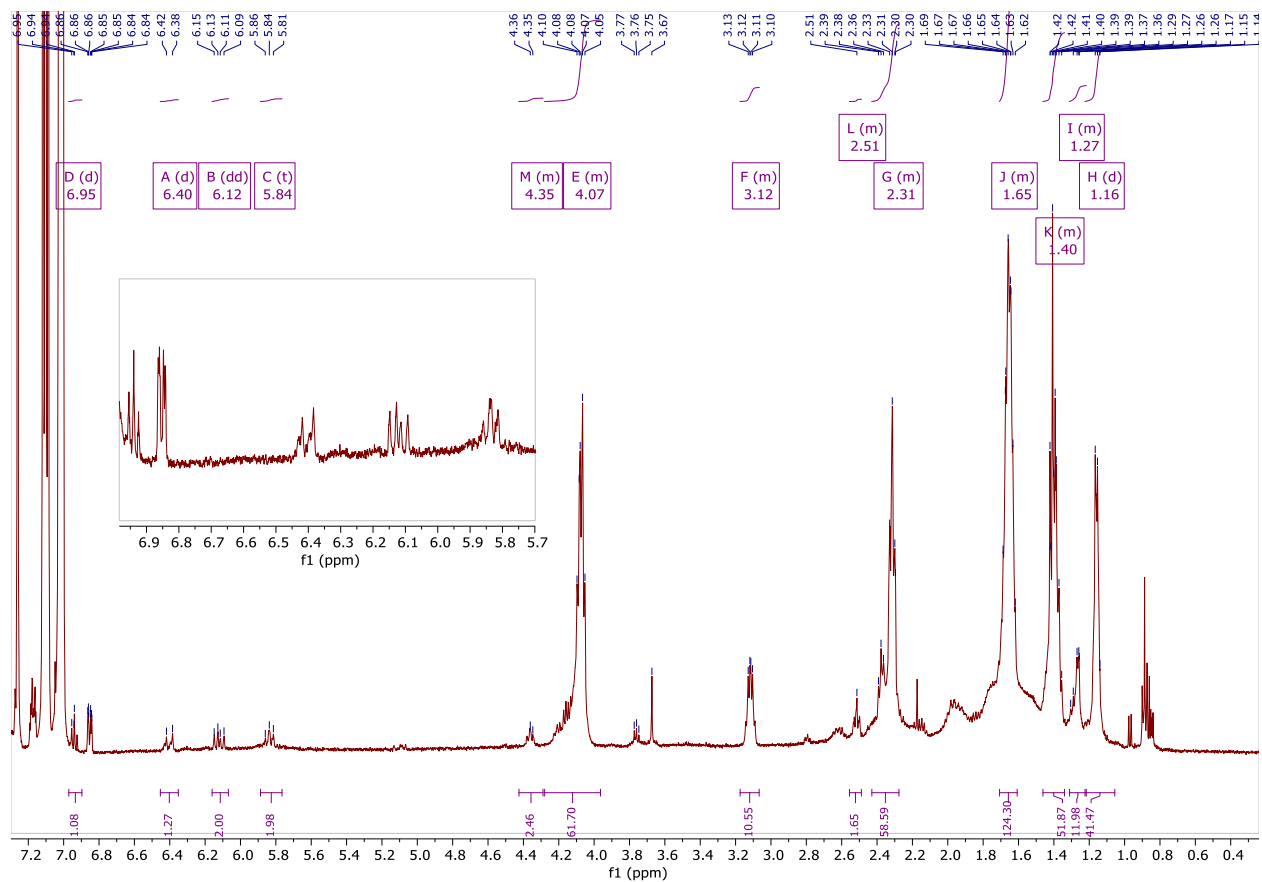


Figure 40. ¹H NMR Spectrum of ADMET-Synthesized Poly-[Oligo-(ϵ -Caprolactone)-*block*-(ϵ -Caprolactone- γ -Isopropyl Amide)] (p[CL_o10-CL_{iPrA}5]). 400 MHz, CDCl₃.

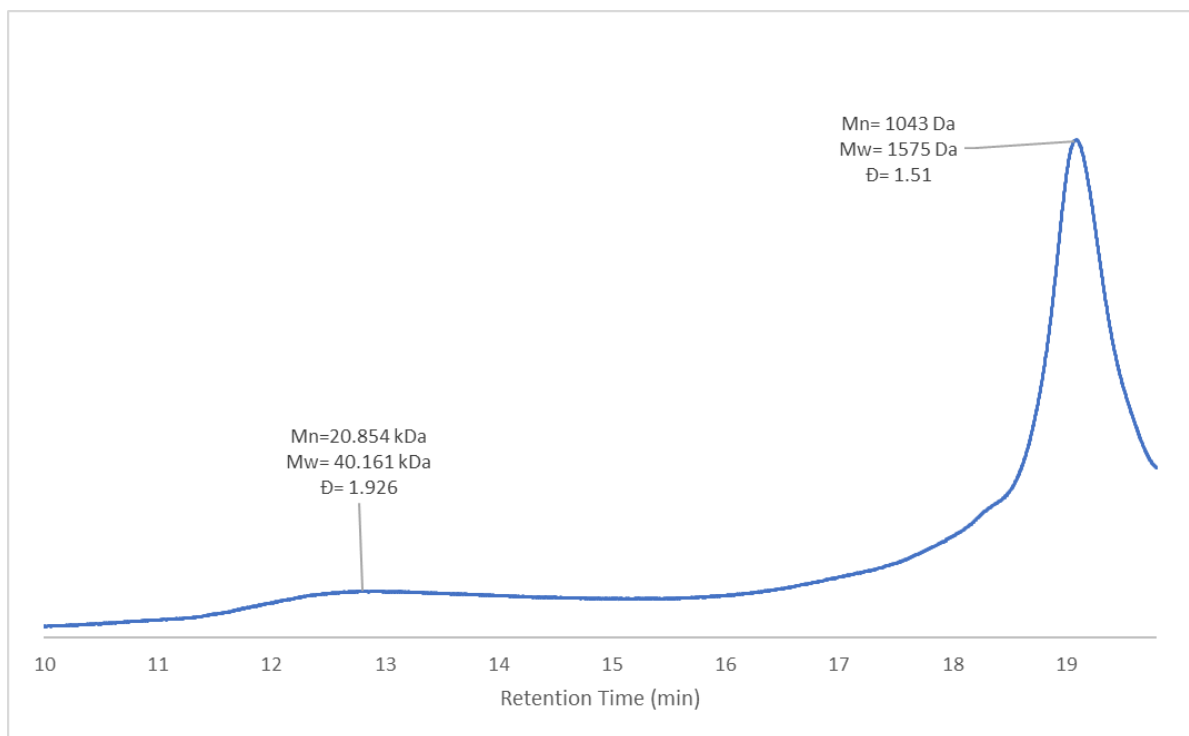


Figure 41. SEC Chromatogram of ADMET-Synthesized Poly-[Oligo-(ϵ -Caprolactone)-*block*-(ϵ -Caprolactone- γ -Isopropyl Amide)] (p[CL_O10-CL_{iPrA}5]).

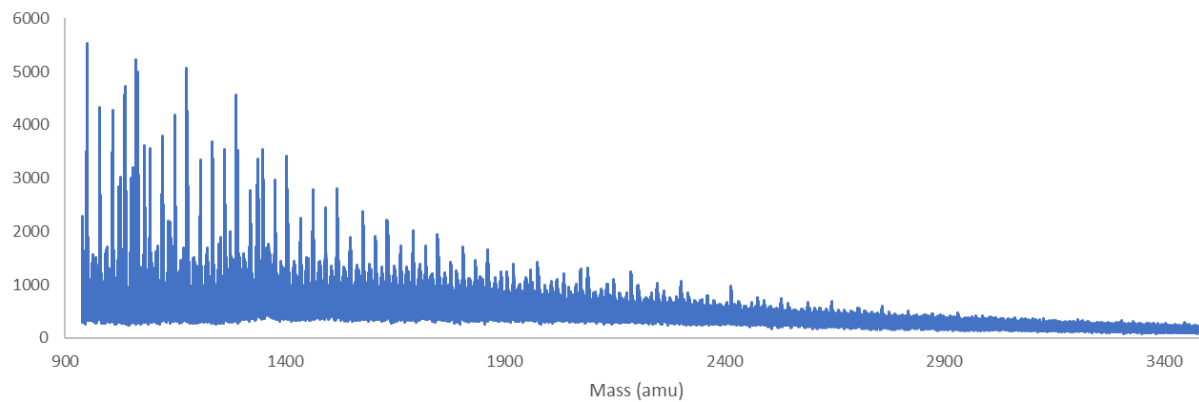
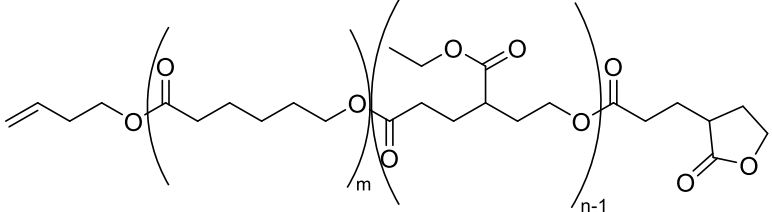


Figure 42. MALDI-TOF Spectra of ADMET-Synthesized Poly-[Oligo-(ϵ -Caprolactone)-*block*-(ϵ -Caprolactone- γ -Isopropyl Amide)] (p[CL_O10-CL_{iPrA}5]).

Appendix E Spectral Data Associated with Syntheses of γ -Ester-Substituted ϵ -Caprolactone Oligomers and Al-Salen Catalyst

Appendix E.1 1,3-Butenol and 2-Oxotetrahydrofuran Capped Oligo-(ϵ -Caprolactone)-*block*-(ϵ -Caprolactone- γ -Ethyl Ester) (CL₀8-CL_{COOEt}_n) Chemical Shift Assignments, NMR Spectra, SEC, and MALDI-TOF

Table 18. ¹H and ¹³C NMR Shift Assignments for 1,3-Butenol and 2-Oxotetrahydrofuran Capped Oligo-(ϵ -Caprolactone)-*block*-(ϵ -Caprolactone- γ -Ethyl Ester) (CL₀8-CL_{COOEt}_n).

				¹³ C-NMR (500 MHz, CDCl ₃)	
				δ (ppm)	Assignment
				178.81	C=O (cyclic)
				173.66	C=O (CL ₀)
				172.88	C=O (linear)
¹ H-NMR (400 MHz, CDCl ₃)				134.17	H ₂ C=CH
δ (ppm)	Mult. (J (Hz))	Int.	Assignment	117.32	H ₂ C=CH
5.77	ddt (17.1, 10.4, 6.9)	1	H ₂ C=CH	66.51	C-O (cyclic)
5.08	m	2	H ₂ C=CH	64.27	C-O (CL ₀)
4.35	td (8.8, 2.7)	5	CL _{COOEt} CH ₂ (cyclic)	60.71	C-O (linear)
4.15	m	12	CL _{COOEt} CH ₂ (cyclic), 2xCH ₂ (linear)	38.53	CH (cyclic)
4.05	t (6.7)	30	CL ₀ CH ₂ , CH ₂ (end group)	34.25	CH ₂ (CL ₀)
2.60	m	5	CL _{COOEt} CH (cyclic)	31.85	CH ₂ (end group)
2.50	t (7.5)	10	CL _{COOEt} CH ₂ (linear/cyclic)	28.91	CH ₂ (cyclic)
2.40	m	5	CL _{COOEt} CH ₂ (cyclic)	28.48	CH ₂ (CL ₀)
2.30	t (7.5)	35	CL ₀ CH ₂	25.67	CH ₂ (CL ₀)
2.15	m	5	CL _{COOEt} CH ₂ (linear/cyclic)	25.62	CH ₂ (end group)
1.95	m	5	CL _{COOEt} CH ₂ (cyclic)	24.71	CH ₂ (CL ₀)
1.84	m	5	CL _{COOEt} CH ₂ (linear/cyclic)	14.34	CH ₃ (linear)CH ₂
1.64	m	72	CL ₀ 2xCH ₂		
1.38	m	35	CL ₀ CH ₂		
1.26	t (7.2)	12	CL _{COOEt} CH ₃ (linear, end group)		

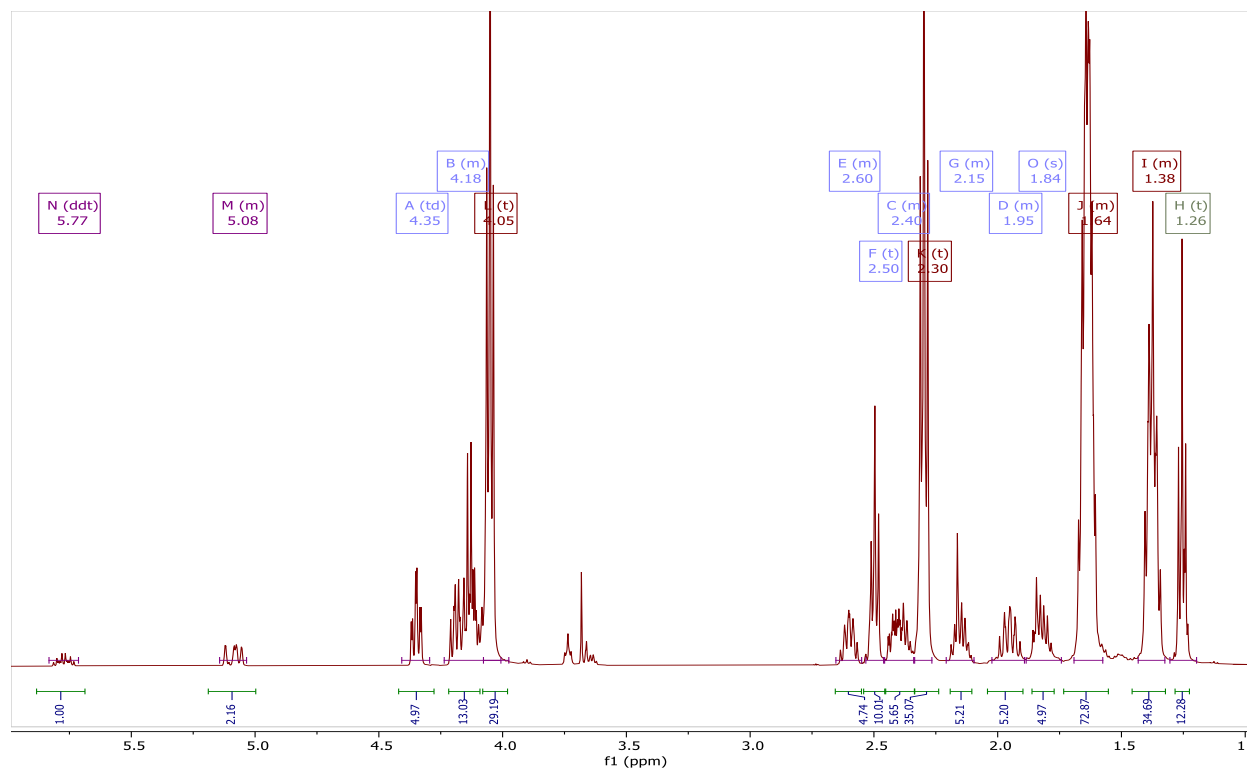


Figure 43. ¹H NMR Spectrum of 1,3-Butenol and 2-Oxotetrahydrofuran Capped Oligo-(ϵ -Caprolactone)-*block*-(ϵ -Caprolactone- γ -Ethyl Ester) (CLo8-CLCOOEIn). 400 MHz, CDCl₃.

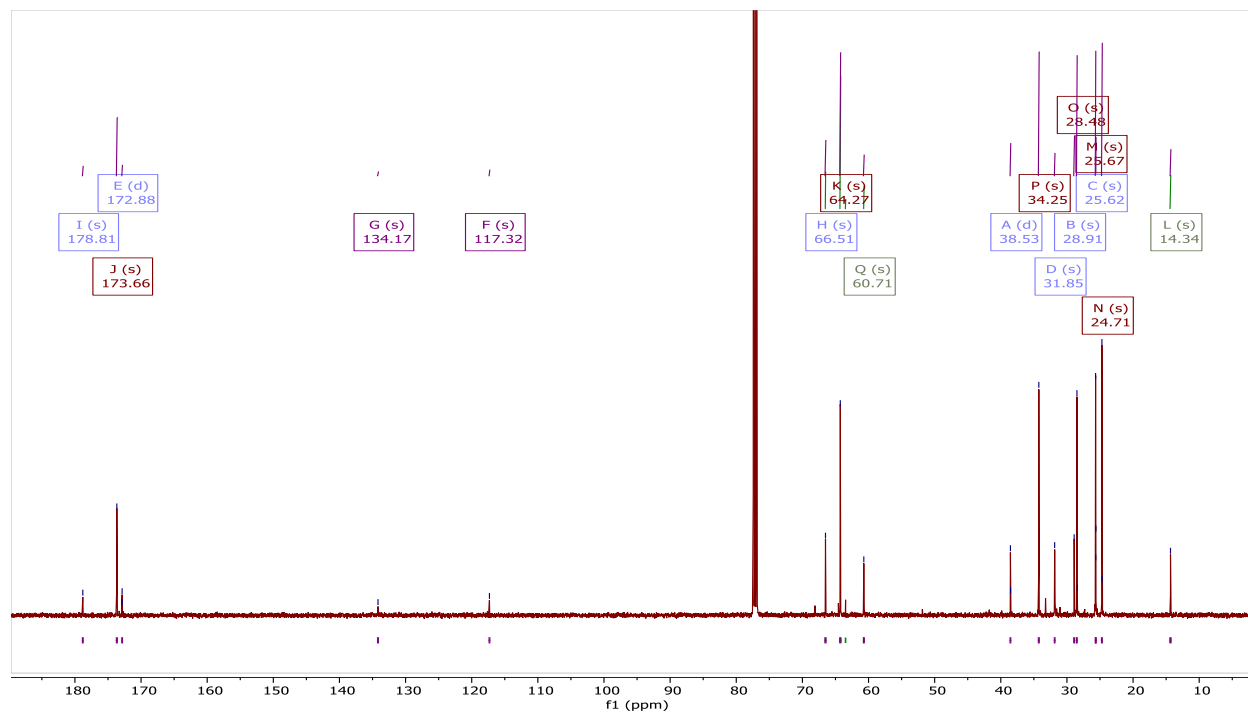


Figure 44. ¹³C NMR Spectrum of 1,3-Butenol and 2-Oxotetrahydrofuran Capped Oligo-(ϵ -Caprolactone)-*block*-(ϵ -Caprolactone- γ -Ethyl Ester) (CLo8-CLCOOEIn). 500 MHz, CDCl₃.

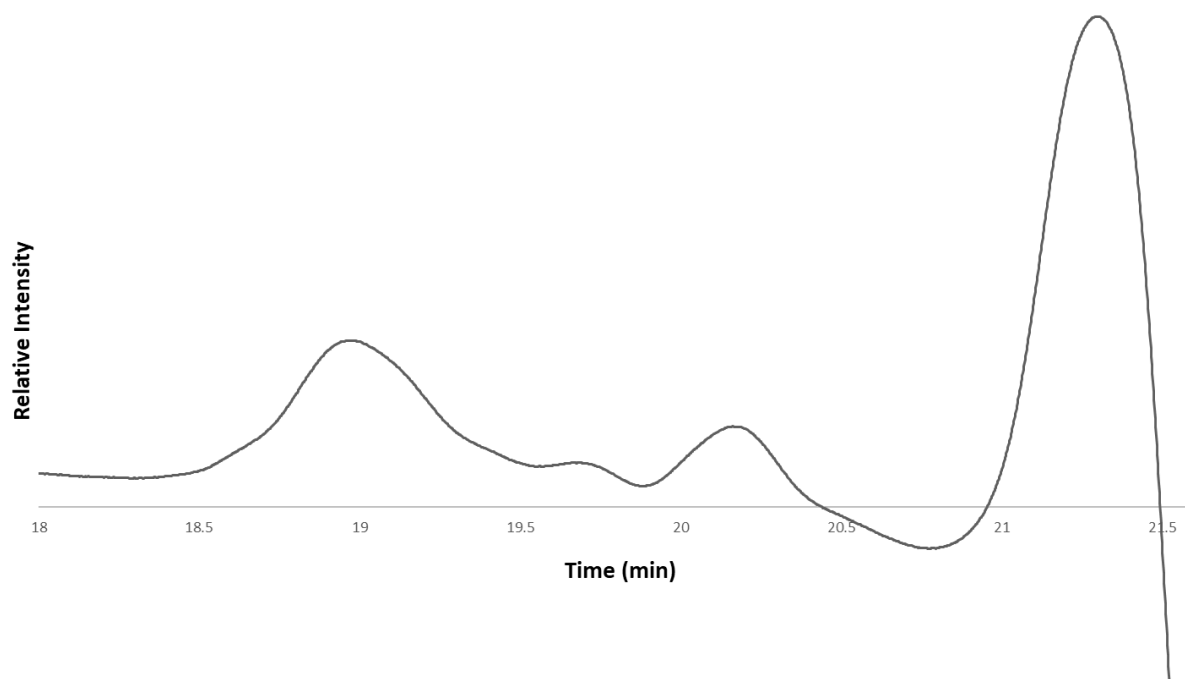


Figure 45. SEC of 1,3-Butenol and 2-Oxotetrahydrofuran Capped Oligo-(ϵ -Caprolactone)-*block*-(ϵ -Caprolactone- γ -Ethyl Ester) (CL₀8-CL_{COOEt}11).

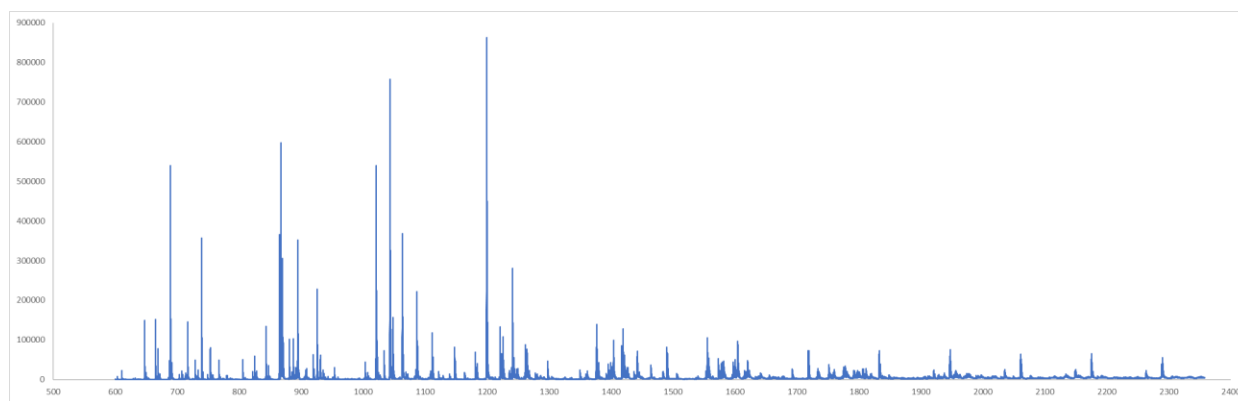
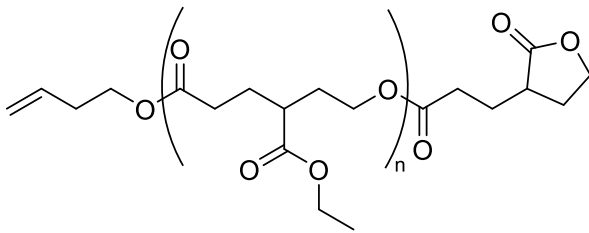


Figure 46. MALDI-TOF Spectra of 1,3-Butenol and 2-Oxotetrahydrofuran Capped Oligo-(ϵ -Caprolactone)-*block*-(ϵ -Caprolactone- γ -Ethyl Ester) (CL₀8-CL_{COOEt}11).

Appendix E.2 Aluminum Tri-1,3-Butenoxide Catalyzed ϵ -Caprolactone- γ -Ethyl Ester Oligomer Chemical Shift Assignments and NMR Spectrum

Table 19. ^1H NMR Shift Assignment for Aluminum Tri-1,3-Butenoxide Catalyzed ϵ -Caprolactone- γ -Ethyl Ester Oligomer.

			
$^1\text{H-NMR}$ (400 MHz, CDCl_3)			
δ (ppm)	Mult. (J (Hz))	Int.	Assignment
5.74	ddt (17.1, 10.2, 6.7)	1	$\text{H}_2\text{C}=\text{CH}$
5.06	m	2	$\text{H}_2\text{C}=\text{CH}$
4.32	td (8.8, 2.7)	5	$\text{CL}_{\text{COOEt}} \text{CH}_2$ (cyclic)
4.13	m	20	$\text{CL}_{\text{COOEt}} \text{CH}_2$ (cyclic), $2 \times \text{CH}_2$ (linear)
2.60	m	6	$\text{CL}_{\text{COOEt}} \text{CH}$ (cyclic)
2.47	m	11	$\text{CL}_{\text{COOEt}} \text{CH}_2$ (linear/cyclic)
2.37	m	9	$\text{CL}_{\text{COOEt}} \text{CH}_2$ (cyclic)
2.12	m	5	$\text{CL}_{\text{COOEt}} \text{CH}_2$ (cyclic)
1.92	m	6	$\text{CL}_{\text{COOEt}} \text{CH}_2$ (linear/cyclic)
1.79	m	5	$\text{CL}_{\text{COOEt}} \text{CH}_2$ (cyclic)
1.23	m	16	$\text{CL}_{\text{COOEt}} \text{CH}_3$ (linear, end group)

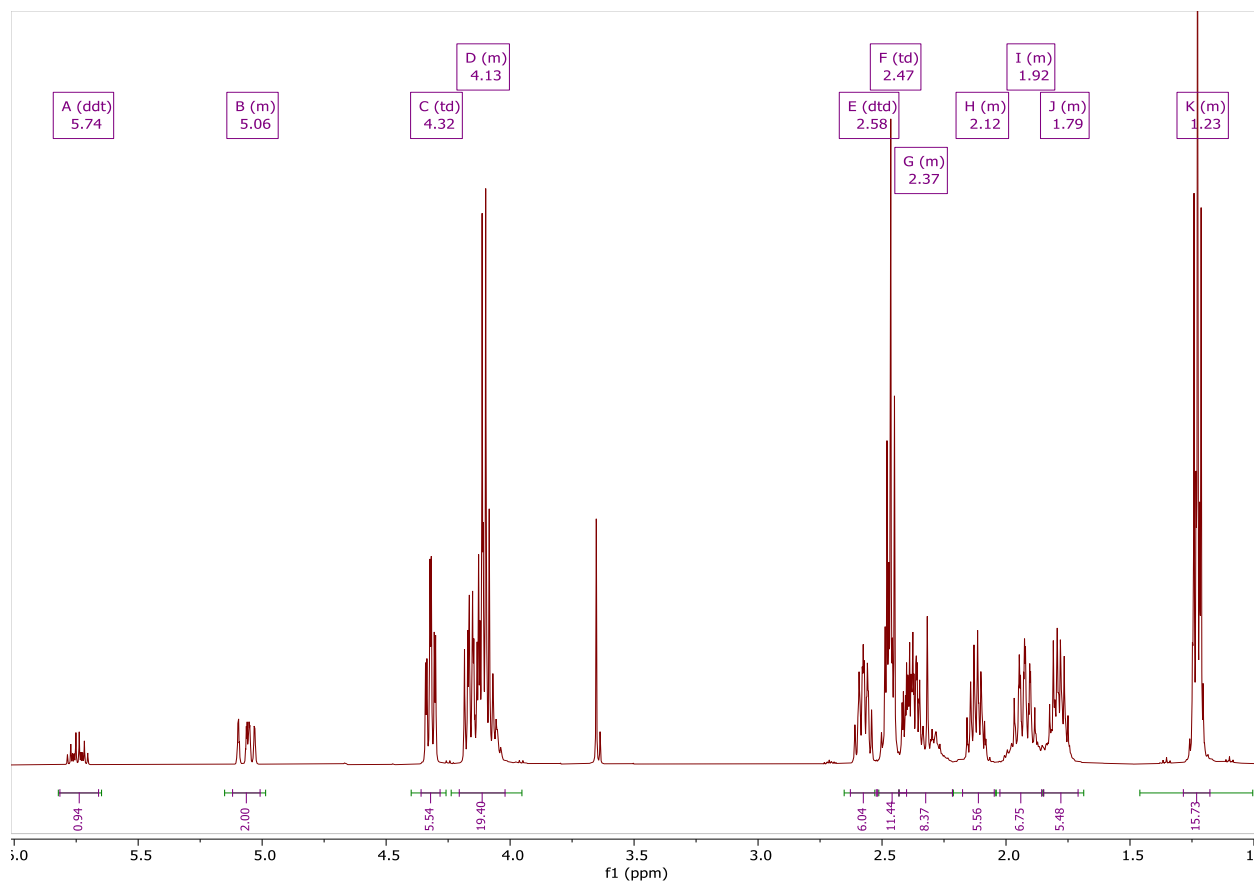


Figure 47. ^1H NMR Spectrum of Aluminum Tri-1,3-Butenoxide Catalyzed ϵ -Caprolactone- γ -Ethyl Ester Oligomer. 400 MHz, CDCl_3 .

Appendix E.3 N,N'-bis(3,5-di-tert-butylsalicylidene)-1,2-cyclohexane-diamino aluminum isopropoxide (Al-Salen) Catalyzed ϵ -Caprolactone Oligomer Chemical Shift Assignments and NMR Spectrum

Table 20. ^1H NMR Shift Assignment for N,N'-bis(3,5-di-tert-butylsalicylidene)-1,2-cyclohexane-diamino aluminum isopropoxide (Al-Salen) Catalyzed ϵ -Caprolactone Oligomer.

$^1\text{H-NMR}$ (400 MHz, CDCl_3)			
δ (ppm)	Mult. (J (Hz))	Int.	Assignment
8.35	d (5.8)	1	(catalyst) N=CH-Ar
8.15	d (7.7)	1	(catalyst) N=CH-Ar
7.49	dt (13.2, 3.3)	2	(catalyst) CH (aromatic)
7.24	m	2	(catalyst) CH (aromatic)
7.05	m	1	(catalyst) CH-N
6.99	m	1	(catalyst) CH-N
4.99	m	6	(catalyst) $(\text{CH}_3)_2$
4.52	m	1	CH (end group)
4.28-3.95	m	14	CH_2 (internal, end group)
3.72	m	2	CH_2 (end group)
3.39	m	1	(catalyst) CH_2 (cyclic)
3.05	m	1	(catalyst) CH_2 (cyclic)
2.59	m	1	(catalyst) CH_2 (cyclic)
2.44	m	1	(catalyst) CH_2 (cyclic)
2.39	tt (6.7, 1.4)	2	CH_2 (end group)
2.28	m	28	2x CH_2 (internal)

¹ H-NMR (400 MHz, CDCl ₃)			
δ (ppm)	Mult. (J (Hz))	Int.	Assignment
2.03	m	2	(catalyst) CH ₂ (cyclic)
1.64	m	30	CH ₂ , CH ₂ (internal, end group)
1.55	s	9	(catalyst) (CH ₃) ₃
1.52	s	9	(catalyst) (CH ₃) ₃
1.47	d (6.4)	6	(CH ₃) ₂ (end group)
1.38	m	14	CH ₂ (internal)
1.30	s	9	(catalyst) (CH ₃) ₃
1.29	s	9	(catalyst) (CH ₃) ₃

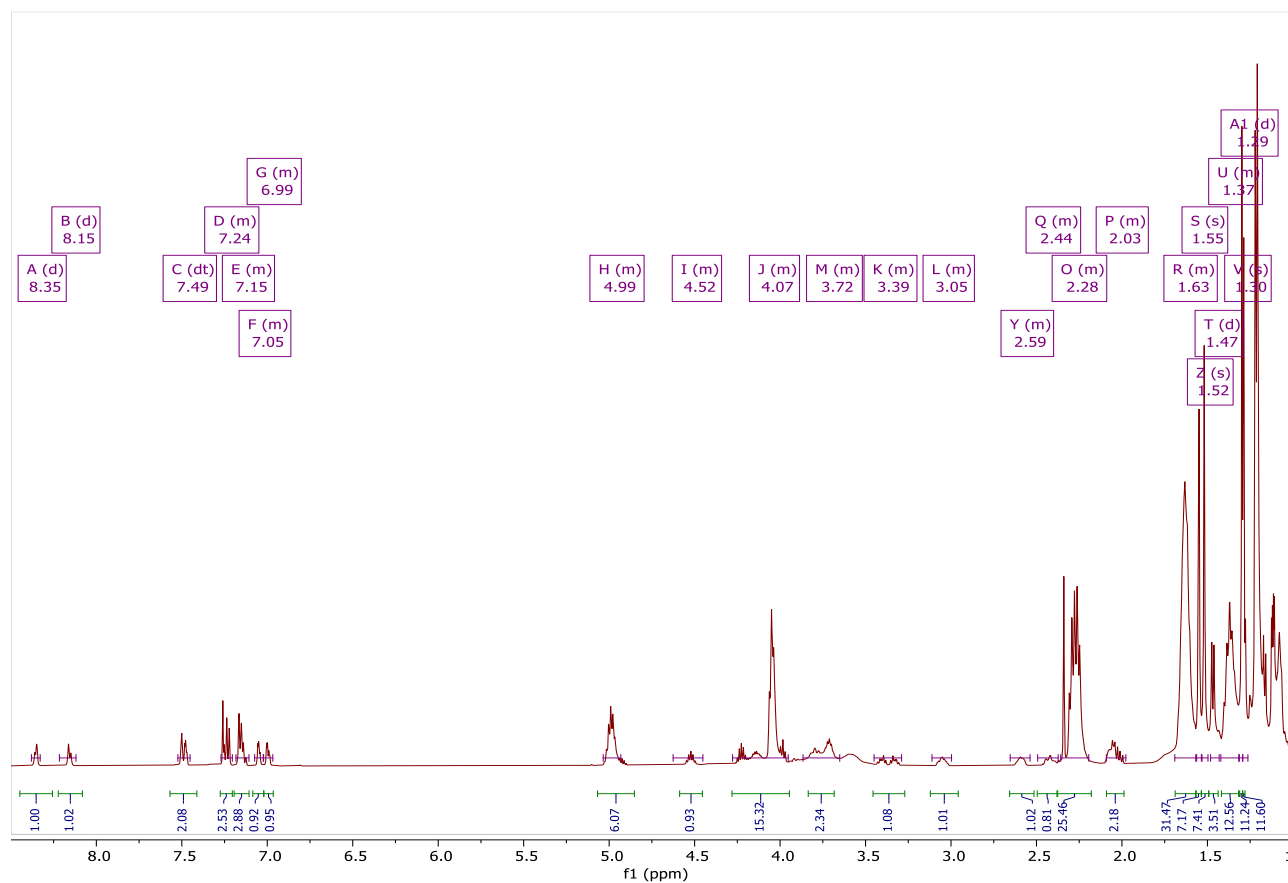


Figure 48. ¹H NMR Spectrum of N,N'-bis(3,5-di-tert-butylsalicylidene)-1,2-cyclohexane-diamino aluminum isopropoxide (Al-Salen) Catalyzed ε-Caprolactone Oligomer after 72 h. 400 MHz, CDCl₃.

Appendix E.4 N,N'-bis(3,5-di-tert-butylsalicylidene)-1,2-cyclohexane-diamino aluminum isopropoxide (Al-Salen) Catalyzed ϵ -Caprolactone- γ -Ethyl Ester Oligomer Chemical Shift Assignments and NMR Spectrum

Table 21. ^1H NMR Shift Assignment for N,N'-bis(3,5-di-tert-butylsalicylidene)-1,2-cyclohexane-diamino aluminum isopropoxide (Al-Salen) Catalyzed ϵ -Caprolactone- γ -Ethyl Ester Oligomer.

$^1\text{H-NMR}$ (400 MHz, CDCl_3)			
δ (ppm)	Mult. (J (Hz))	Int.	Assignment
4.36	td (8.8, 2.7)	4	CL_{COOEt} CH_2 (cyclic, monomer)
4.17	m	19	CL_{COOEt} CH_2 (cyclic), $2\times\text{CH}_2$ (linear), CH_2 CH_2 (monomer)
3.3	m	2	(catalyst) CH_2 (cyclic)
2.79	ddd (14.5, 9.2, 1.8)	1	Monomer CH_2
2.69	tt (9.0, 4.1)	1	Monomer CH
2.60	m	4	CH_2 (cyclic)
2.50	m	11	CL_{COOEt} CH_2 (linear/cyclic)
2.36	m	7	CL_{COOEt} CH_2 (cyclic)
2.16	m	5	CL_{COOEt} CH_2 (cyclic)
1.92	m	5	CL_{COOEt} CH_2 (linear/cyclic)
1.84	m	5	CL_{COOEt} CH_2 (cyclic)
1.41	s	18	$2\times(\text{CH}_3)_3$ (catalyst)
1.31	d (7.8)	11	CL_{COOEt} CH_3 (end group)
1.27	m	11	CL_{COOEt} CH_3 (linear, end group)
1.23	s	18	$2\times(\text{CH}_3)_3$ (catalyst)

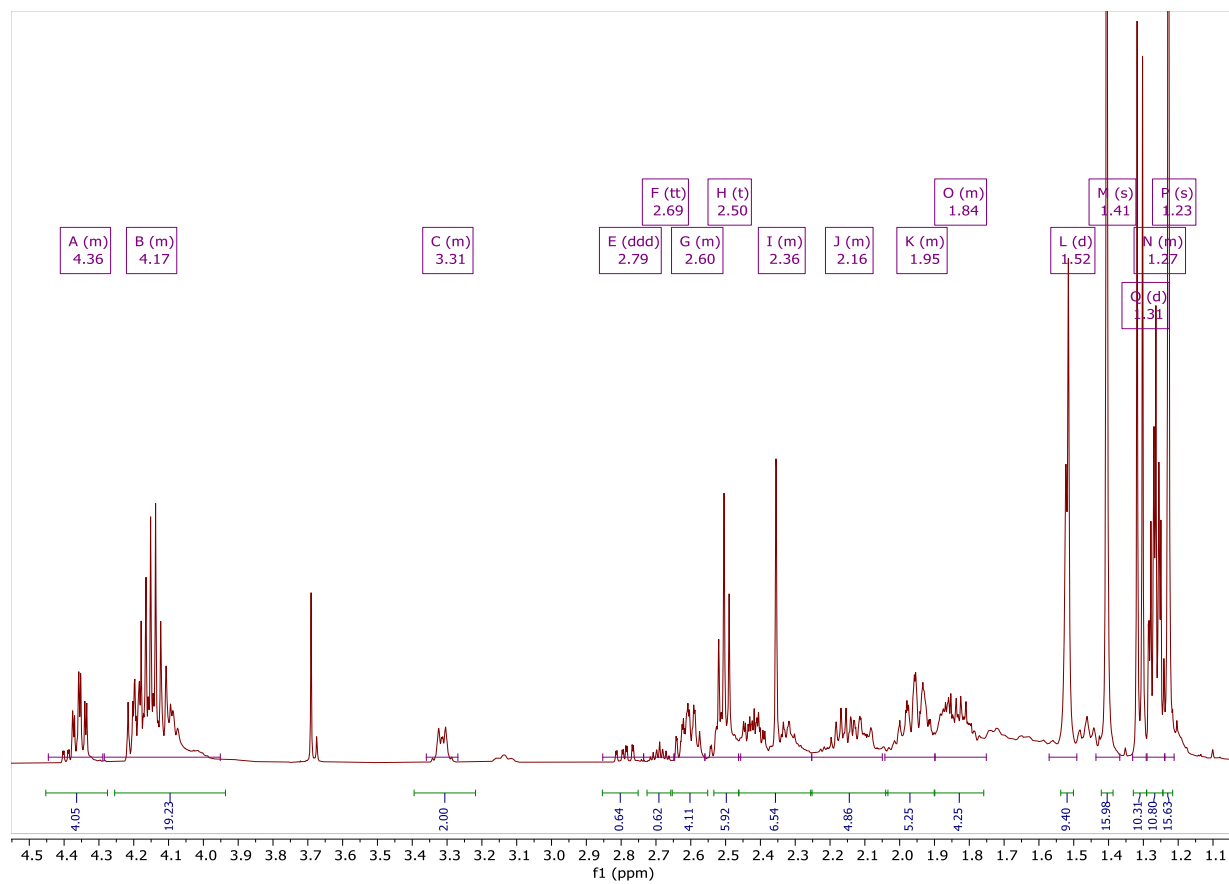


Figure 49. ^1H NMR Spectrum of $\text{N,N}'$ -bis(3,5-di-*tert*-butylsalicylidene)-1,2-cyclohexane-diamino aluminum isopropoxide (Al-Salen) Catalyzed ϵ -Caprolactone- γ -Ethyl Ester Oligomer after 72 h. 400 MHz, CDCl_3 .

Bibliography

1. Hu, X.; Vasanthavada, K.; Kohler, K.; McNary, S.; Moore, A. M. F.; Vierra, C. A., Molecular mechanisms of spider silk. *Cellular and Molecular Life Sciences* **2006**, *63* (17), 1986-1999.
2. Van Beek, J. D.; Hess, S.; Vollrath, F.; Meier, B. H., The molecular structure of spider dragline silk: Folding and orientation of the protein backbone. *Proceedings of the National Academy of Sciences* **2002**, *99* (16), 10266-10271.
3. Berger, O.; Battistella, C.; Chen, Y.; Oktawiec, J.; Siwicka, Z. E.; Tullman-Ercek, D.; Wang, M.; Gianneschi, N. C., Mussel Adhesive-Inspired Proteomimetic Polymer. *Journal of the American Chemical Society* **2022**.
4. Yu, L.; Zhao, J.; Wang, W.; Zong, L.; Ge, S.; Yan, S., Structural stabilization of honeybee wings based on heterogeneous stiffness. *Soft Matter* **2023**, *19* (5), 841-850.
5. Leibler, L., Theory of Microphase Separation in Block Copolymers. *Macromolecules* **1980**, *13* (6), 1602-1617.
6. Geyer, R.; Jambeck, J. R.; Law, K. L., Production, use, and fate of all plastics ever made. *Science Advances* **2017**, *3* (7), e1700782.
7. Takizawa, K.; Tang, C.; Hawker, C. J., Molecularly Defined Caprolactone Oligomers and Polymers: Synthesis and Characterization. *Journal of the American Chemical Society* **2008**, *130* (5), 1718-1726.
8. Jiang, Y.; Golder, M. R.; Nguyen, H. V. T.; Wang, Y.; Zhong, M.; Barnes, J. C.; Ehrlich, D. J. C.; Johnson, J. A., Iterative Exponential Growth Synthesis and Assembly of Uniform Diblock Copolymers. *Journal of the American Chemical Society* **2016**, *138* (30), 9369-9372.
9. Li, G.; Sampson, N. S., Alternating Ring-Opening Metathesis Polymerization (AROMP) of Hydrophobic and Hydrophilic Monomers Provides Oligomers with Side-Chain Sequence Control. *Macromolecules* **2018**, *51* (11), 3932-3940.
10. Mckee, M. L.; Milnes, P. J.; Bath, J.; Stulz, E.; Turberfield, A. J.; O'Reilly, R. K., Multistep DNA-Templated Reactions for the Synthesis of Functional Sequence Controlled Oligomers. *Angewandte Chemie International Edition* **2010**, *49* (43), 7948-7951.
11. Saito, R.; Okuno, Y.; Kobayashi, H., Synthesis of polymers by template polymerization. I. Template polymerization of poly(methacrylic acid) with β -cyclodextrin. *Journal of Polymer Science Part A: Polymer Chemistry* **2001**, *39* (20), 3539-3546.

12. Saito, R.; Yamaguchi, K., Synthesis of Bimodal Methacrylic Acid Oligomers by Template Polymerization. *Macromolecules* **2003**, *36* (24), 9005-9013.
13. O'Reilly, R. K.; Turberfield, A. J.; Wilks, T. R., The Evolution of DNA-Templated Synthesis as a Tool for Materials Discovery. *Accounts of Chemical Research* **2017**, *50* (10), 2496-2509.
14. Feng, L.; Zheng, H.; Gao, B.; Zhao, C.; Zhang, S.; Chen, N., Enhancement of textile-dyeing sludge dewaterability using a novel cationic polyacrylamide: role of cationic block structures. *RSC Advances* **2017**, *7* (19), 11626-11635.
15. Chatterjee, A. K.; Choi, T.-L.; Sanders, D. P.; Grubbs, R. H., A General Model for Selectivity in Olefin Cross Metathesis. *Journal of the American Chemical Society* **2003**, *125* (37), 11360-11370.
16. Brandrup, J.; Immergut, E. H.; Grulke, E. A., *Polymer handbook*. 4th ed ed.; Wiley New York: New York, 1999.
17. Woodruff, M. A.; Hutmacher, D. W., The return of a forgotten polymer—Polycaprolactone in the 21st century. *Progress in Polymer Science* **2010**, *35* (10), 1217-1256.
18. Wen, L.; Zhang, S.; Xiao, Y.; He, J.; Zhu, S.; Zhang, J.; Wu, Z.; Lang, M., Organocatalytic Ring-Opening Polymerization Toward Poly(γ -amide- ϵ -caprolactone)s with Tunable Lower Critical Solution Temperatures. *Macromolecules* **2020**, *53* (13), 5096-5104.
19. Halperin, A.; Kröger, M.; Winnik, F. M., Poly(*N*-isopropylacrylamide) Phase Diagrams: Fifty Years of Research. *Angewandte Chemie International Edition* **2015**, *54* (51), 15342-15367.
20. Bińczak, J.; Dziuba, K.; Chrobok, A., Recent Developments in Lactone Monomers and Polymer Synthesis and Application. *Materials* **2021**, *14* (11), 2881.
21. Clamor, C.; Beament, J.; Wright, P. M.; Cattoz, B. N.; O'Reilly, R. K.; Dove, A. P., Ring-opening polymerisation of alkyl-substituted ϵ -caprolactones: kinetic effects of substitution position. *Polymer Chemistry* **2024**, *15* (12), 1227-1233.
22. Martello, M. T.; Hillmyer, M. A., Polylactide–Poly(6-methyl- ϵ -caprolactone)–Polylactide Thermoplastic Elastomers. *Macromolecules* **2011**, *44* (21), 8537-8545.
23. Batiste, D. C.; Meyersohn, M. S.; Watts, A.; Hillmyer, M. A., Efficient Polymerization of Methyl- ϵ -Caprolactone Mixtures To Access Sustainable Aliphatic Polyesters. *Macromolecules* **2020**, *53* (5), 1795-1808.
24. Tu, Y.-M.; Gong, F.-L.; Wu, Y.-C.; Cai, Z.; Zhu, J.-B., Insights into substitution strategy towards thermodynamic and property regulation of chemically recyclable polymers. *Nature Communications* **2023**, *14* (1).

25. Lenoir, S.; Riva, R.; Lou, X.; Detrembleur, C.; Jérôme, R.; Lecomte, P., Ring-Opening Polymerization of α -Chloro- ϵ -caprolactone and Chemical Modification of Poly(α -chloro- ϵ -caprolactone) by Atom Transfer Radical Processes. *Macromolecules* **2004**, *37* (11), 4055-4061.
26. Mohamed, R. M.; Yusoh, K., A Review on the Recent Research of Polycaprolactone (PCL). *Advanced Materials Research* **2016**, *1134*, 249-255.
27. Sachan, R.; Warkar, S. G.; Purwar, R., An overview on synthesis, properties and applications of polycaprolactone copolymers, blends & composites. *Polymer-Plastics Technology and Materials* **2023**, *62* (3), 327-358.
28. Sisson, A. L.; Ekinici, D.; Lendlein, A., The contemporary role of ϵ -caprolactone chemistry to create advanced polymer architectures. *Polymer* **2013**, *54* (17), 4333-4350.
29. Trollsås, M.; Kelly, M. A.; Claesson, H.; Siemens, R.; Hedrick, J. L., Highly Branched Block Copolymers: Design, Synthesis, and Morphology. *Macromolecules* **1999**, *32* (15), 4917-4924.
30. Calubaquib, E. L.; Soltantabar, P.; Wang, H.; Shin, H.; Flores, A.; Biewer, M. C.; Stefan, M. C., Self-assembly behavior of oligo(ethylene glycol) substituted polycaprolactone homopolymers. *Polymer Chemistry* **2021**, *12* (24), 3544-3550.
31. Rangel, A.; Nguyen, T. N.; Egles, C.; Migonney, V., Different real-time degradation scenarios of functionalized poly(ϵ -caprolactone) for biomedical applications. *Journal of Applied Polymer Science* **2021**, *138* (17), 50479.
32. Barber, V. J.; Borden, M. A.; Alty, J. W.; Tran, L. D.; Koerner, H.; Baldwin, L. A.; Alexanian, E. J.; Leibfarth, F. A., Modifying Poly(caprolactone) Degradation through C–H Functionalization. *Macromolecules* **2023**, *56* (10), 3679-3686.
33. Coudane, J.; Nottelet, B.; Mouton, J.; Garric, X.; Van Den Berghe, H. Poly(ϵ -caprolactone)-Based Graft Copolymers: Synthesis Methods and Applications in the Biomedical Field: A Review *Molecules* [Online], 2022.
34. Shen, J.; Yuan, W.; Badv, M.; Moshaverinia, A.; Weiss, P. S., Modified Poly(ϵ -caprolactone) with Tunable Degradability and Improved Biofunctionality for Regenerative Medicine. *ACS Materials Au* **2023**, *3* (5), 540-547.
35. Bhadran, A.; Shah, T.; Babanyinah, G. K.; Polara, H.; Taslimy, S.; Biewer, M. C.; Stefan, M. C. Recent Advances in Polycaprolactones for Anticancer Drug Delivery *Pharmaceutics* [Online], 2023.
36. Bhadran, A.; Polara, H.; Calubaquib, E. L.; Wang, H.; Babanyinah, G. K.; Shah, T.; Anderson, P. A.; Saleh, M.; Biewer, M. C.; Stefan, M. C., Reversible Cross-linked Thermoresponsive Polycaprolactone Micelles for Enhanced Stability and Controlled Release. *Biomacromolecules* **2023**, *24* (12), 5823-5835.

37. Li, Z.; Tan, B. H., Towards the development of polycaprolactone based amphiphilic block copolymers: molecular design, self-assembly and biomedical applications. *Materials Science and Engineering: C* **2014**, *45*, 620-634.
38. Nguyen, Q. V.; Huynh, D. P.; Park, J. H.; Lee, D. S., Injectable polymeric hydrogels for the delivery of therapeutic agents: A review. *European Polymer Journal* **2015**, *72*, 602-619.
39. Sunnar, B.; Jayakannan, M., Stimuli-Responsive Poly(caprolactone) Vesicles for Dual Drug Delivery under the Gastrointestinal Tract. *Biomacromolecules* **2013**, *14* (12), 4377-4387.
40. Zhai, Y.; Zhou, X.; Jia, L.; Ma, C.; Song, R.; Deng, Y.; Hu, X.; Sun, W. Acetal-Linked Paclitaxel Polymeric Prodrug Based on Functionalized mPEG-PCL Diblock Polymer for pH-Triggered Drug Delivery *Polymers* [Online], 2017.
41. Dubois, P.; Ropson, N.; Jérôme, R.; Teyssié, P., Macromolecular Engineering of Poly lactones and Poly lactides. 19. Kinetics of Ring-Opening Polymerization of ϵ -Caprolactone Initiated with Functional Aluminum Alkoxides. *Macromolecules* **1996**, *29* (6), 1965-1975.
42. Mecerreyes, D.; Atthoff, B.; Boduch, K. A.; Trollsås, M.; Hedrick, J. L., Unimolecular Combination of an Atom Transfer Radical Polymerization Initiator and a Lactone Monomer as a Route to New Graft Copolymers. *Macromolecules* **1999**, *32* (16), 5175-5182.
43. Trollsås, M.; Lee, V. Y.; Mecerreyes, D.; Löwenhielm, P.; Möller, M.; Miller, R. D.; Hedrick, J. L., Hydrophilic Aliphatic Polyesters: Design, Synthesis, and Ring-Opening Polymerization of Functional Cyclic Esters. *Macromolecules* **2000**, *33* (13), 4619-4627.
44. Kularatne, R. N.; Washington, K. E.; Bulumulla, C.; Calubaquib, E. L.; Biewer, M. C.; Oupicky, D.; Stefan, M. C., Histone Deacetylase Inhibitor (HDACi) Conjugated Polycaprolactone for Combination Cancer Therapy. *Biomacromolecules* **2018**, *19* (3), 1082-1089.
45. Ota, T.; Montagna, V.; Higuchi, Y.; Kato, T.; Tanaka, M.; Sardon, H.; Fukushima, K., Organocatalyzed ring-opening reactions of γ -carbonyl-substituted ϵ -caprolactones. *RSC Advances* **2023**, *13* (40), 27764-27771.
46. Baeza, G. P., Recent advances on the structure-properties relationship of multiblock copolymers. *Journal of Polymer Science* **2021**, *59* (21), 2405-2433.
47. Yu, X.; Li, G.; Zheng, B.; Youn, G.; Jiang, T.; Quah, S. P.; Laughlin, S. T.; Sampson, N. S.; Bhatia, S. R., Controlling Rheology of Fluid Interfaces through Microblock Length of Sequence-Controlled Amphiphilic Copolymers. *Macromolecular Chemistry and Physics* **2022**, *223* (18), 2200110.

48. Dykeman-Birmingham, P. A.; Bogen, M. P.; Chittari, S. S.; Grizzard, S. F.; Knight, A. S., Tailoring Hierarchical Structure and Rare Earth Affinity of Compositionally Identical Polymers via Sequence Control. *Journal of the American Chemical Society* **2024**, *146* (12), 8607-8617.
49. Atallah, P.; Wagener, K. B.; Schulz, M. D., ADMET: The Future Revealed. *Macromolecules* **2013**, *46* (12), 4735-4741.
50. Nomura, K.; Chaijaroen, P.; Abdellatif, M. M., Synthesis of Biobased Long-Chain Polyesters by Acyclic Diene Metathesis Polymerization and Tandem Hydrogenation and Depolymerization with Ethylene. *ACS Omega* **2020**, *5* (29), 18301-18312.
51. Walsh, D. J.; Hyatt, M. G.; Miller, S. A.; Guironnet, D., Recent Trends in Catalytic Polymerizations. *ACS Catalysis* **2019**, *9* (12), 11153-11188.
52. Schulz, M. D.; Wagener, K. B., Precision Polymers through ADMET Polymerization. *Macromolecular Chemistry and Physics* **2014**, *215* (20), 1936-1945.
53. Sehlinger, A.; de Espinosa, L. M.; Meier, M. A. R., Synthesis of Diverse Asymmetric α,ω -Dienes Via the Passerini Three-Component Reaction for Head-to-Tail ADMET Polymerization. *Macromolecular Chemistry and Physics* **2013**, *214* (24), 2821-2828.
54. Labet, M.; Thielemans, W., Synthesis of polycaprolactone: a review. *Chemical Society Reviews* **2009**, *38* (12), 3484.
55. Breteler, M. R. T.; Zhong, Z.; Dijkstra, P. J.; Palmans, A. R. A.; Peeters, J.; Feijen, J., Ring-opening polymerization of substituted ϵ -caprolactones with a chiral (salen) AlO*<i>i</i>*Pr complex. *Journal of Polymer Science Part A: Polymer Chemistry* **2007**, *45* (3), 429-436.
56. Zaitsev, K. V.; Piskun, Y. A.; Oprunenko, Y. F.; Karlov, S. S.; Zaitseva, G. S.; Vasilenko, I. V.; Churakov, A. V.; Kostjuk, S. V., Controlled ring-opening homo- and copolymerization of ϵ -caprolactone and $\langle\text{sc}\rangle\text{d,l}\langle\text{sc}\rangle$ -lactide by iminophenolate aluminum complexes: An efficient approach toward well-defined macromonomers. *Journal of Polymer Science Part A: Polymer Chemistry* **2014**, *52* (9), 1237-1250.
57. MacDonald, J. P.; Sidera, M.; Fletcher, S. P.; Shaver, M. P., Living and immortal polymerization of seven and six membered lactones to high molecular weights with aluminum salen and salan catalysts. *European Polymer Journal* **2016**, *74*, 287-295.
58. Miranda, M. O.; DePorre, Y.; Vazquez-Lima, H.; Johnson, M. A.; Marell, D. J.; Cramer, C. J.; Tolman, W. B., Understanding the Mechanism of Polymerization of ϵ -Caprolactone Catalyzed by Aluminum Salen Complexes. *Inorganic Chemistry* **November 12, 2013**, *52* (23).
59. Ding, K.; Miranda, M. O.; Moscato-Goodpaster, B.; Ajellal, N.; Breyfogle, L. E.; Hermes, E. D.; Schaller, C. P.; Roe, S. E.; Cramer, C. J.; Hillmyer, M. A.; Tolman, W.

- B., Roles of Monomer Binding and Alkoxide Nucleophilicity in Aluminum-Catalyzed Polymerization of ϵ -Caprolactone. *Macromolecules* **2012**, *45* (13), 5387-5396.
60. Zhong, Z.; Dijkstra, P. J.; Feijen, J., Controlled and Stereoselective Polymerization of Lactide: Kinetics, Selectivity, and Microstructures. *Journal of the American Chemical Society* **2003**, *125* (37), 11291-11298.
61. Lu, Y.; Swisher, J. H.; Meyer, T. Y.; Coates, G. W., Chirality-Directed Regioselectivity: An Approach for the Synthesis of Alternating Poly(Lactic-co-Glycolic Acid). *Journal of the American Chemical Society* **2021**, *143* (11), 4119-4124.
62. Shen, Z.; Chen, X.; Shen, Y.; Zhang, Y., Ring-Opening polymerization of ϵ -caprolactone by rare earth coordination catalysts. I. Characteristics, kinetics, and mechanism of ϵ -caprolactone polymerization with $\text{Nd}(\text{acac})_3 \cdot 3\text{H}_2\text{O}$ -ALET3 system. *Journal of Polymer Science Part A: Polymer Chemistry* **1994**, *32* (4), 597-603.
63. Wang, H.; Cue, J. M. O.; Calubaquib, E. L.; Kularatne, R. N.; Taslimy, S.; Miller, J. T.; Stefan, M. C., Neodymium catalysts for polymerization of dienes, vinyl monomers, and ϵ -caprolactone. *Polymer Chemistry* **2021**, *12* (47), 6790-6823.
64. Kularatne, R. N.; Taslimy, S.; Bhadran, A.; Cue, J. M. O.; Bulumulla, C.; Calubaquib, E. L.; Gunawardhana, R.; Biewer, M. C.; Stefan, M. C., A binary neodymium catalyst for the polymerization of lactones. *Polymer Chemistry* **2023**, *14* (34), 3962-3970.
65. Gody, G.; Maschmeyer, T.; Zetterlund, P. B.; Perrier, S., Pushing the Limit of the RAFT Process: Multiblock Copolymers by One-Pot Rapid Multiple Chain Extensions at Full Monomer Conversion. *Macromolecules* **2014**, *47* (10), 3451-3460.
66. Blázquez-Blázquez, E.; Pérez, E.; Lorenzo, V.; Cerrada, M. L., Crystalline Characteristics and Their Influence in the Mechanical Performance in Poly(ϵ -Caprolactone) / High Density Polyethylene Blends. *Polymers* **2019**, *11* (11), 1874.
67. Benoit, H.; Hadziioannou, G., Scattering theory and properties of block copolymers with various architectures in the homogeneous bulk state. *Macromolecules* **1988**, *21* (5), 1449-1464.
68. Krause, S., Microphase Separation in Block Copolymers. Zeroth Approximation Including Surface Free Energies. *Macromolecules* **1970**, *3* (1), 84-86.
69. Tan, C.; Zou, C.; Chen, C., Material Properties of Functional Polyethylenes from Transition-Metal-Catalyzed Ethylene-Polar Monomer Copolymerization. *Macromolecules* **2022**, *55* (6), 1910-1922.
70. Halperin, A., On the collapse of multiblock copolymers. *Macromolecules* **1991**, *24* (6), 1418-1419.
71. Weidisch, R.; Schreyeck, G.; Ensslen, M.; Michler, G. H.; Stamm, M.; Schubert, D. W.; Budde, H.; Höring, S.; Arnold, M.; Jerome, R., Deformation Behavior of Weakly

- Segregated Block Copolymers. 2. Correlation between Phase Behavior and Deformation Mechanisms of Diblock Copolymers. *Macromolecules* **2000**, *33* (15), 5495-5504.
72. Thompson, S. W.; Guimarães, T. R.; Zetterlund, P. B., Sequence-Defined Multiblock Copolymer Nanoengineered Particles from Polymerization-Induced Self-Assembly (PISA): Synthesis and Film Formation. *Macromolecules* **2023**, *56* (23), 9711-9724.
73. Hermel, T. J.; Hahn, S. F.; Chaffin, K. A.; Gerberich, W. W.; Bates, F. S., Role of Molecular Architecture in Mechanical Failure of Glassy/Semicrystalline Block Copolymers: CEC vs CECEC Lamellae. *Macromolecules* **2003**, *36* (7), 2190-2193.
74. Daubian, D.; Gaitzsch, J.; Meier, W., Synthesis and complex self-assembly of amphiphilic block copolymers with a branched hydrophobic poly(2-oxazoline) into multicompartement micelles, pseudo-vesicles and yolk/shell nanoparticles. *Polymer Chemistry* **2020**, *11* (6), 1237-1248.
75. Grover, T. L.; Guymon, C. A., Effect of Block Copolymer Self-Assembly on Phase Separation in Photopolymerizable Epoxy Blends. *Macromolecules* **2024**, *57* (10), 4717-4728.
76. Drayer, W. F.; Simmons, D. S., Sequence Effects on the Glass Transition of a Model Copolymer System. *Macromolecules* **2022**, *55* (14), 5926-5937.